2023

Adolescence, alcohol, and astrocytes: the impact of adolescent alcohol use on astrocyte-synaptic interactions, structure, function, and behavior

Christopher Douglas Walker
walker.christopherd@gmail.com

ADOLESCENCE, ALCOHOL, AND ASTROCYTES: THE IMPACT OF ADOLESCENT ALCOHOL USE ON ASTROCYTE-SYNAPTIC INTERACTIONS, STRUCTURE, FUNCTION, AND BEHAVIOR

A dissertation submitted to
Marshall University
in partial fulfillment of
the requirements for the degree of
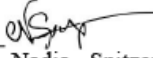Doctor of Philosophy
in
Biomedical Research
by
Christopher Douglas Walker
Approved by
Dr. Mary-Louise Risher, Committee Chairperson
Dr. Richard Egleton
Dr. Brandon Henderson
Dr. Chris Risher
Dr. Nadja Spitzer

Marshall University
August 2023

Approval of Dissertation

We, the faculty supervising the work of Christopher Douglas Walker, affirm that the dissertation, *Adolescence, Alcohol, and Astrocytes: The Impact of Adolescent Alcohol Use on Astrocyte-Synaptic Interactions, Structure, Function, and Behavior,* meets the high academic standards for original scholarship and creative work established by the Biomedical Research Program and the Joan C. Edwards School of Medicine. The work also conforms to the requirements and formatting guidelines of Marshall University. With our signatures, we approve the manuscript for publication.

		07/07/2023
Dr. Mary-Louise Risher, Department of Biomedical Research	Committee Chairperson	Date
		7/7/23
Dr. Richard Egleton, Department of Biomedical Research	Committee Member	Date
		7/10/2023
Dr. Brandon Henderson, Department of Biomedical Research	Committee Member	**Date**
		7/7/23
Dr. Chris Risher, Department of Biomedical Research	Committee Chairperson	Date
		Jul?,2023
Dr. Nadja Spitzer, Department of Biological Sciences	Committee Member	Date

iii

Dedication

I want to dedicate this dissertation to my late mother, Linda Kay Walker. She was a fantastic human; she was strong, fierce, kind, and supportive. While she may no longer be with us, I think of her often and know I would not be the person I am today without her example. I wish she could be here to share in the celebration of these accomplishments. I think she would be proud.

I love you high as the sky and as deep as the ocean.

Acknowledgements

I am grateful for the endless support from my mentors, classmates, friends, and family throughout this journey. Graduate school is difficult under normal circumstances. Once you mix in a pandemic and the death of loved ones, it becomes almost unbearable. I have been fortunate to be surrounded by an endless team of support.

First, I want to thank my mentor, Dr. Louise Risher. I began my rotation in her lab the day I started graduate school and never left. Numerous times, my inner saboteur tried to get the best of me. Dr. Risher would help me realize that I am a good scientist and deserve to be here; she would not let me give up on myself. During this program, I have gone through some of my life's most brutal experiences, and she has always been there to help me get to the other side. I am beyond lucky to have had a mentor like Dr. Risher. I am now and always will be grateful.

Next, I want to thank the other extraordinary members of my committee – Drs. Richard Egleton, Brandon Henderson, Chris Risher, and Nadja Spitzer – for their kindness, support, and always challenging me to think critically and look at the bigger picture.

I want also to acknowledge the many people who have played a considerable role of support over the last five years Hannah Sexton, Cassie Song, Dr. Laura Kutz, Dr. Shreya Mukherji, Dr. Skylar Cooper, Dr. Sarah Brunty, Nate Olszewski, Renat Roytenberg, and Olivia Coulter to name a few. They have been there to listen, provide advice, and have always encouraged me to keep moving forward. We have developed a bond that has and will continue to extend outside this program.

Next, I want to thank my Kentucky 'family,' Dr. Thys Meyer, Karyla Trester, Hannah Thacker, Linda Morely, Steven Blackburn, and Dr. Carman Parker. Each of them enriches my life in more ways than I can describe. They have lifted me even when I didn't know I needed it.

v

A very special thank you to Erica Blackburn. We share over 25 years of friendship that has survived high school, major life events, and sometimes thousands of miles. At this point, we are more like family than we are friends. I know that when we are old, gray, and wrinkled, we will sing songs from 'Grease 2' and plan our next vacation.

Last but certainly not least, I want to thank my unique, kind, successful, and supportive husband, Jerald Hylton. He is my biggest cheerleader and my best friend. He found me when I didn't know I was lost and has never left my side or let me down. I am grateful to have him as my partner for this life adventure. Thank you for loving me for who I am and never asking me to be anything else.

I am looking forward to spending the rest of my life with you.

Table of Contents

x

xiii

List of Abbreviations and Acronyms

* – other NMDAR receptors may be present

µL – microliter

µm – micrometer

AAV – adeno-associated virus

ACC – anterior cingulate cortex

ACSF – artificial cerebrospinal fluid

AIE – adolescent intermittent ethanol

AMPAR – α-amino-3-hydroxy-5-methyl-4-isoxazolepropionic acid receptor

AUD – alcohol use disorder

BAC – blood alcohol concentration

BEC – blood ethanol concentration

C – Celsius

C1q – complement component 1q

C3 – complement 3

CA – cornu ammonis

Ca^{2+} – calcium

$CaCl_2$ – calcium chloride

CDC – Centers for Disease Control and Prevention

CFB – complement factor B

CNS – central nervous system

CO_2 – carbon dioxide

DREADDs – designer receptors exclusively activated by designer drugs

DTI – diffusion tensor imaging

EtOH – ethanol

g – gram

g/L – grams per liter

GABA – gamma-Aminobutyric Acid

GFAP – glial fibrillary acidic protein

GFP – green fluorescent protein

GluN2A – glutamate NMDA Subunit 2A

GluN2B – glutamate NMDA Subunit 2B

H_2O – water

HEPES – N-2-hydroxyethylpiperazine-N-2-ethane sulfonic acid

i.g. – intragastric gavage

IHC – immunohistochemistry

IL – infralimbic cortex

IL-1α – interleukin-1 alpha

IPA – ingenuity pathway analysis

K^+ – potassium

KCl – potassium chloride

kg – kilogram

Lck – lymphocyte protein tyrosine kinase

LC-MS/MS – liquid chromatography with tandem mass spectrometry

LO-OFC – lateral orbitofrontal cortex

LTD – long term depression

LTP – long-term potentiation

M – molar

$MgCl_2$ – magnesium chloride

min – minute

mL – milliliter

mm – millimeter

mM – millimolar

mPFC – medial prefrontal cortex

MRI – magnetic resonance imaging

NaCl – sodium chloride

NaH_2PO_4 – monosodium phosphate

$NaHCO_3$ – sodium bicarbonate

NDS – normal donkey serum

NGS – normal goat serum

NMDA – N-methyl-D-aspartate

NMDAR - N-methyl-D-aspartate receptors

NMDG – N-methyl-D-glucamine

NSDUH – National Survey on Drug Use and Health

OFC – orbitofrontal cortex

PAPs – peripheral astrocyte processes

PB – phosphate buffer

PBS – phosphate buffered saline

PFA – paraformaldehyde

PFC – prefrontal cortex

PL – prelimbic cortex

PND – postnatal day

PPI – prepulse inhibition

P-rats – alcohol-preferring rats

PSD-95 – postsynaptic density marker 95

Str. Gr. – stratum granulosum

Str. L-M – stratum lacunosum-moleculare

Str. Mol. – stratum moleculare

Str. Oriens – stratum oriens

Str. Pyr. – stratum pyramidal

Str. Rad. – stratum radiatum

SUD – substance use disorder

TNFα – tumor necrosis factor-alpha

Str. Luc. – stratum luciderm

v/v – volume per volume

VO-OFC – ventral orbitofrontal cortex

Abstract

Alcohol is the third leading cause of preventable death in the United States and has substantial social and economic burdens. Excessive alcohol consumption in the form of binge drinking is highly prevalent among adolescents and emerging adults. Binge drinking is a form of excessive drinking, defined as consuming enough alcohol on a single occasion to result in blood alcohol concentrations above 0.08%. Approximately 55% of full-time college students aged 18-22 years old have reported consuming alcohol in a binge manner. Furthermore, studies have shown that approximately 20% of college students meet the criteria for an alcohol use disorder (AUD). These statistics are concerning as this period of increased proclivity to participate in binge-type alcohol consumption overlaps with the critical period of adolescent development. During adolescence, the central nervous system (CNS) is undergoing a stage of neurodevelopment in which regions of the brain, such as the prefrontal cortex (PFC) and the hippocampus, which are critical for learning and higher cognitive development, continue to undergo refinement and maturation. Consuming alcohol during early adolescence results in long-term deficits in cognitive function and an increased risk of developing an AUD later in life. There has been a concerted effort to understand the direct contributions of adolescent binge drinking to long-lasting changes in neuronal structure, function, and subsequent cognitive changes that may be associated with the emergence of neuropsychiatric disorders and addiction. However, non-neuronal cells' contribution to alcohol-induced neuronal dysfunction is just beginning to be elucidated. Astrocytes are highly complex non-neuronal glial cells that serve in developing, refining, and maintaining the CNS. Furthermore, very few studies are dedicated to investigating potential sex differences in the effects of adolescent alcohol exposure on astrocytes. Parallels in findings in human clinical data and laboratory studies using rodent models have

allowed our lab and others to use a rat model of adolescent intermittent binge ethanol (EtOH) exposure (AIE) to begin to identify the roles of astrocytes in AIE-induced long-term neuronal dysfunction across multiple brain regions in males and females. This dissertation encompasses the investigation of 1) the short- and long-term effects of AIE on astrocyte morphology and astrocyte-synaptic interactions across multiple subregions of the male PFC, 2) the long-term effects of AIE on astrocyte morphology, astrocyte-synaptic interactions, and astrocyte function at the synapse in the female hippocampus, and 3) the short- and long-term effects of AIE on astrocyte morphology, astrocyte-synaptic proximity and interactions, subsequent astrocyte function at the synapse and hippocampal behaviors in male rodents. Overall, this dissertation aims to fill in gaps of knowledge by identifying how AIE impacts astrocytes across different brain regions undergoing adolescent neurodevelopment and how these effects may vary between sexes.

<center>**Chapter 1**</center>

<center>**Introduction to Alcohol, Adolescence, and Astrocytes**</center>

Alcohol

Alcohol consumption is the third leading cause of preventable death in the United States. Alcohol use plays a significant role in health and social problems and imposes a substantial economic burden (Choenni et al., 2017; Esser et al., 2020; Karriker-Jaffe et al., 2018; Sacks et al., 2015; Xi et al., 2017). The economic burden of alcohol use is staggering, with estimates that alcohol costs roughly $250 billion annually (Sacks et al., 2015). While these statistics are overwhelming, alcohol use remains highly prevalent in the United States, regardless of the societal consequences and personal risks.

Alcohol consumption can be classified as moderate or heavy drinking, often accompanied by intense or binge drinking periods. Moderate alcohol consumption is defined as one standard drink (0.6 oz of alcohol) or less per day for women and two drinks or less per day for men. Heavy drinking is typically defined as eight standard drinks per week for women and 15 standard drinks or more for men (Bohm et al., 2021; Sacks et al., 2015). In comparison, binge drinking is a pattern of alcohol consumption that brings blood alcohol levels (BACs) to 0.08% or more in a single session (Bohm et al., 2021; Sacks et al., 2015). This typically occurs when women consume four or more drinks or five or more drinks are consumed by men within two hours (Bohm et al., 2021; Sacks et al., 2015).

Binge alcohol consumption is highly prevalent among adolescents and emerging adults (Bohm et al., 2021). Adolescence is a time of increased independence and risk-taking behavior that often leads to experimentation with misused substances, including alcohol. As discussed in the next section, this propensity toward binge alcohol consumption coincides with a critical

<center>1</center>

period of neurodevelopment, resulting in long-term cognitive dysfunction and an increase in the likelihood of developing an alcohol use disorder later in life.

Adolescent Neurodevelopment

Adolescence is a transitional period of development that encompasses, but is not limited to, puberty and continues into early adulthood (Holder & Blaustein, 2014). The World Health Organization has historically defined adolescence as the period between the ages of 10 and 19 (World Health Organization, 2001). However, recent work indicates that it is more appropriate to identify individuals 10-24 years of age as among the adolescent/emerging adulthood category (Sawyer et al., 2012). These individuals can be divided into early adolescence (10-14 years of age), late adolescence (15-19), and young or emerging adulthood (20-24; Sawyer et al., 2012). During puberty, hormones are released, triggering sexual maturation. These hormones result in physical and biochemical changes that include increases in growth and metabolic rates, changes in fat and muscle, and the development of breasts and genitalia accompanied by the appearance of secondary sex characteristics. At the same time, changes in social, emotional, and cognitive processes occur that enable individuals to transition from childhood to adulthood to successfully take on adult roles and responsibilities (Choudhury, 2010). This is accompanied by changes in brain structure and function that are influenced by education and socialization (Crone & Dahl, 2012; Davey et al., 2008; Mills & Tamnes, 2014). One way to consider adolescent development is biological changes (i.e., puberty) and social changes (i.e., adolescence), with neurodevelopment mediating the association between these biochemical and psychosocial changes (Crone & Dahl, 2012; Davey et al., 2008; Mills & Tamnes, 2014).

Neurodevelopment is the process of neuronal growth and circuitry refinement that shapes the brain to fit its environment under the influence of experience, biochemistry, and genetic

mechanisms. Adolescent neurodevelopment has been conserved across evolution as common adolescent behaviors observed in humans have also been found in other species. For example, increased peer-direct social interactions (Csikszentmihalyi et al., 1977; Primus & Kellogg, 1989; Steinberg et al., 1989), risk-taking, and novelty- and sensation-seeking (Adriani et al., 1998; Romer et al., 2010; Steinberg, 2010; Trimpop et al., 1998), and greater incidences of alcohol consumption (Doremus et al., 2005) have been observed in humans, non-human primates, rodents, and other species.

One of the hallmarks of adolescent neurodevelopment is synaptic pruning, which is when the brain eliminates excess synapses that are no longer needed. During early development, there are more neurons and synapses produced than will be retained throughout the lifespan (Huttenlocher & Dabholkar, 1997; Oppenheim, 1991). It is thought that the overproduction of neurons and synapses helps to ensure that appropriate circuitry is established, leaving those neurons and synapses that do not make proper connections to be lost to mechanisms of apoptosis and synaptic pruning (Rakic et al., 1994). It has been speculated that synaptic pruning is a mechanism to aid in rewiring neuronal circuitry into more 'adult-like patterns' (Spear, 2013). Furthermore, this rewiring can correlate to increased plasticity, essential in memory and learning (Spear, 2013). However, not all brain regions undergo refinement via synaptic pruning to the same extent. Pruning is precise and results in some regions losing nearly 50% of their synaptic connectivity during adolescence, while others experience little synaptic loss (Rakic et al., 1994). Overall, synaptic pruning during adolescence optimizes the brain's circuits in regions, such as the prefrontal cortex (PFC) that correlate to increased cognitive function, through the strengthening of functionally related brain regions by weakening connections with others (Fair et al., 2008; Johnson, 2001; Stevens et al., 2009; Supekar et al., 2009).

This dissertation focuses on the impact of adolescent ethanol (EtOH) exposure (AIE) on the PFC and the hippocampus (Chapters 4, 5, and 6). We begin by reviewing adolescent development of the PFC and hippocampus (Chapters 2 and 3 respectively). Below, we give a brief overview of the effects of alcohol exposure on the PFC, hippocampus, and astrocytes, highlighting the importance of our research and contributions to the field.

Prefrontal Cortex (PFC)

The PFC continues to undergo structural and functional neuronal refinement during adolescence, during which experience and neurobiological factors work together to shape normal brain development and permanently alter behaviors (Asato et al., 2010; Bourne & Harris, 2008; Cressman et al., 2010; Cunningham et al., 2002; Liston et al., 2006; Markham et al., 2007; Matsuzaki, 2007). Experiences that engage the PFC during adolescence include increased exploration, independence, socialization, sensation-seeking, sexual maturation, and mating behaviors. As these experiences increase in complexity (and as adolescents are increasingly responsible for navigating them without parental instruction), brain areas like PFC that support increasingly complex behaviors, such as socioemotional processing, planning, reasoning, and abstract thought, must be engaged and specialized to meet the demands of the environment. As such, increasingly complex adolescent experiences are the optimal input to drive experience-dependent plasticity. For example, in rats, complex peer-peer social interaction and cognitive flexibility peak during adolescence, which the mPFC mediates, thus engaging mPFC networks and strengthening its neuronal network (Bell et al., 2010; Himmler et al., 2013; Panksepp, 1981; Spinka et al., 2001; van Kerkhof et al., 2013).

Hippocampus

The hippocampus's highly organized architecture undergoes continued maturation throughout adolescence (Gomez & Edgin, 2016). Behavioral development reflects the maturation of the underlying circuitry, making adolescence a transformative time of neurodevelopment. During childhood, synaptogenesis is active in the hippocampus, increasing peak brain volume in early adolescence, followed by the pruning and refinement of synapses and axonal myelination that aid in fine-tuning hippocampal architecture. Social, emotional, and environmental factors can robustly affect remodeling during adolescent development, influencing cognition (see Griffin (2017) for review). Substance use is one of the stimuli that can critically influence these final stages of hippocampal maturation. For example, Risher, Fleming, et al. (2015) have previously shown that early EtOH exposure results in a shift towards increased dendritic spine immaturity and lowered stimulus thresholds for the induction of long-term potentiation (LTP) in the hippocampus of adult male rats. These findings suggest that AIE increases synaptic plasticity in adulthood, reminiscent of an immature or adolescent-like state.

Astrocytes

Astrocytes have emerged as critical regulators of central nervous system (CNS) development and function in the last two decades (Barres, 2008; Chung et al., 2013; Eroglu & Barres, 2010; Kim et al., 2019). Astrocytes have complex morphologies that allow them to interact with the vasculature to form the blood-brain barrier (BBB) via endfeet (Kubotera et al., 2019). Astrocytes also have an extensive network of peripheral astrocyte processes (PAPs) that extend from the cell body and ensheathe presynaptic neuronal compartments and postsynaptic dendritic spines (Ventura & Harris, 1999), forming what is referred to as the 'tripartite synapse.' Each astrocyte can interact with up to 100,000 synapses in the rodent brain and an estimated 2

million synapses in humans (Bushong et al., 2002), providing a wide-ranging network of connectivity that allows a single astrocyte to integrate and influence neuronal activity across independent circuits (Oberheim et al., 2009).

Astrocytes regulate various functions through contact-mediated and secreted signaling factors. Astrocytes have been identified as key drivers in the formation of excitatory synapses in the CNS (Christopherson et al., 2005; Ullian et al., 2001) and, more recently, in the signaling-dependent promotion of synaptic diversity (Farhy-Tselnicker & Allen, 2018). Astrocytes also play significant roles in the regulation of extracellular matrix protein signaling (Wiese et al., 2012; Zamanian et al., 2012), formation and maintenance of the blood-brain barrier (BBB) (Wong et al., 2004), neovascularization (Fan et al., 2008), neurogenesis (Song et al., 2002), axonal growth (Dickson, 2002), and homeostasis of the synaptic microenvironment (Khakh & Sofroniew, 2015).

A growing body of evidence suggests that astrocyte dysregulation can play an essential role in cognitive impairment, neuronal loss, and the emergence of synaptic deficits associated with aging and neurodegenerative diseases (Clarke et al., 2018; Matias et al., 2019). In addition, astrocytes react to various conditions, including excitotoxicity, injury, age, and infection, in a process termed astrogliosis (i.e., astrocyte reactivity (Karve et al., 2016)). Astrogliosis is a heterogeneous response in which these cells undergo context-dependent molecular and morphological changes. Depending on the nature of the insult, astrocytes can take on characteristic functional and molecular profiles termed A1 or A2 reactive astrocytes. The A1 reactive astrocyte subtype is characterized by the upregulation of complement 3 (C3, complement factor B (CFB)) and the MX Dynamin-like GTPase 1, MX1 (Liddelow et al., 2017). The unique combination of microglia-secreted interleukin-1 alpha (IL-1α), tumor necrosis factor-

alpha (TNFα), and complement component 1q (C1q) is required for the induction of A1 reactive astrocytes (Liddelow et al., 2017). Following excitotoxicity, A1 reactive astrocytes contribute to neuronal and oligodendrocyte cell death to promote extensive remodeling of neuronal circuitry. However, if the A1 astrocyte phenotype persists, there can be deleterious effects on synapses and subsequent neuronal function through pro-inflammatory response and neurodegeneration (Pekny et al., 2014). By contrast, the A2 reactive astrocyte subtype is anti-inflammatory and neuroprotective. A2 reactive astrocytes can be induced following ischemia, which results in the transient upregulation of neurotrophic factors, promoting neuronal survival and synaptogenesis (Liddelow et al., 2017). A2 reactive astrocytes are identified by the expression of the S100A10 astrocyte-related gene, which is essential for cell proliferation, membrane repair, and inhibition of apoptosis (Liddelow et al., 2017). A2 astrocytes release TNFα, which acts as an anti-inflammatory cytokine via inhibiting inflammatory cytokines such as IL-12p40 (Zakharova & Ziegler, 2005), contributing to A2 astrocyte synaptogenic and neuroprotective properties (Liddelow et al., 2017). Both A1 and A2 reactive astrocytes are essential in CNS recovery and restoration after injury or insult. Still, the specific pathways underlying A1 and A2 activation remain a primary research focus as we do not know how or if there is a direct link between the two reactive subtypes.

Emergent evidence has revealed that substance misuse can result in reactive astrogliosis, including modification of astrocyte morphology and function through various processes (Lasic et al., 2019; Lee et al., 2016). Substance use can disrupt neuronal circuits by triggering astrocytic changes like those observed in aging, injury, and disease models. Our laboratory has observed long-term perturbations in the reactive astrocyte A2 phenotype, further implicating a role for astrocytes in the studies examining the consequences of AIE on the CNS. These findings suggest

that astrocytes take on a neuroprotective phenotype in response to EtOH exposure. However, these EtOH-induced changes in astrocyte morphology and function may also contribute to long-term cognitive deficits due to EtOH-induced changes in PAP-synaptic interactions and astrocyte function at the synapse. This dissertation tests our hypothesis that AIE results in acute and chronic changes in astrocyte morphology, PAP-synaptic interactions, and astrocyte function at the synapse that differ across brain regions and sexes. To test this hypothesis, we have addressed the following specific aims: 1) determine how AIE influences astrocyte morphology and PAP-synaptic interactions in the male PFC and the hippocampus of male and female rats and 2) determine how AIE induces changes in neuronal-astrocyte communication in the hippocampus in adult male and female rats.

Conclusions

Adolescence is a critical time of neurodevelopment that involves the maturation and refinement of key brain regions, such as the PFC and hippocampus, essential for higher-order executive function. Adolescent neurodevelopment transitions the brain from youth to an adultlike state by refining circuitry within these regions and strengthening their connectivity to other regions. Due to this ongoing maturation and refinement, the adolescent brain is particularly vulnerable to the cytotoxic effects of substance use and misuse. Alcohol consumption in the form of binge drinking is prominent among adolescents and emerging adults, resulting in long-term cognitive deficits and an increased risk of alcohol use disorders (AUDs) later in life. While research has been ongoing to determine the effects of alcohol exposure on neurons, the field is still investigating how astrocytes contribute to the neuronal deficits previously observed in animal models. In the following few chapters, I will review current knowledge of alcohol use and adolescent development of the PFC (Chapter 2) and the hippocampus (Chapter 3). The

8

following chapter represents our most recent publication demonstrating temporal and regional effects of AIE on astrocyte morphology and astrocyte-synaptic interactions across the PFC (Chapter 4). Lastly, I will end with our current research, investigating how AIE impacts astrocyte morphology and function, astrocyte-synaptic interactions, and subsequent neuronal function and behavior in the female and male hippocampus (Chapters 5 and 6, respectively). This dissertation provides insight into the roles of astrocytes in AIE-induced neuronal and non-neuronal dysfunction and provides a novel non-neuronal target for therapeutic interventions.

Chapter 2

The Prefrontal Cortex and Adolescent Development

This chapter will explore the effects of adolescent alcohol exposure on the developing PFC. We will begin by discussing the anatomy and connectivity of the PFC and how maturation continues throughout adolescent development. Then we will explore the acute and chronic consequences of adolescent alcohol exposure on PFC structure and function. This discussion will incorporate findings from human and animal models to provide an overview of the current field that will inform future investigations into the neurobiological effects of adolescent alcohol consumption.

Adolescent Development

The human and rodent PFC continue to undergo structural and functional neuronal refinement during adolescence which is influenced by external experiences and neurobiological factors that work together to shape normal brain development and permanently alter behavior (Asato et al., 2010; Bourne & Harris, 2008; Cressman et al., 2010; Cunningham et al., 2002; Liston et al., 2006; Markham et al., 2007; Matsuzaki, 2007). This ongoing developmental period is suggested to be a time of increased vulnerability to AIE-induced neuronal disruption.

Adolescence is a fascinating period that spans puberty and early adulthood and coincides with the emergence of many higher-order, complex cognitive abilities. This critical developmental period for the PFC is akin to the early developmental period seen within the visual (Wiesel & Hubel, 1963) and language systems (Penfield & Roberts, 1959). Interestingly, adolescence is characterized by distinct cognitive development, driven by specific neurobiological changes, and dependent on many external factors (Blakemore & Mills, 2014; Steinberg, 2008). The transition from seeking parental approval to seeking peer approval

10

emerges during this period. When combined with increased freedom, it leads to a richness of novel experiences and provides an opportunity to participate in more risk-taking behaviors (Dahl, 2004).

Developmental studies have shown that during adolescence, there are brain areas in which loss of gray matter is evident (Gogtay et al., 2004), while an increase in white matter density is observed in other regions (Simmonds et al., 2014) along with synapse proliferation, indicating a significant period of plasticity and neurodevelopment (Bourgeois et al., 1994; Huttenlocher, 1990; Petanjek et al., 2011). Plasticity during critical periods of development (i.e., adolescence) results in reliable and efficient neuronal circuit communication, allowing for robust and optimized cognitive and behavioral outputs in response to a multitude of stimuli and task demands (Knudsen, 2004). In essence, time-dependent neuronal maturation during this critical adolescent developmental period adapts an individual to their surroundings by using experiences to refine neuronal circuits to navigate the demands of their environment.

Once a circuit has become efficient and reliable, the circuit is stabilized to prevent excessive pruning and circuit rewiring. Refined circuits are sculpted by the experiences of the individual in order to be ideally suited to respond to the demands of their environment (Takesian & Hensch, 2013). Critical periods of development are heavily influenced by experience-dependent neuronal activity that engages circuits that will mature and stabilize over time. For example, projections from the hippocampus and amygdala compete for targeted innervation of the PFC during adolescence. This was demonstrated by Guirado and colleagues (2016) when they lesioned the ventral hippocampus at postnatal day (PND) 7 in rats and then allowed the animals to grow to adulthood (PND 70). By adulthood, there was an increase in basolateral

amygdala innervation of the ventral mPFC due to the lesion-dependent loss of ventral

hippocampal competition (Guirado et al., 2016).

Critical periods of development progress in a hierarchical fashion; they start from

primary sensory areas (visual and auditory) and progress to regions of the cortex involved in

higher-order executive function necessary for complex cognition (Takesian & Hensch, 2013;

Toyoizumi et al., 2013). Areas integrating multisensory information to perform higher-order

cognitive functions require stable inputs from multimodal processing streams to drive

experience-dependent development and maturation. These experience-dependent changes in

neuronal architecture are partly due to changes at the receptor biology level. NMDA receptors

(NMDARs) are ionotropic glutamate receptors that are critical for synaptic plasticity, triggering

both long-term potentiation (LTP) and long-term depression (LTD) that contribute to memory

formation (Hunt & Castillo, 2012). During adolescence, excitatory neurons change NMDAR

subunit composition, influencing overall excitatory function. Expression of the NMDAR NR3A

subunit, which inhibits NMDA-regulated plasticity and prevents synaptic maturation peaks in

early development and decreases throughout adolescent development (Das et al., 1998; Henson

et al., 2008; Roberts et al., 2009). In contrast, expression of the NR1 subtype, which is critical in

experience-related plasticity of corticostriatal circuits, peaks, and plateaus in the PFC during this

developmental period (Das et al., 1998; Henson et al., 2008; Santos et al., 2015). This shift in the

ratio of NR1 and NR3A NMDAR subtypes is essential for activity-dependent plasticity and

maturation and can be considered a defining characteristic of adolescent neuronal development.

There is also evidence of increased NR2B-driven plasticity during adolescence (Morales

& Spear, 2014). This increase in the NR2B subtype is associated with longer-lasting excitatory

postsynaptic currents (EPSCs) of the mPFC layer V pyramidal cells in response to hippocampal

input, facilitating LTP-driven plasticity (Flores-Barrera et al., 2014). The emergence of hippocampus-to-PFC circuitry during adolescence further emphasizes that the shift in context-dependent plasticity is a key characteristic of adolescent development (Murty et al., 2016).

All developmental periods are partly driven by experience, but the nature of the experience necessary to optimally drive developmental neuronal plasticity varies according to region-specific function. To promote plasticity in PFC regions critical for complex cognitive function, experiences that engage higher-order cognitive processes are necessary. Experiences that engage the PFC during adolescence include increased exploration, independence, socialization, sensation-seeking, sexual maturation, and mating behaviors. As these experiences increase in complexity (and as adolescents are increasingly responsible for navigating these experiences without parental instruction), brain areas like PFC that support increasingly complex behaviors, such as socioemotional processing, planning, reasoning, and abstract thought, must be engaged and specialized to meet the demands of the environment. As such, increasingly complex adolescent experiences are the optimal input to drive experience-dependent plasticity. For example, it has been shown in rats that complex peer-peer social interaction and cognitive flexibility peaks during adolescence and is mediated by the mPFC, which is in turn strengthened by these interactions (Bell et al., 2010; Himmler et al., 2013; Panksepp, 1981; Spinka et al., 2001; van Kerkhof et al., 2013). Similarly, sexual experience leads to greater spine density within the PFC and enhanced cognitive flexibility in the rat (Glasper et al., 2015).

While outside the scope of this chapter, it is also essential to note that there are sex differences in the development and maturation of the PFC. Although the basic neural systems involved in positive and negative reinforcement and PFC-dependent behavioral control are similar in males and females, sex differences have been observed in PFC organization, activation

patterns, and anatomical connectivity (Murray et al., 2021; Nephew et al., 2020). These differences are thought to underlie sex-specific brain responses to experiences such as stress and drug exposure and sex-dependent vulnerabilities to the development of alcohol and substance misuse.

Histology of the Prefrontal Cortex

The PFC is a region of 6 laminae defined based on cellular composition and input and output circuitry (for review, see (Akkoc & Ogeturk, 2017)).

- Layer I – Lamina zonalis (molecular layer): This layer, located on the surface of the cortex, contains mainly apical dendrites of the pyramidal cells from layers III and V and projections from the thalamic nuclei. Here resides a small concentration of Cajal-Retzius neurons that have excitatory effects on the resident pyramidal cells.

- Layer II – Lamina granularis externa (external granular layer): This layer primarily consists of inhibitory basket cells interspersed with small pyramidal cells. The basket cells of layer II exhibit a significant inhibitory effect on layer III pyramidal neurons.

- Layer III – Lamina pyramidalis externa (layer of pyramidal cells): This layer contains loosely arranged medium-sized pyramidal neurons that receive information from stellate interneurons from layer IV as well as thalamocortical projections. Commissural fibers projecting to the contralateral hemisphere and fibers leading to the ipsilateral cortex arise in layer III.

- Layer IV – Lamina granularis interna (internal granular layer): This layer has the highest number of cells and is composed mainly of stellate, pyramidal neurons, and granular cells. The majority of the thalamocortical projections terminate here.

- Layer V – Lamina pyramidalis interna (large pyramidal cell layer): This layer has the least number of cells compared to the other laminae. Layer V consists of well-developed, large (sometimes called giant) pyramidal neurons that project to the basal ganglia.

- Layer VI – Lamina multiformis (layer of fusiform or polymorphic cells): As the name suggests, this layer consists of an assortment of different cells (Martinotti cells, fusiform cells, and pyramidal cells) which can influence neuronal activity from other laminae. This is also the location of axons that comprise the corticothalamic pathway.

The primary source of projecting circuits of the cortex is found in layers V and VI. Projections to the striatum, tectum, reticular formation, mesencephalon, medulla oblongata, and spinal cord arise from layer V. Projections to the thalamus arise from layer VI.

Anatomy of the Prefrontal Cortex

The PFC consists of multiple subregions that are associated with the modulation of specific behaviors.

Anterior Cingulate Cortex

The ACC is the frontal part of the cingulate cortex that resembles a collar surrounding the frontal part of the corpus callosum in the human brain. The anatomy of the ACC can be divided into dorsal and ventral components, which are associated with cognitive and emotional behaviors, respectively (Bush et al., 2000). The ACC has been implicated in a range of behaviors. Most notably, the ACC plays critical roles in fundamental cognitive processes such as motivation, learning, empathy, impulse control, emotion, cost-benefit association, decision-making, as well as conflict and error monitoring (Bush et al., 2000; Holroyd & McClure, 2015; Holroyd & Yeung, 2012; Kolling et al., 2016; Laubach et al., 2015; Rushworth et al., 2012; Shackman et al., 2011; Shenhav et al., 2013; Ullsperger et al., 2014; Verguts et al., 2015).

Disruption of the ACC is associated with psychopathology and emotional dysregulation (Stevens et al., 2011).

Medial Prefrontal Cortex

Like the ACC, the mPFC can be divided into dorsal and ventral areas with associated behaviors. The dorsal mPFC is more associated with complex cognitive operations, while the ventral region is more closely associated with emotional behaviors (Bush et al., 2000; Morris et al., 1999; Ongur & Price, 2000; Paus, 2000; Petrides & Pandya, 1999). The mPFC comprises the prelimbic cortex (PL) and infralimbic cortex (IL). These two subregions are strongly associated with the activation and suppression of fear circuits, respectively (Laurent & Westbrook, 2009; Sotres-Bayon & Quirk, 2010).

Orbitofrontal Cortex

The OFC receives inputs from sensory cortices about taste, smell, and touch, as well as auditory and visual stimuli (Rolls, 2019; Rolls et al., 2020). Direct outputs from the OFC project to the cingulate cortex, striatum, and inferior frontal gyrus, with indirect connectivity to the brainstem via the habenula (Rolls, 2019; Rolls et al., 2020). The OFC is associated with sensory integration and modulation of visceral reactions, participation in learning, and decision-making for emotional, adaptive, and goal-directed behavior (Rolls et al., 2020). Within the OFC, the lateral (sometimes referred to as the ventrolateral (LO-OFC)) and ventral (VO-OFC) aspects appear to have diverging roles. The LO-OFC is involved in obsessive-compulsive behavior (Lei et al., 2019) and decision-making through the integration of immediate prior information and current information (Nogueira et al., 2017), while the VO-OFC appears to be involved in value assessment in tasks such as delayed discounting (Jobson et al., 2021).

Damage or degeneration of the PFC can manifest as a deficit in impulse control, poor performance on tasks that require long-term planning, blunted emotional responses, aggression, and irritability (Wood & Worthington, 2017). Therefore, it is unsurprising that PFC dysfunction has been implicated in many human psychiatric disorders, the emergence and persistence of drug and alcohol use, and as a predictor of increased risk of drug and alcohol relapse (Camchong et al., 2013).

Alcohol and the Prefrontal Cortex

Adolescence is the developmental period in which many psychiatric disorders emerge, some characterized by deficits in higher-order cognition, including substance use disorder, schizophrenia, depression, and anxiety disorders (Paus et al., 2008). Though treatments are available, and recovery is possible, many of these disorders typically persist throughout the lifespan (Davydov et al., 2010; Demyttenaere et al., 2004; Jaaskelainen et al., 2013). This suggests that while cognitive functions are normatively refined during adolescence, the enhanced plasticity of cortical circuits may present a window of vulnerability to abnormal neurodevelopment following toxic insults with long-lasting and potentially severe consequences. Evidence from human literature and animal models of adolescent alcohol use supports this. However, whether the impact of alcohol use on neuronal development and maturation during adolescence is PFC-subregion specific is unknown. Significant work has been conducted to determine the impact of adolescent alcohol on neuronal development within the ACC (Mashhoon et al., 2014) and mPFC (Abernathy et al., 2010). However, the contributions of the OFC subregions have not been fully explored. Taken together, these data provide a rationale for continued investigation into how adolescent alcohol exposure: 1) impacts PFC structural and functional development, 2) contributes to the emergence of long-term PFC-dependent

neurological deficits, and 3) contributes to the increased probability of developing an alcohol use disorder later in life.

Using an animal model of adolescent intermittent ethanol (AIE) exposure, a standard approach in the field to replicate adolescent binge drinking in humans, Broadwater et al. (2018) showed that AIE perturbed resting-state connectivity using functional MRI connectivity between OFC-striatum and OFC-nucleus accumbens in rats, that persisted into adulthood (Broadwater et al., 2018). These findings correlate with multiple studies demonstrating AIE-induced deficits in PFC-dependent behaviors, such as behavioral flexibility, increased disinhibition, and increased propensity to self-administer EtOH. Once again, all of these deficits persisted into adulthood (Broadwater et al., 2018; Coleman et al., 2011; Coleman et al., 2014; Supekar et al., 2010), suggesting long-term changes to neuronal function. However, growing evidence shows that behavioral outputs heavily rely on astrocyte modulation of neuronal function. This has been demonstrated in several studies using designer receptors exclusively activated by designer drugs (DREADDs) that specifically target astrocytes and result in subsequent modulation of rodent behavior (for review, see (Gass et al., 2014)). Erickson and colleagues conducted one study of particular importance (Erickson et al., 2021). They showed that activation of astrocyte-specific excitatory DREADDs within the PFC (IL, PL, and ACC combined) can contribute to regulating EtOH consumption, supporting a critical role for astrocytes in behaviors associated with substance misuse. Taken together, these data provide a rationale for continued investigation into how adolescent alcohol exposure: 1) impacts PFC structural and functional development, 2) contributes to the emergence of long-term PFC-dependent neurological deficits, and 3) contributes to the increased probability of developing an alcohol use disorder later in life.

Conclusion

In this chapter, we have provided an overview of the histology and neuroanatomy of the PFC and discussed the current state of knowledge on the effects of EtOH in adolescent human and adolescent rodent models. While not overly discussed, it is essential to note that the field is beginning to acknowledge that non-neuronal cells, such as microglia and astrocytes, contribute to neuronal function and dysfunction. Moving forward, it will be essential to continue to include these non-neuronal targets to garner a more complete and accurate picture of the effects of EtOH use on adolescent development and EtOH-induced neuronal dysfunction.

Chapter 3

The Effects of Peri-Adolescent Alcohol Use on The Developing Hippocampus

C.D. Walker[1], C.M. Kuhn[3], M-L. Risher [1,2]

[1]Department of Biomedical Research, Joan C Edwards School of Medicine Marshall University,

Huntington, WV, USA

[2]Neurobiology Research Laboratory, Hershel Woody Williams Veteran Affairs Medical Center,

Huntington, WV, USA

[3]Department of Pharmacology and Cancer Biology, Duke University Medical Center, Durham

NC, USA

Author Note

Abstract

    Adolescence is a period of continued brain development. Regions of the brain, such as the hippocampus, continue to undergo refinement and maturation throughout adolescence and into early adulthood. Adolescence is also a time of heightened sensitivity to novelty and reward, which contribute to an increase in risk-taking behaviors including the use of drugs and alcohol. Importantly, binge drinking is highly prevalent among adolescents and emerging adults. The hippocampus which is important for the integration of emotion, reward, homeostasis, and memory is particularly vulnerable to the neurotoxic effects of alcohol. In this chapter, we cover the fundamentals of hippocampal neuroanatomy and the current state of knowledge of the acute and chronic effects of ethanol in adolescent humans and adolescent rodent models. We focus on the hippocampal-dependent behavioral, structural, and neurochemical changes and identify knowledge gaps in our understanding of age-dependent neurobiological effects of alcohol use.

Binge drinking is highly prevalent among adolescents and emerging adults. One in six adolescents in the United States have participated in binge drinking (Chung et al., 2018). Growing evidence from studies in humans reveals that alcohol use is associated with acute and long-term deficits across several domains of cognition including verbal and non-verbal skills, attention, visuospatial function, and learning in which the hippocampus is critical (Brown et al., 2000; Chin et al., 2010; Hanson et al., 2011; Tapert and Brown, 1999). Furthermore, studies in both humans and rats have shown that adolescents and young adults are more vulnerable to alcohol-induced memory impairment than older subjects, while effects on motor function are relatively minimal (Acheson et al., 1998; Land & Spear, 2004; Little et al., 1996; Markwiese et al., 1998; Spear, 2000).

This chapter will explore the consequences of drinking on the hippocampus during adolescence. We will begin by discussing hippocampal architecture, interconnectivity, and how this region critical for learning and memory continues to develop and refine throughout this time period. We will then consider how the structure and function of the hippocampus may be disrupted by the acute and chronic effects of adolescent ethanol (EtOH) exposure. This discussion will incorporate findings from neuroimaging, behavior, circuits, and synapses in order to provide a thorough overview of the current state of the field and potentially inform future investigations into the neurobiology of adolescent drinking.

Hippocampus Anatomy and Adolescent Development

Anatomy of the Hippocampus

The sixteenth century anatomist, Julius Caesar Arantius coined the term 'hippocampus', derived from the Greek word for sea horse, because of the region's unique architecture (Arantius, 1587). While this is the term we use today, there were several other anatomists who attempted to

define this region with their own terminology. Some described the region as reminiscent of a ram's horn. This led to De Garengeot naming the hippocampus 'cornu ammonis' or 'Ammon's horn' after the Egyptian god Amun Kneph whose symbol was a ram (RJC, 1742). While the term 'hippocampus' remains the official name for this region of the brain, conru ammonis or CA is used to denote some hippocampal subregions.

Figure 1
Interconnectivity Between the Hippocampal Subregions. Perforant Path Fibers Innervate the Mossy Fibers of the Dentate Gyrus.
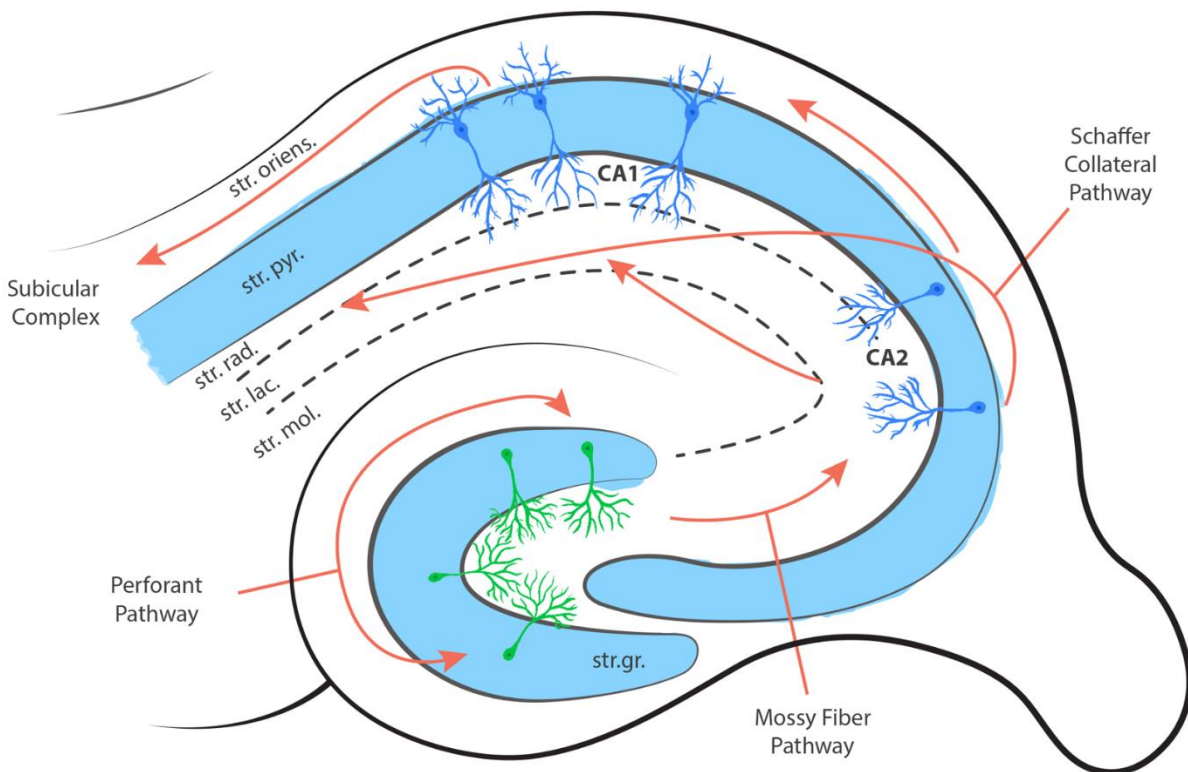
The mossy fibers project to the apical dendrites of in the stratum luciderm of the CA3. The Schaffer collateral pathway projects from the pyramidal neurons of the CA3 to synapse with the pyramidal neurons of the stratum radiatum, lacunosum, and moleculare. CA3 Schaffer collaterals also project to CA1 pyramidal neurons in the stratum oriens. The subicular complex is the major output from the hippocampus and contains projections from the CA1 stratum oriens. From "The Effects of Peri-Adolescent Alcohol Use on The Developing Hippocampus," by C.D. Walker, C.M. Kuhn, and M-L. Risher, 2021, *International Review of Neurobiology, 160*, p. 254 (https://doi.org/10.1016/bs.irn.2021.08.003). Copyright 2021 by Elsevier Inc. Reprinted with permission.

The hippocampus is an elegantly laminated region of the brain that has precise and complex connectivity (Figure 1). The hippocampus is divided into distinct subregions, the CA1, CA2, CA3, CA4, and dentate gyrus that differ in cellular composition and neuronal connectivity. The CA2 field is a narrow zone of cells interposed between the CA3 and CA1 and consists of large pyramidal cell bodies similar to those in the CA3. The principal 'granule' cells of the dentate gyrus give rise to axons called mossy fibers that synapse onto pyramidal cells of the CA3 field of the hippocampus. The CA3 pyramidal cells are the source of major input to the CA1 hippocampus via the Schaffer collateral axons. Neurons within the CA1 hippocampus then project to the subiculum, providing major excitatory input to the entorhinal cortex. The CA4 is often called the hilus or hilar region and is considered part of the dentate gyrus. Unlike the pyramidal neurons in the CA1 and CA3, the neurons here include mossy cells that primarily receive inputs from the granule cells in the dentate gyrus.

The CA subregions of the hippocampus are further divided into laminated strata, the stratum oriens (str. oriens), stratum pyramidal (str. pyr.), stratum luciderm (str. luc.), stratum radiatum (str. rad.), stratum lacunosum (str. lac.), and the stratum moleculare (str. mol.) (Figure 2). The striatum oriens is the most dorsal layer of the hippocampus. This region contains inhibitory basket cells that innervate the oriens, pyramidal, and radiatum strata. Next is the stratum pyramidal containing the pyramidal cell bodies, which are the primary excitatory neurons of the hippocampus. The stratum pyramidal of the CA3 contains synapses from mossy fibers as well as the cell bodies of interneurons. The stratum luciderm is found ventral to the stratum pyramidal in the CA3 and contains mossy fibers from the dentate gyrus. The stratum radiatum contains the Schaffer collateral fibers that project from the CA3 and innervate the CA1. The stratum lacunosum is a thin layer that also contains Schaffer collateral fibers as well as perforant path fibers from the

superficial layers of the entorhinal cortex (Figure 1). As this is such a thin layer, it is often grouped

together with the stratum moleculare and is referred to as the stratum lacunosum-moleculare (str.

l-m.). The stratum moleculare contains perforant path fibers that synapse onto the apical dendrites

of hippocampal pyramidal cells.

Figure 2
Laminated Strata Detailing the Lamination of the CA1 Hippocampus and Pyramidal Cell
Innervation.
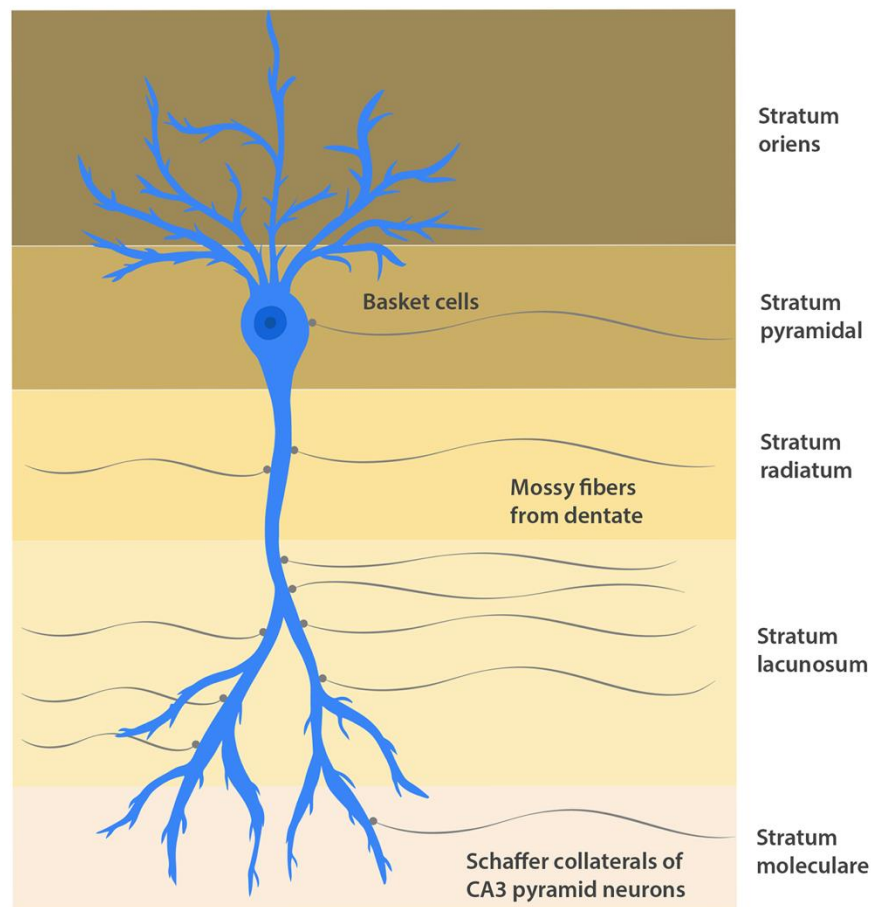
The stratum moleculare, stratum lacunosum, and stratum radiatum contains Schaffer collaterals from the CA3 and perforant path fibers. The stratum radiatum not only contains Schaffer collaterals from the CA3 pyramidal neurons, but also contains mossy fibers from the dentate. The stratum pyramidal contains the cell bodies of the pyramidal neurons in the CA1. The stratum pyramidal and stratum oriens contain inhibitory basket cells. From "The Effects of Peri-Adolescent Alcohol Use on The Developing Hippocampus," by C.D. Walker, C.M. Kuhn, and M-L. Risher, 2021, *International Review of Neurobiology, 160*, p. 262 (https://doi.org/10.1016/bs.irn.2021.08.003). Copyright 2021 by Elsevier Inc. Reprinted with permission.

Like the CA subregions of the hippocampus, the dentate gyrus has similar lamination. The most superficial layer of the dentate gyrus is the polymorphic layer (poly. lay.) and contains interneurons and the axons of the dentate's granule cells that synapse in the CA3. The next layer of the dentate gyrus is the stratum granulosum (str. gr.), which contains the granule cell bodies. The dentate's stratum molecular (str. mol.) is where commissural fibers from the contralateral dentate form synapses. This is also where perforant path fibers form excitatory synapses with distal apical dendrites of granule cells.

The hippocampus receives major afferents and sends major efferents to and from the entorhinal cortex (Figure 1), which is part of the medial temporal lobe. The entorhinal cortex acts as the gateway between the hippocampus and the parietal, temporal, and prefrontal cortex. The ventral hippocampus also receives direct inputs from the anterior cingulate cortex (ACC (Bian et al., 2019)) and sends direct outputs to the basolateral amygdala (Yang et al., 2016). It has reciprocal connections with the hypothalamus and receives major subcortical inputs from the medial septum (see (Muller & Remy, 2018) for review). Through this network of interactions, the hippocampus acts as an integrative hub for the limbic system and is critically involved in emotion, anger, reward, homeostasis, and memory.

Adolescent Development of the Hippocampus

The hippocampus has a highly organized architecture that undergoes continued maturation throughout adolescence (Gomez & Edgin, 2016). The World Health Organization has historically defined adolescence as being the period of time between the ages of 10 and 19 years of age (World, 2001). However, as further research is conducted, it has become appropriate to identify individuals 10-24 years of age as among the adolescent/emerging adulthood category (Sawyer et al., 2012). These individuals can be divided into early adolescence (10-14 years of age), late adolescence (15-

19), and young or emerging adulthood (20-24 years of age) (Sawyer et al., 2012). The adolescent time-period encompasses puberty, which typically occurs from 10 to 16 years of age in females and 11 to 17 years of age in males (Holder & Blaustein, 2014). In rats, adolescence spans from postnatal day (PND) 35 to PND ~60 (McCutcheon & Marinelli, 2009; Spear, 2000). Within that time span, puberty generally occurs between PND 28 and 42 in females and PND 42 and 49 in males (Holder & Blaustein, 2014). Rat adolescence is generally defined by the period in which they exhibit peak adolescent-typical neurobehavioral characteristics (Spear, 2000), the presence of an adolescent growth spurt, changes in neurotransmitter receptor expression, and the emergence of nest burrowing, some of which will be discussed further in upcoming segments of this chapter.

Behavioral maturation reflects the maturation of the underlying circuitry, making adolescence a transformative time of brain development. During childhood, synaptogenesis is active, resulting in an increase in peak brain volume in early adolescence followed by the pruning and refinement of synapses as well as axonal myelination throughout adolescence and into early adulthood. The latter processes are ultimately responsible for fine tuning the architecture of the brain. This adolescent period provides an opportunity for robust brain remodeling that can be heavily influenced by social, emotional, and environmental factors ((Griffin, 2017) for review). Substance use is one of the stimuli that can critically influence these final stages of brain maturation. This is particularly important when so many vital brain regions involved in drug-seeking and novelty seeking behaviors are undergoing complicated late-stage refinement. The hippocampus is one such area that shows distinct vulnerability to the acute and long-term effects of EtOH, as will be demonstrated in this chapter.

Figure 3:

Longitudinal Sections of a Human and Rat Brain Showing Similarities in Structure (However Proportionally Different) and Hippocampal Connectivity.
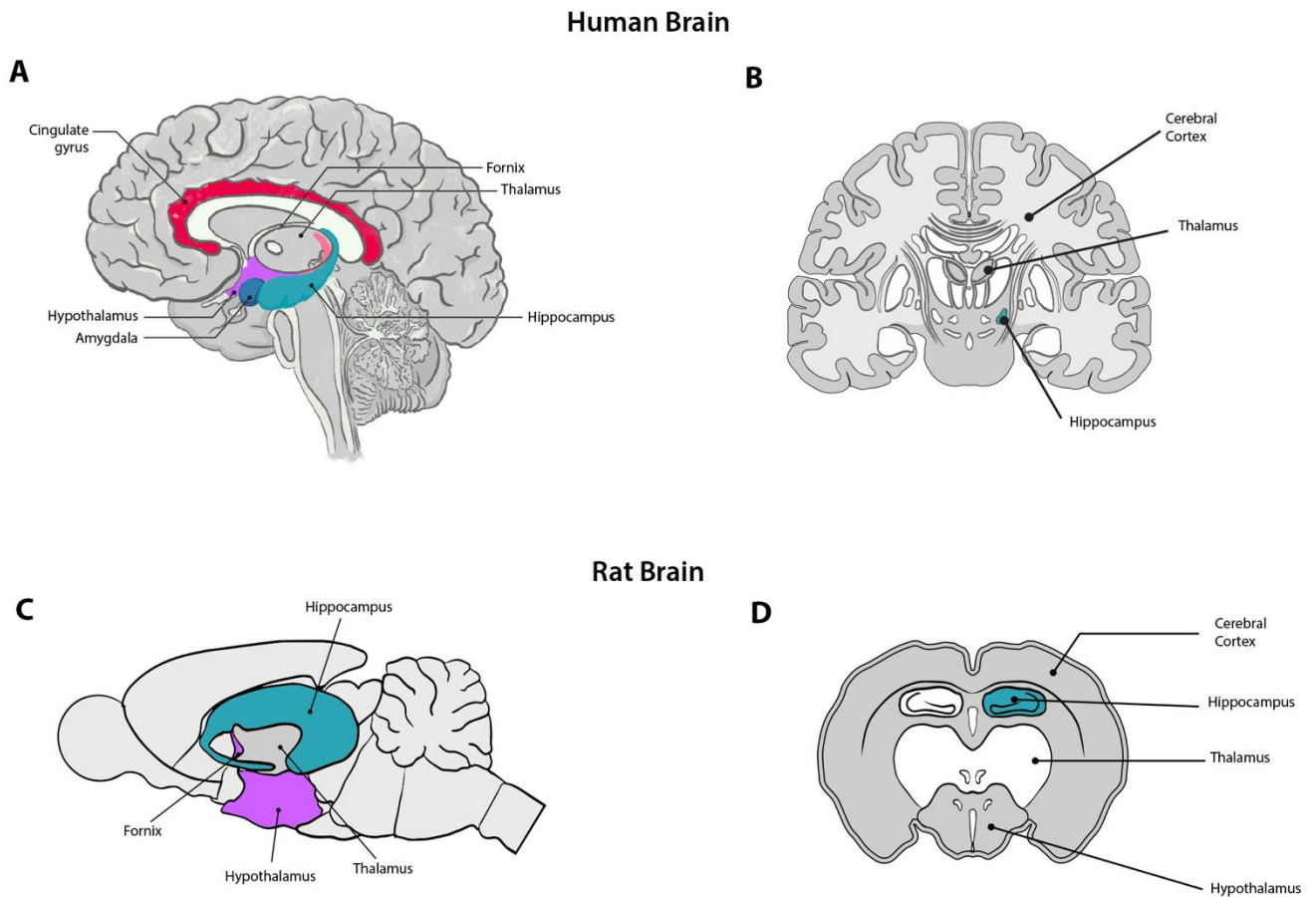
(A-B). Transverse section of a human and rat brain showing the structural similarities of the hippocampus in different locations within the brain. While the human and rat hippocampus have similar structures, function, and connectivity, the human hippocampus is located ventral, while the rat hippocampus is more dorsally located (C-D). From "The Effects of Peri-Adolescent Alcohol Use on The Developing Hippocampus," by C.D. Walker, C.M. Kuhn, and M-L. Risher, 2021, *International Review of Neurobiology, 160*, p. 256 (https://doi.org/10.1016/bs.irn.2021.08.003). Copyright 2021 by Elsevier Inc. Reprinted with permission.

The Effects of Alcohol on the Peri-Adolescent Hippocampus

Effects of Alcohol on Adolescent Hippocampal Structure and Connectivity

Understanding the underlying changes that occur specifically in response to adolescent alcohol use has become an emerging topic of interest because adolescence is a time in which substance and alcohol use are escalating and, in some cases, reaching peak consumption. These events may also impact the development of various brain regions through alcohol-induced changes in hippocampal efferent innervation.

Magnetic resonance imaging (MRI) imaging studies have revealed that frontal lobes, limbic system, and cerebellum have unique vulnerabilities to degeneration as demonstrated in adults with AUD. There is ample evidence that the hippocampus, in particular, is a prime target for alcohol toxicity. This is observed in both adults and adolescents with alcohol use disorders that show a reduction in hippocampal volume, which is accompanied by neuronal loss (De Bellis et al., 2000; Harper, 1998; Jernigan et al., 1991). No relationship has been found between loss of hippocampal volume and changes in total brain volume or intracranial volumes suggesting that the hippocampus may be particularly vulnerable to the detrimental effects of alcohol (Beresford et al., 2006).

Adolescents with chronic AUD show reduced hippocampal volume (De Bellis et al., 2000; Medina et al., 2007; Nagel et al., 2005). Recent work using MRI looked more specifically at hippocampal subregions. This study assessed the effects of alcohol and lifetime psychological trauma on hippocampus and amygdala development during adolescence in 803 male and female participants from 12 to 21 years of age. The participants completed questionnaires to identify drinking behaviors and lifetime psychological trauma. Phillips et al. (2021) observed smaller whole hippocampus, smaller left hippocampus tail volumes, larger right CA3 head, and larger left subiculum volumes in participants with greater alcohol consumption (Phillips et al., 2021). They also observed an interaction between adolescents who reported greater alcohol use with

greater psychological trauma. These participants showed smaller right hippocampal CA1 head and hippocampal head but larger whole hippocampus volume overall. While this study did not parse out the differences in hippocampal volume of males and females, it has been well established that there are sex specific effects of alcohol on cortical gray and white matter (Pfefferbaum et al., 2001). Moreover, it is not clear if the reduced hippocampal volume observed in heavy drinkers is a result of excessive alcohol use or demonstrates a genetic predisposition to the development of excessive, heavy drinking. Animal models provide an opportunity to investigate these nuances.

Ehlers et al. (2013) addressed the question of whether EtOH exposure directly influences hippocampal size using adolescent male Wistar rats. Animals were exposed to intermittent EtOH vapor for 35 days (PND23-58) so they would reach an average BEC of 169mg/dl (Ehlers et al., 2013). Two weeks and 10 weeks following EtOH exposure animals were assessed for changes in hippocampal volume using diffusion tensor imaging (DTI) to measure axonal organization (i.e. white matter). At the earlier timepoint (PND72) there was no change in hippocampal volume. However, at the later timepoint (PND128) rats exposed to EtOH exhibited smaller hippocampal volume when compared to age-matched controls, suggesting a delayed loss of hippocampal volume. This study showed hippocampal growth between PND72 and PND128 in control animals, as indicated by an increase in total hippocampal volume, suggesting ongoing hippocampal development well into the typical "adult" age range. This is consistent with previous MRI studies conducted in alcohol-preferring rats (P-rats) in which hippocampal and whole-brain volume continued to increase until PND400 and 450, respectively, and was most prominent in the dorsal hippocampal region when compared to other hippocampal sub regions (Sullivan et al., 2006). It was observed that EtOH exposure reduced hippocampal volume in

30

PND128 rats to the equivalent of PND72 EtOH-naïve rats, leading us to question whether chronic EtOH exposure results in a decrease in hippocampal volume through cell death pathways or simply disrupts the normal developmental maturation and impedes the corresponding increase in hippocampal volume.

Ehlers and colleagues (Ehlers et al., 2013) paired the imaging studies with a behavioral test called prepulse inhibition (PPI), a measure of sensory gating. The authors found a significant correlation between hippocampal volume loss and deficits in PPI. This is consistent with correlations that have previously been made between PPI response and hippocampal volume using MRI volumetric studies conducted in normally developing rats (Schubert et al., 2009) as well as pharmacologic manipulation of hippocampal cholinergic signaling (Caine et al., 1992). A follow-up study was conducted by Vetreno and colleagues (Vetreno et al., 2016), using DTI in a model of adolescent intermittent EtOH exposure to assess long-term effects on brain structure, volume, and integrity at PND80 and PND220, 25 and 165 days after the last EtOH dose, respectively. There was a reduction in the magnitude and directionality of water movement parallel to axons (axial diffusivity) in EtOH exposed rats that emerged by PND220. This type of measure, also known as fractional anisotropy, provides information regarding axon density and myelination ((Beaulieu, 2002) for review). Radial diffusivity, which measures water movement perpendicular to axonal fibers and can suggest demyelination or impairment of glia cell activity, was not significantly reduced at either PND80 or PND 220. These imaging studies were paired with behavioral measures including object recognition, open field, and light-dark box to assess anxiety that were conducted between imaging timepoints. The studies demonstrated a positive correlation between EtOH-induced deficits in object recognition and axial diffusivity. This is consistent with human studies in which decreased axial diffusivity is associated with deficits in

31

cognitive performance (Grieve et al., 2007). More specifically, in these animal studies they observed that lower axial diffusivity in EtOH animals was associated with diminished performance on the object recognition task (Vetreno et al., 2016).

Effects of Ethanol on Adolescent Hippocampal-Dependent Behavior

Acute Effects of Ethanol on Adolescent Hippocampal-Dependent Behavior. The acute effects of EtOH on cognition are primarily mediated through the disruption of hippocampal function. Acute EtOH exposure in humans results in impaired hippocampal-dependent learning and memory processes ((Mira et al., 2019) for review). Work by Weissenborn and Duka (Weissenborn & Duka, 2003) demonstrated that college-age students (18-34 years of age) with a history of binge-pattern drinking performed worse on memory tasks while intoxicated when compared to non-binge counterparts. Acheson et al., 1998 (Acheson et al., 1998) took this one step further by narrowing the age range and assessing the acute effects of alcohol (0.6 g/kg) on the acquisition of semantic and figural memory in young adults from 21 to 29 years of age. Intoxicated subjects 21-24 years of age had significantly more impaired immediate and delayed recall than those within the 25-29 age group, suggesting a critical period of heightened sensitivity to the cognitive-impairing effects of alcohol. These effects are not unique to the hippocampus, as there are also age dependent lack of sensitivities to the sedating effects and motor impairing effects of alcohol as well as an increased sensitivity to the social facilitating effects of alcohol that likely contribute to the increased consumption typically observed in this younger age.

Rodent models that recapitulate these findings have allowed researchers to look beyond the role of genetic background and the contributions of environmental stressors and look more specifically at adolescent responsiveness to acute and chronic EtOH exposure during

developmental stages that align with the time when heaviest drinking occurs (late teens to early twenties in humans) and when excessive alcohol consumption has been associated with an increased likelihood of developing an alcohol use disorder (Caspi et al., 2002). These are described below.

In the traditional hippocampal-dependent learning and memory task, the Morris Water Maze, acute EtOH intoxication produced by administering 1.0 or 2.0 g/kg EtOH to rats prior to task training impaired learning (spatial memory acquisition) when compared to age-matched vehicle-treated controls. These impairments in learning were much more robust in adolescent versus adult rats (Markwiese et al., 1998), suggesting an increased sensitivity to the memory impairing effects of EtOH in adolescence. Land and Spear (2004) showed that EtOH (0, 0.5, or 1g/kg, ip) administration impaired performance in an odor discrimination task (animals dug in scented sand for a cereal reward) in adolescent, but not adult Sprague Dawley rats. Further testing revealed that this difference was not due to changes in taste or odor aversions but was attributed to the strong EtOH effects on adolescent memory (Land & Spear, 2004). Studies have also revealed other, non-hippocampal-dependent, and age-dependent differences in response to acute EtOH such as reduced sensitivity to the sedating effects (Silveri & Spear, 1998) and motor impairing (Little et al., 1996; White et al., 2002), and increased sensitivity to the social facilitating effects of EtOH (Varlinskaya & Spear, 2002) in adolescent rats when compared to adults. Combined, these findings demonstrate unique adolescent characteristics of acute EtOH intoxication when compared to adults across a wide range of behavioral measures in predominantly male rats. Further work is necessary to characterize these behavioral changes in a sex-dependent manner following acute EtOH exposure.

Chronic Effects of Ethanol on Adolescent Hippocampal-Dependent Behavior.

Parallels are beginning to emerge between human findings and rat models (Figure 3) of binge drinking (or chronic intermittent EtOH exposure) that are consistent across laboratories (Crews et al., 2019; Spear & Swartzwelder, 2014). Multiple studies have demonstrated long-term, selective, hippocampal-dependent changes in response to chronic intermittent EtOH exposure that has been observed in humans ((Crews et al., 2016; Silvers et al., 2003) for review). In animal studies, in the radial arm maze, a task that relies heavily on hippocampal function, chronic EtOH exposure resulted in working memory deficits after a 67-day washout period but only after an acute EtOH challenge (1.5g/kg, i.p.) 30 minutes prior to the acquisition trial (Risher et al., 2013). However, there was a lack of spatial learning deficit using the Barnes maze following chronic EtOH exposure (Vetreno & Crews, 2012). Further work by Vetreno and Crews (Vetreno & Crews, 2015) demonstrated impaired novel object recognition in chronic intermittent EtOH exposed animals after an extensive washout period (PND163-165), suggesting task- and domain-selective sensitivity in the assessment of hippocampal-dependent function. The lack of spatial learning deficits in response to chronic intermittent EtOH exposure have also been observed in the Morris Water Maze which is a task often used in behavioral neuroscience to observe the psychological processes and neuronal mechanisms of spatial learning (Swartzwelder et al., 2015). However, when an additional challenge was added, such as EtOH challenge or more complex decision making was required, the Morris Water Maze revealed some interesting findings. Rats treated with EtOH demonstrated behavioral inefficiency in this task, as indicated by a prolonged path length to reach the stable invisible platform (Acheson et al., 2013). However, these modifications push this traditionally hippocampal-dependent task towards a more cortical/prefrontal cortex-reliant task in which reversal learning is required to navigate the

maze effectively. These laboratory studies are consistent with human studies that have revealed deficits in cognitive domains that rely heavily on hippocampal function, such as visuospatial construction (Hanson et al., 2011; Tomlinson et al., 2004), verbal learning and working memory (Hanson et al., 2011), and executive function (Giancola et al., 1998; Parada et al., 2012) in adolescents with AUD.

Some age-specific sensitivities appear to persist in human subjects (Sullivan et al., 2016). and rodent models following chronic intermittent EtOH exposure across the limbic system. Sullivan et al. (2016) observed decreased performance in accuracy and speed during cognitive testing of adolescent subjects with a history of alcohol consumption. These observations suggest that alcohol consumption can have a detrimental impact on decision-making in adolescent subjects. In animal studies, Varalinskaya et al., (2014) demonstrated that chronic EtOH exposure during adolescence preserves adolescent sensitivity to the social facilitating effects of alcohol into adulthood (Varlinskaya et al., 2014), while White et al., (2002) showed that adults exposed to chronic intermittent EtOH exposure in adolescence retained the adolescent lack of sensitivity to the motor impairing effects of alcohol. However, it should be noted that not all adolescent behavioral sensitivities are retained following chronic intermittent EtOH exposure. For example, adolescent rats are more sensitive to the rewarding effects of alcohol when compared to adults (Pautassi et al., 2008; Ristuccia & Spear, 2008), while the effects of chronic intermittent EtOH exposure in adolescence on adult sensitivity to the rewarding effects of EtOH are inconclusive. Some studies have reported increased EtOH consumption (Alaux-Cantin et al., 2013; Amodeo et al., 2018; Doremus et al., 2005; Pascual et al., 2009) and some have not (Broadwater et al., 2013; Gilpin et al., 2012; McBride et al., 2005; Nentwig et al., 2019). These differences may be due to the route of administration during adolescence and the type of self-administration paradigm

implemented particularly since rats do not like to self-administer high quantities of EtOH without the presence of sweeteners. Exposure to sweeteners during adolescence appears to influence drinking in adulthood only when paired with the familiar sweetener (Broadwater et al., 2013). A pressing question is whether the retention of adolescent behavioral and cognitive sensitivities (and lack of sensitivities) is due to delayed maturation of the neuronal circuitry or simply impairment that manifests with an immature phenotype.

Effects of Ethanol on Synapse and Synaptic Circuitry in the Adolescent Hippocampus

Acute Effects of Ethanol on Synapse and Synaptic Circuitry in the Adolescent Hippocampus. There is extensive literature characterizing the effects of alcohol on the dominant neurotransmitters in the hippocampus, GABA and glutamate. One "classic" effect of alcohol is its agonist activity at (some) GABA-A receptors. Combined with GABA subtype-specific sensitivity to the acute effects of EtOH ((Kumar et al., 2009) for review), it is evident that EtOH potently modulates excitatory:inhibitory balance at the synaptic level. Importantly, the effects of EtOH are not limited to glutamate and GABAergic modulation. EtOH actions span a diverse range of receptors and ion channels critical for hippocampal function either due to being located directly in the hippocampal region or due to projections such as those from the amygdala or to the cingulate gyrus ((Abrahao et al., 2017) for review).

It has been demonstrated that acute EtOH significantly reduces glutamate release in the dorsal hippocampus (Shimizu et al., 1998) and inhibits NMDA-activated ion currents in a concentration-dependent manner (Lovinger et al., 1989). Acute EtOH also inhibits long-term potentiation (LTP) in hippocampal slices (Blitzer et al., 1990; Morrisett & Swartzwelder, 1993), which is consistent with acute deficits in hippocampal-dependent memory processes (Shimizu et al., 1998). However, there are inconsistencies across studies (Fujii et al., 2008; Swartzwelder et

36

al., 1995). These differences may be due to the age of the animal, subregion assessed, or stimulus strength applied. More recent work demonstrates that these nuances may exist because acute EtOH blocks LTP in apical dendrites but only reduces LTP in basal dendrites (Ramachandran et al., 2015).

Chronic Effects of Ethanol on Synapse and Synaptic Circuitry in the Adolescent Hippocampus. The most concerning effects of adolescent alcohol exposure are those that persist into adulthood. In humans, these data are difficult to collect because it is difficult to quantitate exposure or eliminate other life circumstances. Rodent models have proved especially useful in probing these important outcomes. Adolescent rats exposed to a two-binge dose paradigm administered 9 hours apart developed short-term deficits in the hippocampal-dependent novel object recognition task that correlated with the abolishment of NMDA-R activity and impaired long-term depression (LTD) (Dong et al., 2013; Dong et al., 2012; Ge et al., 2010; Silvestre de Ferron et al., 2015). However, longer, more intermittent patterns of EtOH exposure, caused a different outcome on LTP measures. Following a 12-week EtOH liquid diet Fujii et al. (Fujii et al., 2008) showed decreased threshold for LTP when assessed within 24 hours of the final dose. This is similar to Sabeti and Gruol (Sabeti & Gruol, 2008), who demonstrated age-dependent changes in LTP in an EtOH vapor chamber model in rats 24 hour after the last exposure. However, none of these studies addressed the long-term effects of adolescent binge EtOH exposure, i.e., how adult hippocampal circuit function is changed following adolescent exposure. Work by Risher et al., (Risher, Fleming, et al., 2015) addressed that question using a rat model of adolescent intermittent EtOH exposure in which rats received 5g/kg of EtOH intermittently over 16 days via gastric gavage. Similar to Fujii et al (Fujii et al., 2008), they demonstrated that adolescent rats exposed to EtOH had a lowered threshold for LTP when compared to age-

matched controls that persisted 26 days after the final dose of EtOH, in adulthood (Risher, Fleming, et al., 2015). These data suggest the persistence of more responsive/plastic CA1 hippocampal circuitry that is reminiscent of the plasticity that is typically observed in adolescent hippocampal slices (Swartzwelder et al., 1995). It would be tempting to hypothesize that the lowered threshold for LTP (a physiological representation of learning) would make learning easier, however based on the behavioral data collected by various groups, it more likely reflects an inability to filter unnecessary information that could theoretically make decision making more difficult. This is best demonstrated in results of the modified version of the Morris Water Maze task in which rats were assessed for behavioral efficiency (discussed above) (Acheson et al., 2013).

LTP also results in changes in dendritic spine morphology, typically resulting in enlargement of the spine head and spine neck that coincides with spine neck shortening (Harris et al., 2003). This structural change has been referred to as the transition from a 'learning spine' into a 'memory spine' (Harris et al., 2003), resulting in a shift from a more plastic, immature spine type to a more mature, stable spine. The importance of dendritic spines to overall neuronal excitability has generated interest in how neuronal structures could change in response to adolescent EtOH exposure. Using the adolescent intermittent EtOH exposure gavage model in rats, recent work has demonstrated that there is a corresponding shift towards an immature dendritic spine phenotype and a reduction in mature dendritic spine number in CA1 pyramidal neurons in adulthood with no overall reduction in spine density (Risher, Sexton, et al., 2015), suggesting that there is more plasticity and less stability in dendritic spines following adolescent EtOH exposure. This increase in plasticity corresponds nicely with the lowered threshold for LTP previously reported (Risher, Fleming, et al., 2015). Further work is required to determine

whether the emergence of an EtOH-induced immature dendritic spine phenotype and increased plasticity within the CA1 hippocampal circuitry demonstrates the elimination and replacement of old spines with new immature spines or a failure of normally emerging dendritic spines to mature into adulthood. However, there does appear to be the persistence of an adolescent phenotype into adulthood that correlates with the persistence of select adolescent-typical behavioral characteristics. Whether the circuit-level and dendritic spine-level changes drive the persistence of these adolescent-typical behavioral characteristics is yet to be determined. Moreover, caution should be used with this interpretation of adolescent-typical phenotype. The shift towards a more immature phenotype may represent dysregulation and not necessarily a 'lock in' of an adolescent phenotype or impedance of maturation.

Synapses do not form alone in a vacuum; they require heavy input from peripheral astrocyte processes that ensheathe the synapses creating the tripartite synapse. Given the critical role of astrocytes in the formation and maturation of dendritic spines (Nishida & Okabe, 2007; Risher, Patel, et al., 2014) and for the formation of functional synapses (Allen, 2014a, 2014b; Blanco-Suarez et al., 2017; Gavrilov et al., 2018), it is feasible that astrocyte dysregulation may be contributing to the aberrant dendritic spine morphology or impeded spine maturation that may be occurring following adolescent intermittent EtOH exposure. Evidence is emerging that this may be the case. Using the gavage model of adolescent intermittent EtOH exposure in rats, Risher et al (Risher, Sexton, et al., 2015) demonstrated that adolescent EtOH exposure dysregulates astrocyte signaling factors, called thrombospondins, that are critical for synaptogenesis and the formation of functional synapses. However, astrocyte signaling factors specifically involved in dendritic spine maturation were not investigated. More recent work by Healey et al., (Healey et al., 2020) demonstrated that astrocyte ensheathment of synapses is

disrupted following adolescent EtOH exposure, however this was reversed by high dose

gabapentin administration (100mg/kg, i.p. daily) for five days. This is an interesting finding

given that gabapentin can antagonize thrombospondins interaction with its neuronal,

synaptogenic receptor α2δ-1 (Eroglu et al., 2009) preventing synapse formation. Interestingly,

the authors looked at the AMPAR subunit, GluA1 which is a marker for excitatory synapses, and

found no reduction in synapse formation. Further analysis to determine whether inhibition of

synaptogenesis was the driver of this effect was not investigated. However, these findings add

the accumulating evidence for the astrocyte's role in the enduring effects of adolescent EtOH.

Further work is required to determine the extent of astrocytic participation in these events.

Sex Differences

Alcohol consumption is rising in females while male drinking remains steady, this has

resulted in a growing number of studies that focus on female drinking behavior and sex-

dependent differences in the emergence of AUD. Clinical studies demonstrate that male binge

drinkers perform worse on working memory tasks than female subjects (Parada et al., 2012) but

are equally impaired when assessing declarative memory tasks (Parada et al., 2011), suggesting

that deficits may be domain specific, as is seen in rodent models. Multiple studies have reported

that alcohol-dependent men and women experience comparable deficits in brain volume or

volume of specific areas including the hippocampus despite lower lifetime alcohol consumption

in women (Agartz et al., 1999; Jacobson, 1986; Mann et al., 1992; Zahr et al., 2019) which has

led to the conclusion that women are more vulnerable to alcohol-induced brain structure changes

than men. However, differences in the size of various brain structures as well as the

aforementioned difference in lifetime consumption have made these comparisons difficult and

comparable findings in both sexes and even opposite findings exist. Pfefferbaum and colleagues

(2001) observed that there was less brain shrinkage in women who suffer from AUD than men, although this study was conducted after a longer recovery time than most studies (2-3 months vs. 1 month (Pfefferbaum et al., 2001)). A very recent study (Rossetti et al., 2021) of men and women with current AUD reported similarly comparable decreases in the areas of brain volume including hippocampus in men and women with current AUD despite female lifetime alcohol consumption that was 60% of males. Finally, Sawyer et al, (2020) reported comparable decrease in the volume of all hippocampal subfields of men and women despite 25% lower alcohol consumption by women and a longer length of sobriety (Sawyer et al., 2020). These authors raised the possibility that AUD resulted in accelerated age-related loss of hippocampal volume.

Gianoulakis and colleagues (2003) took this a step further to study how this may affect neuronal function by conducting a population study to investigate the effect of alcohol consumption on the activity of the hypothalamic-pituitary-adrenal axis. Their study revealed that alcohol dependence results in sex and age specific deficits in neuronal activity. There was a robust decrease in plasma β-endorphin and adrenal corticotropic hormone levels in heavy drinking adult females (30-44 and 45-60 years of ages) when compared to males that was accompanied by an increase in cortisol levels that was observed in all heavy drinkers compared to nondrinkers (Gianoulakis et al., 2003). Moreover, adolescent female binge drinkers demonstrate decreased activation in frontal cortical and hippocampal areas when compared to male binge drinkers (Squeglia et al., 2011). Despite this emerging evidence at the clinical level, rodent models focusing on sex differences in the hippocampus are lagging behind work that has been conducted in males only. A fairly recent study (Maynard et al., 2018) in rats in which investigator-administered alcohol of comparable doses was given to males and females resulted in cell loss in the dentate gyrus in females but not males. This supports the speculations raised in

human studies above in a more controlled environment (Maynard et al., 2018). Much more work is required to determine the sex-dependent effects of adolescent intermittent EtOH exposure and the long-term impact of hippocampal remodeling.

Conclusion

In this chapter, we have provided an overview of hippocampus neuroanatomy and discussed the current state of knowledge on the acute and chronic effects of EtOH in adolescent humans and adolescent rodent models in the context of hippocampal-dependent behavioral, structural, and neurochemical changes. We have identified knowledge gaps in our understanding of sex and age-dependent neurobiological effects of binge drinking that will be critical in understanding the relationship between adolescent binge drinking and the development of cognitive impairments and higher prevalence of AUD. While not discussed at length in this chapter it should be noted that as the field moves forward the integration of knowledge about the role of non-neuronal cells such as microglia and astrocytes will be pivotal in generating a complete picture of the effects of EtOH on adolescent development and the repercussions of early EtOH-induced perturbations.

Chapter 4

Diverging Effects of Adolescent Ethanol Exposure on Tripartite Synaptic Development Across Prefrontal Cortex Subregions

C.D. Walker[1,2], H.G. Sexton[1,2], J. Hyde[1], B. Greene[1], and M-L. Risher[1,2]

[1]Department of Biomedical Research, Joan C. Edwards School of Medicine, Marshall University, Huntington, WV 25701, USA

[2]Neurobiology Research Laboratory, Hershel 'Woody' Williams Veterans Affairs Medical Center, Huntington, WV 25704, USA

Author Note

Abstract

Adolescence is a developmental period that encompasses, but is not limited to, puberty and continues into early adulthood. During this period, maturation and refinement are observed across brain regions such as the prefrontal cortex (PFC), which is critical for cognitive function. Adolescence is also a time when excessive alcohol consumption in the form of binge drinking peaks, increasing the risk of long-term cognitive deficits and the risk of developing an alcohol use disorder later in life. Animal models have revealed that adolescent ethanol (EtOH) exposure results in protracted disruption of neuronal function and performance on PFC-dependent tasks that require higher-order decision-making. However, the role of astrocytes in EtOH-induced disruption of prefrontal cortex-dependent function has yet to be elucidated. Astrocytes have complex morphologies with an extensive network of peripheral astrocyte processes (PAPs) that ensheathe pre- and postsynaptic terminals to form the 'tripartite synapse.' At the tripartite synapse, astrocytes play several critical roles, including synaptic maintenance, dendritic spine maturation, and neurotransmitter clearance through proximity-dependent interactions. Here, we investigate the effects of adolescent binge EtOH exposure on astrocyte morphology, PAP-synaptic proximity, synaptic stabilization proteins, and dendritic spine morphology in subregions of the PFC that are important in the emergence of higher cognitive function. We found that adolescent binge EtOH exposure resulted in subregion specific changes in astrocyte morphology and astrocyte-neuronal interactions. While this did not correspond to a loss of astrocytes, synapses, or dendritic spines, there was a corresponding region-specific and EtOH-dependent shift in dendritic spine phenotype. Lastly, we found that changes in astrocyte-neuronal interactions were not a consequence of changes in the expression of key synaptic structural proteins neurexin, neuroligin 1, or neuroligin 3. These data demonstrate that adolescent EtOH

exposure results in enduring effects on neuron-glia interactions that persist into adulthood in a subregion-specific PFC manner, suggesting selective vulnerability. Further work is necessary to understand the functional and behavioral implications.

Despite declining rates of alcohol consumption since 1975, alcohol remains the most commonly used licit substance and a leading cause of death and injury in the United States (Patrick & Schulenberg, 2013), while alcohol-related deaths have been steadily rising by ~2.2% per year over the past two decades (White et al., 2022). According to the World Health Organization, 3 million deaths every year result from the harmful use of alcohol, representing 5.3% of all deaths worldwide (World Health Organization, 2019). The emergence of the COVID-19 pandemic has compounded this problem resulting in an increase of 25.5% in alcohol-related deaths during the period 2019–2020 (White et al., 2020).

In the United States, alcohol consumption typically begins and escalates during adolescence. Although adolescents drink less frequently than adults, adolescents typically consume more alcohol per occasion, most commonly in a binge-like manner (Chung et al., 2018; Hingson & White, 2014). Early alcohol use, in the form of binge drinking, increases the risk of acute and chronic physical and mental health problems, as well as alcohol dependence later in life (Grifasi et al., 2019; Kandel et al., 1997; Kuntsche et al., 2017; Miller et al., 2007). It has been proposed that this is, in part, due to the ongoing development of the adolescent brain, in which excessive alcohol use drives maladaptive neuronal changes that alter brain connectivity and result in remodeling of the reward network (for a review, see Koob and Volkow (2016)).

Select cortical regions, such as the prefrontal cortex (PFC) are known to undergo the final stages of neuronal maturation during adolescence, occurring via the pruning of synapses and the refinement of neuronal circuitry. Through this process, local and projecting neuronal networks are refined and stabilized. The PFC is composed of multiple subregions, including the anterior cingulate cortex (ACC), the medial prefrontal cortex (mPFC), and the orbitofrontal cortex (OFC) that play distinct roles in higher-order executive functions such as reasoning, planning, language,

and social interactions (Wood & Grafman, 2003), all of which are important aspects of the addiction/reward circuitry. The ACC has been associated with complex cognitive functions such as empathy, impulse control, emotion, and decision-making (Bush et al., 2000), while impaired ACC function is associated with psychopathology and emotional dysregulation (Stevens et al., 2011). The mPFC is essential in regulating cognitive function, including attention, inhibitory control, habit formation, and working, spatial, and long-term memory (Jobson et al., 2021). The mPFC is also important in the regulation of conditioned behavior and suppression of these behaviors (Warren et al., 2016), with the mPFC's prelimbic cortex (PL) and infralimbic cortex (IL) being strongly associated with the activation and suppression of fear circuits (Laurent & Westbrook, 2009; Sotres-Bayon & Quirk, 2010). The OFC is associated with sensory integration and modulation of visceral reactions, participation in learning, and decision-making for emotional, adaptive, and goal-directed behavior (Rolls et al., 2020). Within the OFC the lateral (sometimes referred to as the ventrolateral (LO-OFC)) and ventral (VO-OFC) aspects appear to have diverging roles. The LO-OFC is involved in obsessive compulsive behavior (Lei et al., 2019) and decision making through the integration of immediate prior information and current information (Nogueira et al., 2017), while the VO-OFC appears to be involved in value assessment in tasks such as delayed discounting (Jobson et al., 2021). Damage or degeneration of the PFC can manifest as a deficit in impulse control, poor performance on tasks that require long-term planning, blunted emotional responses, aggression, and irritability (Wood & Worthington, 2017). Therefore, it is not surprising that PFC dysfunction has been implicated in many human psychiatric disorders, the emergence and persistence of drug and alcohol use, and as a predictor of increased risk to drug and alcohol relapse (Camchong et al., 2013).

Previous studies have shown a positive correlation between ACC activation and excessive drinking (Vollstadt-Klein et al., 2010), while the mPFC has been implicated in the development and persistence of addictive behaviors through reinforcement of rewarding stimuli, compulsive drug taking, drug-associated memories, and relapse (Hogarth et al., 2013; Kalivas, 2009; Van den Oever et al., 2010). The OFC, which is critical for impulse control, has shown to be impaired in individuals with alcohol use disorders (Boettiger et al., 2007; Miguel-Hidalgo et al., 2006) however the contributions of OFC subregions have not been explored. Taken together, these data provide a rationale for continued investigation into the impact of adolescent binge alcohol exposure on PFC development, contribution to the emergence of long-term PFC-dependent neurological deficits (Crews et al., 2000), and increased propensity to develop alcohol dependence (DeWit et al., 2000).

Despite strong evidence of neuronal deficits following adolescent binge alcohol exposure across many PFC subregions, much of this research ignores the potential contribution of astrocytes to these cognitive impairments. Growing evidence is beginning to reveal the critically important role of astrocytes across numerous domains of cognition and a wide variety of brain regions including PFC subregions (for a review, see Lyon and Allen (2021)), as such the involvement of the ACC in remote memory tasks and novel open field exploratory behavior (Iwai et al., 2021; Kol et al., 2020). Interestingly, PFC astrocytes have also been implicated in bidirectionally modulating ethanol (EtOH) consumption in male mice (Erickson et al., 2021).

Astrocytes are complex non-neuronal glial cells with extensive peripheral astrocytic processes (PAPs) that ensheathe presynaptic axonal and postsynaptic dendrite components to form the 'tripartite synapse' (for a review, see Walker et al. (2020)). It is estimated that a single astrocyte can be connected with up to 2 million synapses in humans (Oberheim et al., 2009).

This connectivity establishes a wide-ranging network, allowing a single astrocyte to integrate and influence neuronal activity across independent circuits (Oberheim et al., 2009). The role of astrocytes at the tripartite synapse is multifaceted (for reviews, see Farhy-Tselnicker and Allen (2018); Kim et al. (2017); Lyon and Allen (2021)). However, many astrocyte functions involve contact mediated signaling or the release of astrocyte secreted signaling factors, both of which rely heavily on appropriate PAP-synaptic proximity and localization. For example, astrocytes are heavily involved in dendritic spine maturation through direct contact mediated signaling (Nishida & Okabe, 2007) and the release of astrocyte secreted factors (Risher, Patel, et al., 2014). Moreover, the further away the PAP is from the synapse, the more likely the dendritic spine will be structurally immature (Witcher et al., 2007). These data suggest that tight regulatory control of PAP-synaptic proximity may be critical for appropriate dendritic spine maturity.

PAP-synaptic proximity relies on the availability of stabilizing proteins. For example, disruption of eph-ephrin located on astrocyte processes and dendritic spines, respectively, has been shown to be important for dendritic stabilization (Nishida & Okabe, 2007). More recently, the role of the cell adhesion molecules, neuroligins (located on postsynaptic terminals and astrocytes depending on the subtype) and neurexins (located on presynaptic terminals) have been shown to play a critical role in astrocyte complexity, synaptic contact, and synaptic function (Stogsdill et al., 2017). Moreover, disruption of neurexin binding prevented increases in pre- and post-synaptic size (Ko et al., 2009), suggesting that the ability of neurexin to bind its appropriate synaptic partner is critical for dendritic spine and overall synaptic maturity.

It is well established that neuronal maturation is ongoing within the PFC throughout adolescence and into early adulthood. Recently, we demonstrated that the relationship between synapses and astrocytes also continues to develop throughout adolescence into early adulthood in

the mPFC (IL and PL), as demonstrated by an increase in PAP-synaptic interactions/proximity across this time period (Testen et al., 2019). Given the emerging appreciation for the critical role that astrocytes play in synaptic maturation, regulation, and cognition, and the critical PAP-synaptic developmental processes that are ongoing during adolescence, we sought to investigate the impact of adolescent binge ethanol exposure on astrocyte morphology, PAP-synaptic proximity, dendritic spine maturation, and determine whether loss of neuroligin-neurexin cell adhesion proteins was a driving factor in the observed changes. We hypothesize that adolescent intermittent binge EtOH exposure (AIE) disrupts PAP-synaptic proximity in a region-dependent manner and is associated with changes in dendritic spine maturation.

Methods

All procedures used in this study were conducted in accordance with the guidelines of the American Association for the Accreditation of Laboratory Animal Care and the National Research Council's Guide for Care and Use of Laboratory Animals and were approved by the Huntington VA Medical Center and Marshall University.

Animals and Surgical Procedures

A total of 46 male Sprague Dawley rats (Hilltop, Scottdale, PA, USA) were received on postnatal day (PND) 21 and were double-housed and maintained in a temperature- and humidity-controlled room with access to food and water ad libitum. All animals, regardless of treatment group or experiment, were housed together in a randomly assigned order on a 12 h:12 h reverse light:dark cycle (lights on at 6:00 p.m.) and allowed to acclimatize for five days. Surgical procedures were performed as previously described in Testen et al. (2019) with minor modifications. On PND 26, rats (n = 10/treatment group, total = 40 rats) were administered mannitol (0.3 mL/kg, 25% w/v, i.p.; (Carty et al., 2013; Testen et al., 2019)) and anaesthetized

with a cocktail of ketamine (30 mg/ kg), xylazine (2.5 mg/kg), and acepromazine (0.5 mg/kg) before being secured to the stereotaxic frame (Figure 4A). For visualization of astrocytes, a green fluorescent protein (GFP) with the lymphocyte protein tyrosine kinase (Lck) tag was used to enhance the visualization of the finer PAPs (Benediktsson et al., 2005; Shigetomi et al., 2013; Zlatkine et al., 1997). Lck-GFP was expressed under the control of the astrocyte-specific GfaABCID promoter using adeno-associated virus (AAV) type 5 (a gift from Kate Reissner (UNC Chapel Hill) and purchased from Addgene Plasmid #105598, RRID:Addgene_105598; (Scofield et al., 2016; Shigetomi et al., 2013; Testen et al., 2019; Testen et al., 2018)). The AAV was microinjected with a 26-gauge needle (1.0 µL per side, 7.3×10^{12} particles/mL at 1 µL/min) with a dwell time of 10 min at the following coordinates: +2.7 mm anterior/posterior, +/−0.6 mm medial/lateral, −3.8 mm dorsal/ventral for mPFC and ACC and −5.2 mm anterior/posterior, +/−2.5 mm medial/lateral, −2.9 mm dorsal/ventral for OFC (Figure 4B). No animals died during the surgery/post-surgical period. Following surgery, animals were double-housed with their original cagemate and randomly assigned into experimental groups (by cage) using an online random number generator, in preparation for binge EtOH exposure. Experimenters were blinded for all experiments and data collection. Analysis was conducted with letter assignments ensuring that treatment groups remained unknown. All animal numbers are described for the individual experimental groups below and based on a prior power analysis using G*Power version 3.1.9.4 (Axel Buchner, Heinrich Heine University, Dusseldorf, Germany) for sample size estimation. This analysis was based on data from previously published and pilot data with a significance criterion of $\alpha = 0.05$ and power $\beta = 0.8$ to determine the required minimum sample size.

Figure 4
Experimental Design.
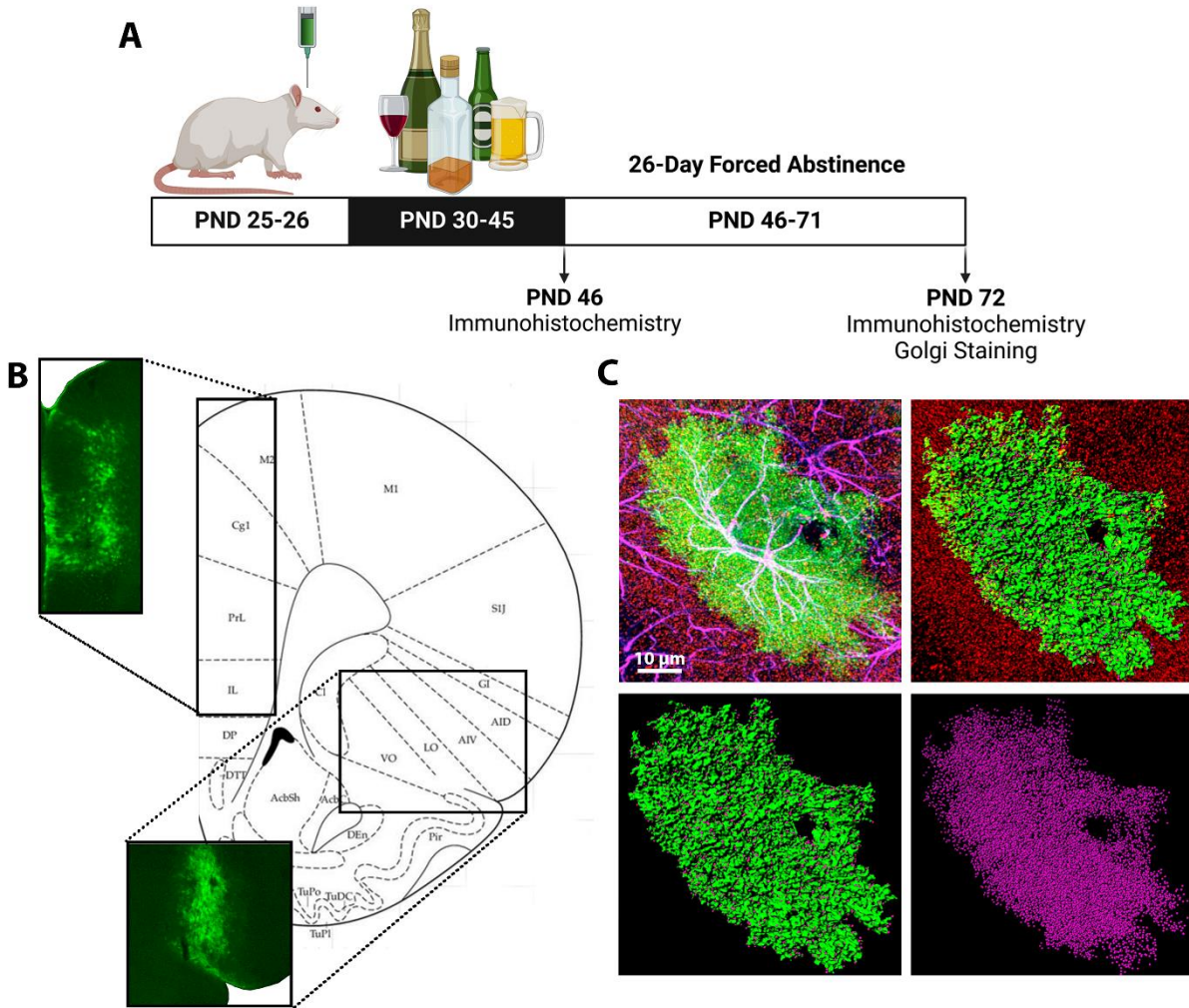
(A) Animals received intracranial injections of an astrocyte-specific adeno-associated virus directly into the ACC, mPFC, or OFC on PND 25–26. Beginning PND 30, animals received 5 g/kg of EtOH or water via oral gavage on an intermittent, two days on, one day off, two days on, two days off, schedule. Tissue was collected on PND 46, during peak withdrawal, or after a 26-day forced abstinence period, on PND 72. **(B)** Validation of Lck-GFP expression in the ACC and mPFC (upper left image) and the OFC (bottom image). **(C)** Representative images of AAV+ astrocyte imaging with confocal microscopy and reconstruction using Imaris. The top left image is a confocal image of an AAV+ astrocyte (green), with GFAP (magenta), co-localization of AAV+ and GFAP (white), and PSD-95 (red), scale bar, 10 μm. The top right image is a reconstructed astrocyte (green) and PSD-95 (red). The bottom left image is a reconstructed

surface rendered astrocyte (green) with PSD-95 (magenta) within 0.5 μm of the astrocyte. The bottom right image is isolated PSD-95 (magenta) that is colocalized with the astrocyte of interest. From "Diverging Effects of Adolescent Ethanol Exposure on Tripartite Synaptic Development Across Prefrontal Cortex Subregions," C.D. Walker, H.G. Sexton, J. Hyde, B. Greene, and M-L. Risher, 2022, *Cells*, *Open*, 11(19), p.4 (https://doi.org/10.3390%2Fcells11193111). CC BY 4.0.

Intermittent Binge EtOH Exposure

Prior to EtOH/water (H_2O) exposure, animals were habituated to handling. Beginning PND 30, animals were exposed to EtOH or H_2O consisting of 10 doses of 5 g/kg EtOH (35% v/v in H_2O) or H_2O by intragastric gavage (i.g.) using two days on, one day off, two days on, two days off intermittent schedule of 16 days (Figure 4A), as previously described in Risher, Sexton, et al. (2015). While all experimenters were blinded, this is difficult to maintain during EtOH administration due to the strong smell of EtOH. The experimenter that administers the EtOH is also responsible for ensuring that the animals recover from intoxication, once again making blinding at this stage of the experiment difficult. The experimenter conducting the EtOH administration was responsible for ensuring that everyone involved in the experiments listed below remained blinded until completion of the study. Animals were euthanized 24 h after the 10th/last dose (PND 46) or following a 26-day forced abstinence period (PND 72), allowing animals to reach adulthood prior to tissue collection. EtOH doses were selected to produce blood EtOH concentrations (BECs) consistent with those of adolescent humans that are achieved during binge drinking episodes (Donovan, 2009).

Immunohistochemistry (IHC)

Slice Preparation. At PND 45 or 72, animals were anesthetized with isoflurane (10 animals/treatment group, total = 40), then perfused with phosphate-buffered saline (PBS, pH7.4; Sigma P5368) for 5 min followed by 4% paraformaldehyde (PFA; cat# 19210, Electron

Microscopy Solutions, Hatfield, PA, USA) for 12 min (20 mL/min). Brains were harvested and postfixed in 4% PFA at 4 C overnight followed by 30% glycerol (cat# G5516-1L, Sigma-Aldrich, St Louis, MO, USA) in PBS at 4 C for 1–2 days. Brains were placed in 2:1 of 30% sucrose to OCT freezing compound (Electron Microscopy Sciences, Hatfield, PA, USA) and stored at −80 C. 80 µm slices were collected using a cryostat (CM 1950, Leica Biosystems, Richmond, IL, USA). Sections underwent antigen retrieval as described in (Jiao et al., 1999; Testen et al., 2019). Briefly, free-floating sections were rinsed three times (5 min each) in 0.1 M PB (3.1 g/L NaH_2PO_4, 10.9 g/L Na_2HPO_4, pH 7.4) then transferred to 10mM sodium citrate buffer preheated to 80 C for 30 min, shaking the slices every 10 min. Sections were cooled and washed three times (5 min each) in 0.1M PB (pH 7.4).

PSD-95 and GFAP. Sections were blocked with 5% normal goat serum (NGS, Jackson Immunolabs,, West Grove, PA, USA, cat# 005-000-121) in PBST (2% triton 100-X, Roche, cat#13134900) for one hour at room temperature. Sections were then incubated for four days in mouse anti-PSD-95 (1:450 Thermo Fisher Scientific Cat# MA1-045, RRID:AB_325399) and rabbit anti-GFAP (1:500 Agilent Cat# Z0334, RRID:AB_10013382) in PBST (2% triton, 5% NGS) at 4 C. Sections were washed three times in PBST (0.2% triton) and incubated for six h at room temperature in Alexa Fluor goat anti-mouse 594 (1:200 Molecular Probes Cat# A-11032, RRID:AB_2534091) and Alexa Fluor goat anti-rabbit 647 (1:200 Thermo Fisher Scientific Cat# A-21245, RRID:AB_2535813) in PBST (2% triton X-100, 5% NGS). Sections were washed three times in PBST (0.2% triton) and once in PBS. Slices were mounted with Vectashield+DAPI (Vector Laboratories West Grove, PA, USA, cat# H-1200) and coverslips were sealed with nail varnish.

Neuroligin 1, 3, and Neurexin. Sections were blocked with 5% normal natural donkey serum (NDS, Jackson Immunolabs, cat# 005-000-121) in PBST (2% triton 100-X, Roche, cat# 13134900) for one hour at room temperature. Then, incubated for four days in rabbit anti-Neurexin 1 2 /3 (1:500 Synaptic Systems Cat# 175 003, RRID:AB_10697815) with either mouse anti-Neuroligin 1 (1:500 Synaptic Systems, cat# 129111) or mouse anti-Neuroligin 3 (1:500 Synaptic Systems Cat# 129 111, RRID:AB_887747) in PBST (2% triton, 5% NDS) at 4 C. Sections were washed three times in PBST (0.2% triton) and incubated for six h at room temperature in Alexa Fluor goat anti-mouse 594 (1:200) and Alexa Fluor goat anti-rabbit 647 (1:200) in PBST (2% triton X-100, 5% NDS). Sections were washed three times in PBST (0.2% triton) and once in PBS. Slices were mounted with Vectashield+DAPI and coverslips were sealed with nail varnish.

Data Acquisition and Processing

Astrocyte-Synaptic Co-Localization. A Leica SP5 laser-scanning confocal microscope with 63× oil-immersive objective, NA 1.45 (Leica, Wetzlar, Germany) was used for image acquisition. Acquisition parameters for AAV$^+$ astrocyte-PSD-95 imaging were set at 1024 × 1024 pixels frame size, 16-bit depths, 4× lines averaging, 1 μm z-step size. Lck-GFP expression pattern is diffuse, aiding in the acquisition of single, isolated astrocytes. Individual, whole GFP$^+$ astrocytes were randomly selected by the experimenter. GFP$^+$, GFAP, and PSD-95 were then imaged within the region of interest: ACC, mPFC (infralimbic (IL) and prelimbic (PL)), and OFC (ventral orbital area (VO-OFC) and lateral orbital area (LO-OFC)). 8–11 individual astrocytes were captured per brain region. A total of 5 brains were used per treatment group.

Co-localization was performed as previously described in Testen et al. (2019), with modifications. AutoQuant X3.1.2 software (Media Cypernetics, Rockville, MD, USA) was used

to deconvolve raw images before digitally reconstructing z-stacks (Figure 4C). AutoQuant's algorithm for blind deconvolution with 10 iterations was run on each z-stack prior to reconstruction. Parameters for blind deconvolution are automatically optimized by the software based on confocal, objective, and imaging specifications. Output files were directly imported to Imaris x64 (Bitplane, Santa Barbara, CA, USA) for 3-dimensional reconstruction. Using Imaris, each individual astrocyte was first isolated from a Lck-GFP background signal using a surface building feature. Surface rendering enables the extraction of morphometric values, including surface area and volume, and generates a new Lck-GFP channel devoid of background noise, revealing only a signal from a single isolated astrocyte (Figure 1C). Close attention was paid to verify that collected Lck-GFP signal accounted for a single astrocyte, in its entirety. Co-localization of the Lck-GFP and GFAP signals was used to confirm astrocyte identity for quantification. Only confirmed astrocytes that were captured in their entirety were used for quantification and analysis. The isolated Lck-GFP channel (surface mask) was used, in conjunction with the PSD-95 channel, to perform colocalization analysis to determine the proximity between the astrocytes and post-synaptic neuronal terminals (Figure 1C). Before co-localization analysis, the threshold for the PSD-95 signal was manually determined by measuring the fluorescence intensity of unambiguous PSD-95 positive puncta on multiple optical planes by a blinded experimenter. This was achieved by rotating the reconstructed astrocyte image in 3D space while adjusting voxels to ensure that PSD-95 expression could be observed without the interference of background noise. An average of these measurements was used as a final PSD-95 signal threshold value. Co-localization is reported as a % of astrocyte volume (identified as Lck-GFP^{+} surface reconstruction) co-localized with the PSD-95 channel.

Neuroligin 1, 3, and Neurexin. Confocal z-stacks (5 µm thick, optical section depth 0.33 µm, and 1024 × 1024 image size) of the ACC, mPFC (IL and PL), LO-OFC, and VO-OFC were imaged on a Leica SP5 laser-scanning confocal microscope with 63× oil-immersive objective, NA 1.45 (Leica, Wetzlar, Germany). A total of 3 randomly selected image stacks from a randomly selected hemisphere were captured from 3 separate brain slices per animal (9–10 brains/treatment group). AutoQuant X3.1.2 software was used to deconvolve raw images before quantifying protein expression and co-localization. Output files were directly imported to Imaris for analysis. Before analysis, the threshold for protein expression was manually determined by measuring fluorescence intensity of unambiguous neuroligin 1, 3, and neurexin markers on multiple optical planes by a blind experimenter. This was achieved by rotating the reconstructed astrocyte image in 3D space while adjusting voxels to optimize the signal for each protein of interest (neuroligin 1, 3, and neurexin). An average measurement for each protein of interest was used as the final signal threshold value. The Imaris 'Spot' function was used to create individual markers for neuroligin 1, 3, and neurexin. Expression of individual proteins were observed based on the number of individual markers. Neurexin-neuroligin interactions were analyzed based on co-localization of neurexin-neuroligin 1 and neurexin-neuroligin 3. Representative images for publication were created by importing LIF files into ImageJ and selecting the Z-stack of interest. After converting the Z-stack to a maximum projection image, brightness and contrast were adjusted, then the images were saved as TIF files. Finally, the TIF files were uploaded into Photoshop (Adobe, San Jose, CA, USA) and cropped into a 4 × 4 grid section.

Golgi-Cox Staining

Golgi-Cox staining was performed as previously described (Risher, Sexton, et al., 2015; Risher, Ustunkaya, et al., 2014). The animals (PND 72, n = 3/treatment group, total = 6) were

deeply anesthetized with isoflurane, decapitated, and the brain was quickly removed. One hemisphere was randomly selected, quickly rinsed in distilled water, and immersed in a 1:1 mixture of solutions A and B (Rapid Golgi Stain Kit; cat#PK401; FD Neurotechnologies, Baltimore, MD, USA). After two weeks of impregnation in solutions A and B, brains were transferred to solution C for 48 h, then removed and frozen in tissue freezing medium (cat#72592 Electron Microscopy Sciences, Hatfield, PA, USA). Coronal slices (100 µm) were sectioned using a cryostat and mounted onto 2% gelatin-coated slides (cat#PO101; FD Neurotechnologies, Baltimore, MD, USA). Sections were stained with a mixture containing Rapid Golgi Stain solutions D and E, then dehydrated, cleared, and coverslipped with Permount Mounting Medium (Electron Microscopy Sciences; cat#17986-05).

Dendritic Spine Analysis. Golgi-impregnated neurons were visualized using the Leica Microscope DM5500B, and image stacks were generated using a 63× oil immersion lens. Image stacks were imported into RECONSTRUCT software (available from http://synapses.clm.utexas.edu/ tools/index.stm (accessed on 21 March 2022); Fiala, 2005) for analysis as described in Risher, Sexton, et al. (2015); Risher, Ustunkaya, et al. (2014), with modifications. Secondary dendritic branches of ACC, mPFC (IL and PL), LO-OFC and VO-OFC neurons were analyzed (blinded) using an unbiased rating system by measuring the length and width of each protrusion with visible connections to the dendritic shaft from dendritic segments 10 µm in length. Average spine densities were calculated using 2 to 3 separate dendrites from at least 4 to 5 separate image stacks per animal (a total of 15 dendritic branches/animal). Spine types were determined on the basis of the ratio of the width (W) of the spine head to the length (L) of the spine neck and classified as (in µm): filopodia (L > 1.5), thin/long thin (L < 1.5 & L:W > 1), stubby (L:W < 1), and mushroom (W > 0.6), also see Risher, Ustunkaya, et al. (2014).

Representative images for publication were created by importing TIF file with dendrite of interest into ImageJ. The background was removed, using the 'Subtract Background' function with a rolling ball radius of 10 pixels with light background. TIF files were imported into Photoshop where dendrite sections of interest were isolated. Final representative images were created by adjusting brightness and contrast.

Blood EtOH Concentrations (BECs)

To minimize confounds associated with stress and avoid stress/EtOH interaction in our experimental group, a parallel group of animals (n = 6) were dosed separately to assess BECs obtained in our intermittent binge EtOH paradigm. Animals received intermittent oral gavage (as described above) of 5 g/kg EtOH beginning on PND 30. Blood was collected from the lateral saphenous vein 60 min after EtOH administration on the first and last days of the EtOH administration. Blood samples were centrifuged for 5 min then serum was removed and stored at −80C. Samples were analyzed in triplicate using an Analox AM1 alcohol analyzer (Analox Instruments LTD, Stourbridge, UK).

Statistical Analysis

Data were grouped using Excel 365 (Microsoft, Redmond, WA, USA) and analyzed using GraphPad Prism Version 9.3.1 (GraphPad Software, San Diego, CA, USA). Two-way ANOVA was performed (treatment × subregion) with a Tukey's post hoc test for all comparisons. The Shapiro–Wilk and Kolmogorov–Smirnov were performed to assess normality. Statistical significance was assessed using an alpha level of 0.05. Data are presented as intercleaved box and whisker plots with minimum and maximum values and individual plot points for each data set. All statistical comparisons (Figure S1) and all raw data (represented as mean ± SEM; Figure S2) have been included in the supplemental section, regardless of significance.

Results

Blood EtOH Concentrations (BECs)

Blood EtOH concentrations were obtained 60 min after EtOH administration at two timepoints: after the first and last dose. We were unable to obtain sufficient blood from one animal when collecting samples at the first timepoint, therefore we had n = 5 for the first time point and n = 6 samples for the second timepoint. Results show that 60 min after EtOH administration, BECs were (mean ± SEM, mg/dL) = 139.21 ± 9.46 and 119.39 ± 2.14 after the first and last dose, respectively. These BECs are consistent with the ranges seen within previous human adolescent drinking analyses (Donovan, 2009).

AIE Induced Changes in PFC Astrocyte Morphology and PAP-Synaptic Proximity in a Subregion-Dependent Manner, but Only After a Period of Forced Abstinence

Before assessing AIE-induced changes in PAP-synaptic interactions, we measured changes in astrocyte morphology based on whole-cell volume. Using Imaris, we quantified the volume of individual Lck-GFP$^+$ astrocytes from the ACC, mPFC (IL and PL), LO-OFC, and VO-OFC (Figure 2A–D) 24 h after the last dose (i.e., PND 46) and after a 26-day forced abstinence period (i.e., PND 72). There was no treatment (AIE) effect on astrocyte volume during peak withdrawal (F (1, 476) = 1.251, p = 0.2639; Figure 5A,B) or after the 26-day forced abstinence period (F (1, 471) = 0.1942, p = 0.6597; Figure 5C,D). However, there was a significant subregion effect at both timepoints ((F (1, 476) = 84.85, p < 0.001 and F (1, 471) = 208.4, p < 0.001, respectively). When we compared the generalized characteristics of astrocyte volume in EtOH-naïve animals (i.e., comparison of H$_2$O controls across subregions), we found that there were distinct differences in astrocyte volume that were dependent on the PFC subregion. At PND 46, ACC and mPFC had the lowest astrocyte volume when compared with LO-OFC and VO-

OFC (p's < 0.0001; Figure 5A,B). There was no significant difference between ACC and mPFC astrocyte volume (p = 0.1199) or LO-OFC and VO-OFC astrocyte volume (p > 0.9999). Interestingly, by adulthood (PND 72), the subregion-dependent effect on astrocyte volume became more refined (F (1, 471) = 208.4, p < 0.001). At the adult timepoint, a significant difference emerged between ACC astrocyte volume and mPFC astrocyte volume, with mPFC emerging as having the larger astrocyte volume (p = 0.0349). As demonstrated at PND 46, LO-OFC and VO-OFC astrocytes remained significantly smaller than both ACC (p < 0.0001 and p < 0.0001, respectively) and mPFC (p < 0.0001 and p < 0.0001, respectively) astrocytes. There was no significant difference between astrocyte volume when comparing LO-OFC and VO-OFC (p = 0.1322).

Figure 5

Single Cell Imaging and Analysis of Astrocyte Volumes 24 H After AIE During Withdrawal and 26-Days After AIE.
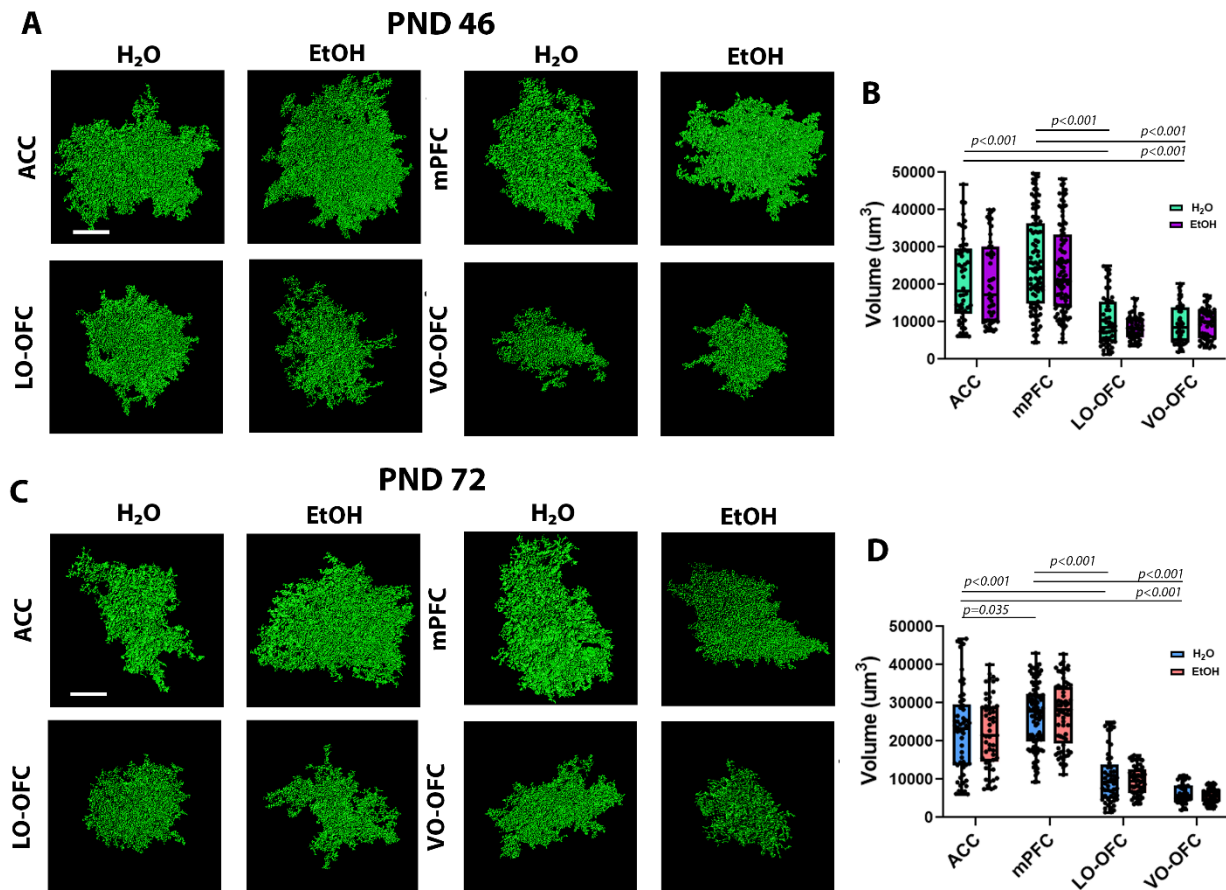
(**A**) Representative images of astrocyte surface rendering from the ACC, mPFC, LO-OFC, and VO-OFC 24 h after the final dose of EtOH. Scale bar, 20 μm. (**B**) Quantification of astrocyte volumes 24 h after the final dose of EtOH. When comparing astrocyte volume across subregions within the control groups, there was a significant decrease in astrocyte volume in LO-OFC and VO-OFC when compared to ACC and mPFC. There was no significant treatment effect (H_2O vs. EtOH) within subregions. (**C**) Representative images of astrocyte surface rendering from the ACC, mPFC, LO-OFC, and VO-OFC following a 26-day forced abstinence period. Scale bar 20 μm. (**D**) Quantification of astrocyte volumes following a 26 day-day forced abstinence period. When comparing control conditions across subregions, there was a significant decrease in astrocyte volume in LO-OFC and VO-OFC when compared to ACC and mPFC. There was no significant treatment effect (H_2O vs. EtOH) within subregions ($p > 0.05$). Error bars represent minimum and maximum values in each data set. Data presented as box and whisker plots with interquartile range with mean, minimum, and maximum measures indicated along with individual data points. Analysis: two-way ANOVA with Tukey's *post hoc* comparison, n = 5/treatment group. From "Diverging Effects of Adolescent Ethanol Exposure on Tripartite Synaptic Development Across Prefrontal Cortex Subregions," C.D. Walker, H.G. Sexton, J. Hyde, B. Greene, and M-L. Risher, 2022, *Cells, Open*, 11(19), p.9 (https://doi.org/10.3390%2Fcells11193111). CC BY 4.0.

Figure 6

Single Astrocyte Co-Localization With PSD-95 and Analysis 24 Hours (PND 46) and 26-Days (PND 72) After AIE.
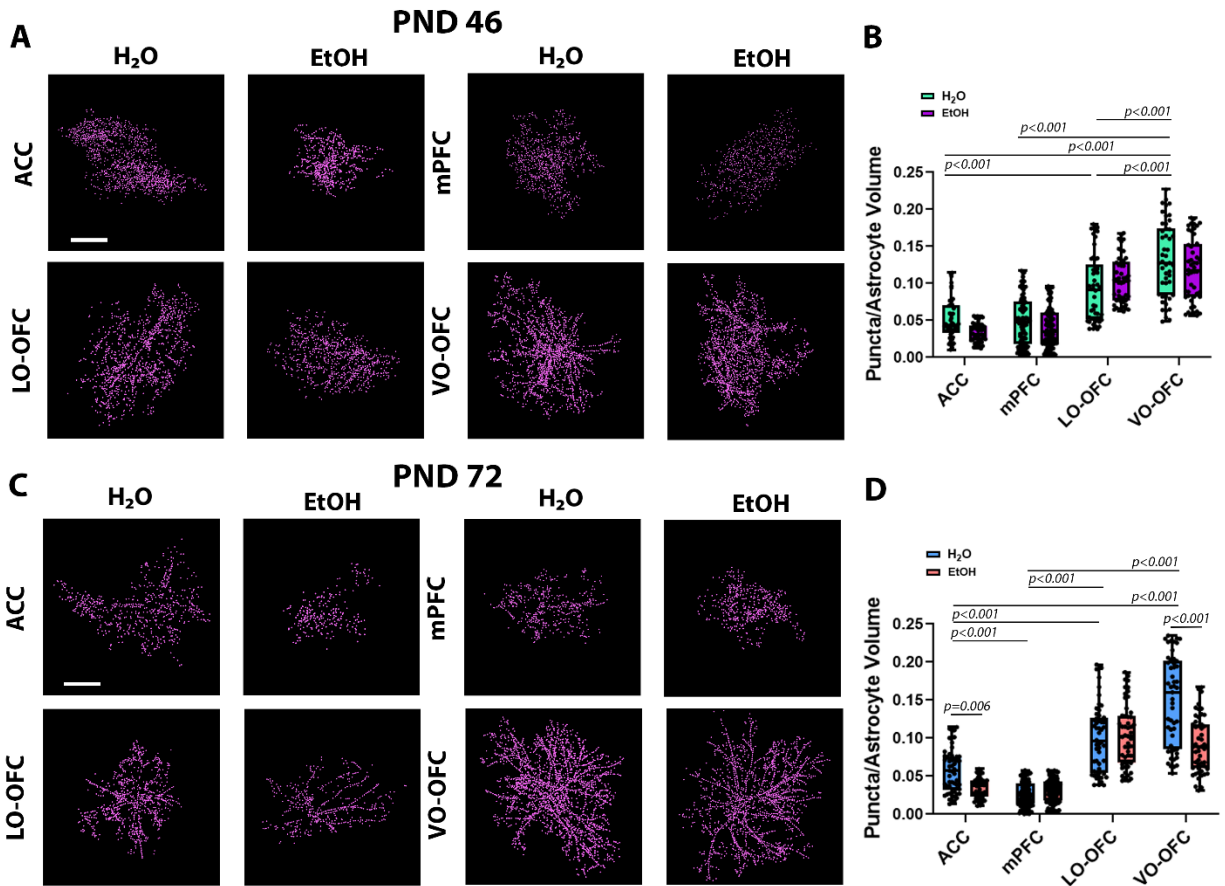
(**A**) Representative images of PSD-95 colocalized within 0.5 µm of a Lck-GFP$^+$ astrocyte in the ACC, mPFC (IL and PL), LO-OFC, and VO-OFC 24 hours after AIE. Scale bar 20 µm. (**B**) Quantification of puncta/astrocyte volume (puncta/µm^3) in each of the PFC subregions. When comparing puncta number across subregions within the control groups, there was a significant increase in puncta number/astrocyte volume in LO-OFC and VO-OFC when compared to ACC and mPFC. There was no significant treatment effect on puncta number (H$_2$O vs. EtOH) within subregions. (**C**) Representative images of PSD-95 colocalized within 0.5 um of an AAV$^+$ astrocyte in the ACC, mPFC (IL and PL), LO-OFC, and VO-OFC 26-days after AIE. Scale bar 20 µm. (**D**). When comparing puncta number across subregions within the control groups, there was a significant increase in puncta number/astrocyte volume in LO-OFC and VO-OFC when compared to ACC and mPFC. There was a significant treatment effect on puncta number (H$_2$O vs. EtOH) demonstrated by a decrease in astrocyte-synapse co-localization in the ACC ($p < 0.006$) and the VO-OFC ($p < 0.001$). Data presented as box and whisker plots with interquartile range with mean, minimum, and maximum measures indicated along with individual data points. Analysis: two-way ANOVA with Tukey's *post hoc* comparison, n = 5/treatment group. From "Diverging Effects of Adolescent Ethanol Exposure on Tripartite Synaptic Development Across

To determine the effects of AIE on PAP-synaptic proximity, we used immunohistochemistry to probe for the postsynaptic density marker, PSD-95, in tissue along with Lck-GFP$^+$ astrocytes (Figure 6A–C). There was a significant treatment effect (AIE), subregion effect, and interaction on PAP-synaptic co-localization during peak withdrawal (24 h after the last dose) (treatment effect: $F_{(1, 476)} = 5.097$, $p = 0.0244$; subregion effect: $F_{(1, 476)} = 160.5$, $p < 0.0001$; interaction: $F_{(1, 476)} = 3.480$, $p = 0.0159$; Figure 6A,B). However, upon *post hoc* analysis, there were no significant effects of AIE within subregions when compared to controls. When we compared the generalized characteristics of astrocyte PAP-synaptic proximity in EtOH-naïve animals (i.e., comparison of H_2O controls across subregions) at this early timepoint, there was no significant difference between ACC and mPFC co-localization ($p > 0.9999$). There were significantly more PAPs co-localizing with synapses in LO-OFC and VO-OFC subregions when compared to ACC ($p < 0.0001$ and $p < 0.0001$, respectively) and mPFC ($p < 0.0001$ and $p < 0.0001$, respectively). There were significantly more PAPs co-localizing with synapses within the VO-OFC when compared with LO-OFC ($p < 0.0001$). By adulthood (PND 72), the subregion-dependent effect of PAP-synaptic colocalization became more refined. PAP-synaptic co-localization was significantly lower in mPFC than ACC ($p < 0.0001$), LO-OFC ($p < 0.0001$), and VO-OFC ($p < 0.0001$). PAP-synaptic co-localization was significantly higher in LO-OFC ($p < 0.0001$) and VO-OFC ($p < 0.0001$) subregions when compared to ACC, while VO-OFC had significantly more PAP-synaptic co-localization than LO-OFC ($p < 0.0001$).

After the 26-day forced abstinence period (PND 72) there was a robust treatment effect (AIE), subregion effect, and interaction on PAP-synaptic co-localization (treatment effect: $F_{(1, 502)} = 35.35$, $p < 0.0001$; subregion effect: $F_{(1, 502)} = 237.6$, $p < 0.0001$; interaction: $F_{(1, 502)}$

= 24.70, $p < 0.0001$; Figure 6C,D). When we compared the generalized characteristics of astrocyte PAP-synaptic proximity in EtOH-naïve animals (i.e., comparison of H_2O controls across subregions) at this adult timepoint, there was significantly less PAP-synaptic co-localization in the mPFC when compared to ACC ($p < 0.0001$), LO-OFC ($p < 0.0001$), and VO-OFC ($p < 0.0001$). Once again, PAP-synaptic co-localization was significantly higher in LO-OFC ($p < 0.0001$) and VO-OFC ($p < 0.0001$) subregions when compared to ACC. However, at this adult timepoint, we began to see a differentiation between OFC subregions. Treatment-naïve astrocytes within the VO-OFC showed significantly higher PAP-synaptic co-localization when compared to LO-OFC astrocytes ($p < 0.0001$).

Post hoc analysis of the treatment effect following forced abstinence demonstrated a significant decrease in PAP-synaptic co-localization in the ACC (Figure 6C,D) and VO-OFC ($p < 0.0001$; Figure 6C,D). There was no effect of AIE on PAP-synaptic co-localization within the mPFC ($p = 0.9444$) or the LO-OFC ($p = 0.9974$).

To rule out the loss of synapses as a driver in the loss of PAP-synaptic interactions in the ACC and VO-OFC, we quantified PSD-95 protein expression in all prefrontal subregions during peak withdrawal (PND 46) and following the 26-day forced abstinence period (PND 72). We used the Imaris 'Spot' function to count the number of individual PSD-95 puncta within the ROI in which our Lck-GFP$^+$ astrocytes were imaged. We found no effect of AIE on PSD-95 expression in the ACC, mPFC (PL and IL), LO-OFC, or VO-OFC at PND 72 ($p > 0.05$; Figure S3) when loss of PAP-synaptic coupling occurs.

AIE Results in Cortical Subregion Dependent Shifts in Dendritic Spine Maturation after

Forced Abstinence

PAP-synaptic proximity is critical for appropriately targeted astrocyte contact-mediated and astrocyte-secreted signaling, particularly with regard to regulating dendritic spine maturation (Risher, Patel, et al., 2014). We wanted to determine if the AIE-induced PAP-synaptic loss of proximity after the 26-day forced abstinence period was associated with changes in dendritic spine maturation and density (Bourne & Harris, 2008; Matsuzaki, 2007). Since the AIE-induced effects on PAP-synaptic colocalization were only observed in adulthood, and to avoid any potential confounding withdrawal effects, we focused on the adult timepoint (after the 26-day forced abstinence period) for all remaining experiments. There was no significant effect of subregion on spine density ($F_{(1, 352)} = 0.7979$, $p = 0.3723$; Figure S4). There was a significant effect of treatment on spine density ($F_{(3, 352)} = 3.764$, $p = 0.011$; Figure S4); however, *post hoc* analysis revealed no significant treatment effects when comparing AIE to control within a subregion ($p > 0.05$; Figure S4). The lack of AIE-induced change in dendritic spine density is consistent with the quantification of PSD-95, an indicator of synaptic number. The absence of changes in dendritic spine density and PSD-95 expression suggests that synaptic loss is not driving the AIE-induced changes in PAP-synaptic interactions.

Based on morphological measures of spine neck length and spine head width (Figure 7A–C), we observed no effect of treatment (AIE) ($F_{(3, 86)} = 3.368$, $p = 0.0699$), subregion ($F_{(3, 86)} = 1.331$, $p = 0.2696$), or interaction ($F_{(3, 86)} = 1.188$, $p = 0.3192$) on the % of immature (i.e., filopodia) spines (Figure 7D). When comparing the % of intermediate (i.e., long/thin) spines, there was a significant effect of treatment ($F_{(3, 440)} = 4.040$, $p = 0.0450$) and subregion ($F_{(3, 440)} = 12.04$, $p < 0.0001$) and a significant interaction ($F_{(3, 440)} = 8.833$, $p < 0.0001$). When

subregion differences in dendritic spine type were compared in EtOH-naïve animals (i.e.,
comparison of H_2O controls across subregions), there was a significantly higher % of
intermediate spines within the LO-OFC (when compared with the ACC ($p < 0.0001$; Figure 7D),
mPFC ($p < 0.0001$; Figure 4E), and VO-OFC ($p < 0.0001$; Figure 7E). There were no differences
in the % of intermediate spines when comparing all other subregions ($p > 0.05$, Figure 7E). *Post
hoc* analysis also revealed that there were no AIE-induced changes in the % of intermediate
spines in the ACC ($p = 0.5438$) and mPFC ($p = 0.2931$); however, there was a significant AIE-
induced decrease in the number of intermediate spines within the LO-OFC ($p = 0.0226$; Figure
7E) and an increase in the number of intermediate spines within the VO-OFC (Figure 7E).

Figure 7
The Effects of AIE on Dendritic Spine Maturation After a 26-Day Forced Abstinence Period.
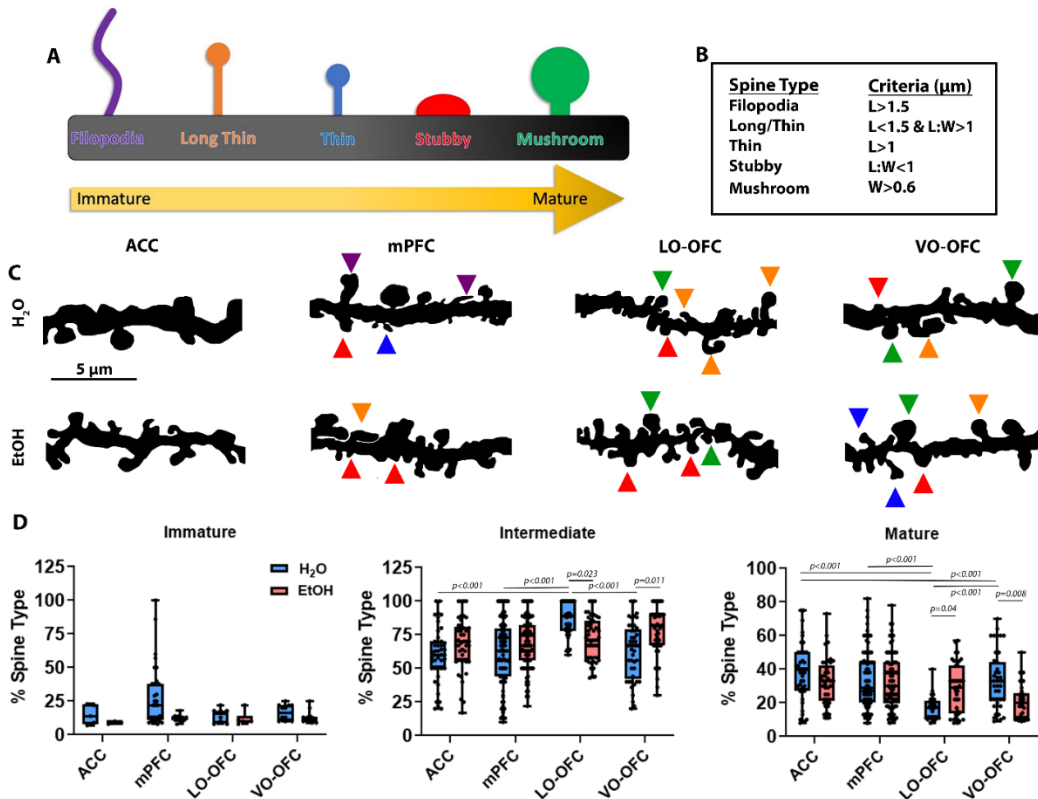
(**A**) Cartoon representation of the classification of different dendritic spine types and how they
correlate to maturation. (**B**) Table depicting how dendritic spines are classified. (**C**)
Representative images of secondary dendrites depicting spine types in the ACC, mPFC (IL/PL),

LO-OFC, and VO-OFC. Triangles indicate spine type based on color: Filopodia – purple; Long Thin – orange; Thin – blue; Stubby – red; Mushroom – green. (**D**) Analysis of dendritic spine maturation in the ACC, mPFC (IL and PL), LO-OFC, and VO-OFC. There was no change in the % of immature dendritic spines in any subregion ($p > 0.05$) following AIE or when comparing subregions ($p > 0.05$). In the LO-OFC, there was a significant decrease in intermediate spines ($p = 0.023$) and an increase in mature spines ($p = 0.04$) following AIE. In the VO-OFC, there was a significant increase in intermediate spines ($p = 0.011$) and a significant decrease in mature spines ($p = 0.008$) following AIE. Data presented as box and whisker plots with interquartile range with mean, minimum, and maximum measures indicated along with individual data points. Average spine densities were calculated using 2-3 separate dendrites from at least 4-5 separate image stacks per animal for a total of 15 dendritic branches/animal, n = 3/treatment group). Analysis: two-way ANOVA with Tukey's *post hoc* comparison. From "Diverging Effects of Adolescent Ethanol Exposure on Tripartite Synaptic Development Across Prefrontal Cortex Subregions," C.D. Walker, H.G. Sexton, J. Hyde, B. Greene, and M-L. Risher, 2022, *Cells*, *Open*, 11(19), p.12 (https://doi.org/10.3390%2Fcells11193111). CC BY 4.0.

Assessment of the % of mature (i.e., mushroom) dendritic spines following AIE treatment and within/across subregions revealed a subregion effect ($F_{(3, 390)} = 11.32$, $p < 0.0001$), no treatment effect ($F_{(1, 390)} = 1.530$, $p = 0.2168$), and an interaction between the two measures ($F_{(3, 390)} = 8.043$, $p < 0.0001$). *Post hoc* analysis revealed that when subregion differences in dendritic spine type were compared in EtOH-naïve animals (i.e., comparison of H_2O controls across subregions) there were significantly less mature spines within the LO-OFC when compared to the ACC ($p < 0.0001$; Figure 4D), mPFC ($p < 0.0001$; Figure 4F), and VO-OFC ($p = 0.0003$; Figure 7F). Interestingly, when assessing the effects of treatment, there was no AIE-induced change in the % of mature dendritic spines in the ACC ($p = 0.6307$) or mPFC ($p = 0.9996$). However, complementary to the changes in intermediate spines, there was a significant increase in the % of mature spines within the LO-OFC ($p = 0.0403$) and a significant decrease in the % of mature spines within the VO-OFC ($p = 0.0079$).

AIE-Induced loss of PAP-Synaptic Co-localization Is Not Driven by Changes in Expression of

Synaptic Stabilization Proteins

To determine if the loss of PAP-synaptic proximity in adulthood was due to a loss of

bridging proteins involved in tripartite synapse stabilization, we investigated changes in the

expression of neuroligins 1 and 3 and their presynaptic partner, neurexin. Analysis of these

critical stabilizing proteins revealed no AIE-induced changes in the expression in any of the PFC

subregions, indicating that a loss of these proteins is not a driver of the AIE-induced PAP-

synaptic decoupling (Figure S5). To further explore the effects of AIE on neurexin-neuroligin

interactions at the tripartite synapse, we assessed the co-localization of neurexin-neuroligin 1 and

neurexin-neuroligin 3.

Analysis of neurexin-neuroligin 1 co-localization revealed a significant treatment effect

(F (3, 286) = 14.08, p = 0.0002), subregion effect (F (3, 286) = 48.01, p < 0.0001), and a

significant interaction (F (3, 286) = 7.137, p = 0.0001). When subregion differences in neurexin-

neuroligin 1 co-localization were compared in EtOH-naïve animals (i.e., comparison of H_2O

controls across subregions), there was significantly higher co-localization within the ACC when

compared to mPFC (p < 0.0001; Figure 8B), LO-OFC (p = 0.0009; Figure 5B), and VO-OFC (p

< 0.0001; Figure 8B), with VO-OFC having the lowest neurexin-neuroligin 1 co-localization of

all four subregions. *Post hoc* analysis also revealed an effect of AIE on two PFC subregions.

Specifically, AIE resulted in a significant decrease in neurexin-neuroligin 1 co-localization in the

ACC (p = 0.0002; Figure 8B) and within the VO-OFC (p = 0.0394), consistent with the loss of

PAP-synaptic coupling within these two specific subregions. There was no AIE-induced change

in neurexin-neuroligin 1 co-localization within the mPFC (p = 0.9979; Figure 5B) or the LO-

OFC (p = 0.9392; Figure 8B).

Analysis of neurexin-neuroligin 3 co-localization revealed a significant treatment effect (F (3, 286) = 6.664, p = 0.0103), subregion effect (F (3, 286) = 19.97, p < 0.0001), and a significant interaction (F (3, 286) = 7.874, p < 0.0001). When subregion differences in neurexin-neuroligin 3 co-localization were compared in EtOH-naïve animals (i.e., comparison of H_2O controls across subregions), there was significantly higher co-localization within the ACC when compared to mPFC (p < 0.0001; Figure 9B) and VO-OFC (p < 0.0001; Figure 9B), but not when compared to the LO-OFC (p = 0.5565; Figure 9B). As with neurexin-neuroligin 1, co-localization of neurexin-neuroligin 3 was the highest within the ACC and lowest within the VO-OFC when all subregions were compared. Further *post hoc* analysis revealed an effect of AIE on two PFC subregions: specifically, AIE resulted in a significant decrease in neurexin-neuroligin 3 co-localization in the ACC (p = 0.00184; Figure 9B) and within the VO-OFC (p = 0.0635; Figure 9B), once again consistent with the loss of PAP-synaptic coupling within these two specific subregions. There were no AIE-induced changes in neurexin-neuroligin 3 co-localization within the mPFC (p = 0.2768; Figure 6B) or the LO-OFC (p > 0.9999; Figure 9B).

Figure 8
The Effect of AIE on Neurexin-Neuroligin 1 Interactions After a 26-Day Forced Abstinence Period.
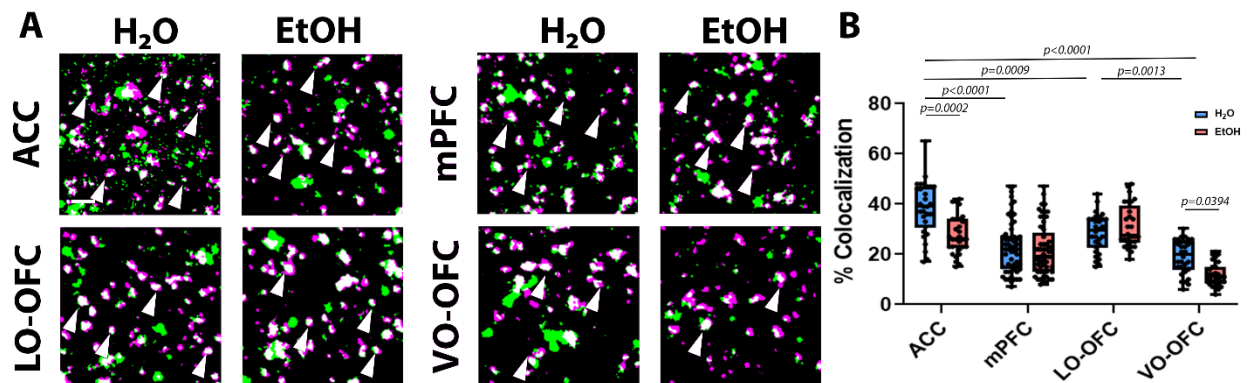
We found that AIE did not change neurexin or neuroligin 1 expression following a 26-day forced abstinence period (see supplemental data). (**A**) Representative images of neurexin (green) and neuroligin 1 (magenta) in the ACC, mPFC (IL and PL), LO-OFC, and VO-OFC. Scale bar, 2 μm. (**B**) Quantification of neurexin and neuroligin 1 co-localization. There was a significant decrease

in neurexin-neuroligin 1 co-localization in the ACC ($p = 0.0002$) and the VO-OFC ($p = 0.0394$) following AIE. Data presented as box and whisker plots with interquartile range with mean, minimum, and maximum measures indicated along with individual data points. Three 5 μm image stacks from randomly selected hemispheres were captured from 3 separate brain slices per animal (n = 9-10 brains/treatment group). Analysis: two-way ANOVA with Tukey's *post hoc* comparison. From "Diverging Effects of Adolescent Ethanol Exposure on Tripartite Synaptic Development Across Prefrontal Cortex Subregions," C.D. Walker, H.G. Sexton, J. Hyde, B. Greene, and M-L. Risher, 2022, *Cells*, *Open*, 11(19), p.14 (https://doi.org/10.3390%2Fcells11193111). CC BY 4.0.

Figure 9
The Effect of AIE On Neurexin-Neuroligin 3 Interactions After a 26-Day Forced Abstinence Period.
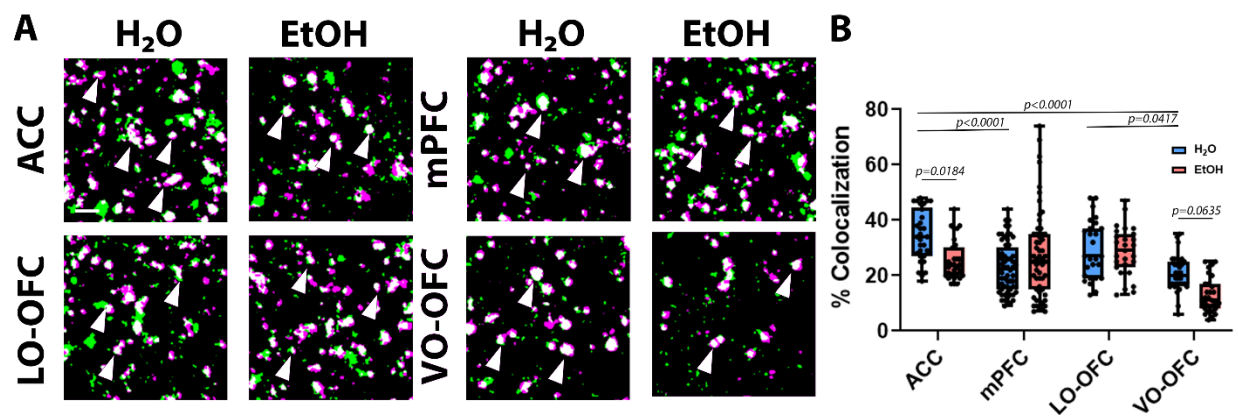
We found that AIE did not change neurexin or neuroligin 3 expression following a 26-day forced abstinence period (see supplemental data). (**A**) Representative images of neurexin (green) and neuroligin 3 (magenta) in the ACC, mPFC (IL and PL), LO-OFC, and VO-OFC. Scale bar, 2 μm. (**B**) Quantification of neurexin and neuroligin 3 co-localization. There was a significant decrease in neurexin-neuroligin 3 co-localization in the ACC ($p = 0.0184$) and the VO-OFC ($p = 0.0635$). Data presented as box and whisker plots with interquartile range with mean, minimum, and maximum measures indicated along with individual data points. Three 5 μm image stacks from randomly selected hemispheres were captured from 3 separate brain slices per animal (n = 9-10 brains/treatment group). Analysis: two-way ANOVA with Tukey's post-hoc comparison. From "Diverging Effects of Adolescent Ethanol Exposure on Tripartite Synaptic Development Across Prefrontal Cortex Subregions," C.D. Walker, H.G. Sexton, J. Hyde, B. Greene, and M-L. Risher, 2022, *Cells*, *Open*, 11(19), p.14 (https://doi.org/10.3390%2Fcells11193111). CC BY 4.0.

Discussion

The aim of this study was to investigate the impact of adolescent EtOH exposure on astrocyte morphology, PAP-synaptic proximity, and dendritic spine maturation in different PFC subregions, as well as to determine whether loss of neurexin-neuroligin cell adhesion proteins were a driving factor in the changes observed. Overall, we found a cortical subregion-specific

loss of PAP-synaptic co-localization/proximity after a 26- day forced abstinence period (in adulthood) within the ACC and VO-OFC that were not present during acute withdrawal. AIE-induced loss of PAP-synaptic co-localization was not due to an overall reduction in astrocyte volume or a loss of synapses; however, the loss of PAP-synaptic proximity did correlate with a significant shift towards a less mature dendritic spine phenotype in adulthood within the VO-OFC, as illustrated by an increase in intermediate spines and a corresponding decrease in mature spines (not seen in other subregions). Lastly, despite no changes in neurexin, neuroligin 1, or neuroligin 3 protein expression following AIE, there was a reduction in neuroligin-neurexin co-localization in the ACC and VO-OFC that correlated with a loss of PAP-synaptic co-localization and the VO-OFC-specific loss of dendritic spine maturity. Additional analysis demonstrated robust differences in AIE-naïve animals across PFC subregions, which included baseline differences in astrocyte volume, PAP-synaptic co-localization, dendritic spine morphology, and neurexin-neuroligin co-localization.

The human and rodent PFC continues to undergo structural and functional neuronal refinement during adolescence (Asato et al., 2010; Cressman et al., 2010; Cunningham et al., 2002; Liston et al., 2006; Markham et al., 2007; Rubia, 2013; Supekar et al., 2010). This ongoing developmental period is suggested to be a time of increased vulnerability to AIE-induced neuronal disruption. This has been demonstrated by Broadwater et al. (2018) in which they showed that AIE perturbed resting state connectivity using functional MRI connectivity between OFC-striatum and OFC-nucleus accumbens in rats. These findings correlate with multiple studies demonstrating AIE-induced deficits in PFC-dependent behaviors such as behavioral flexibility, increased disinhibition, and increased propensity to self-administer EtOH; all of which persist into adulthood (Coleman et al., 2011; Coleman et al., 2014; Gass et al., 2014;

Vetreno & Crews, 2012). However, there is growing evidence that behavioral outputs are highly reliant on astrocyte modulation of neuronal function. This has been demonstrated in a number of studies using designer receptors exclusively activated by designer drugs (DREADDs) that specifically target astrocytes and result in subsequent modulation of rodent behavior (for a review, see Hwang et al. (2021)). One study of particular importance was conducted by Erickson et al. (2021) in which they showed that activation of astrocyte-specific excitatory DREADDs within the PFC (IL, PL, and ACC combined) can regulate EtOH consumption, supporting a critical role for astrocytes in addiction-related behavior.

Astrocytes are able to modulate neuronal function and thus behavior via the uptake of neurotransmitter from the synaptic cleft, the release of gliotransmitters, and through contact-mediated and astrocyte-secreted signaling factors (for a review, see Allen (2014a) and Blanco-Suarez et al. (2017)). One structural characteristic that all of these signaling mechanisms require is astrocyte proximity to the synapse. In the current study, we found that the ACC and VO-OFC appear to be particularly vulnerable to disruption of PAP-synaptic co-localization, suggesting a loss of astrocyte proximity to the synapse. Despite assessing this measure acutely within 24 h of the last dose, the loss of PAP-synaptic coupling only emerged in adulthood after prolonged abstinence, and not in all subregions of the PFC. It is unclear whether these subregion differences are due to astrocyte heterogeneity or variations in the state of developmental maturation of the PAP-synaptic relationship, within the different PFC subregions. However, there are indications from our data that suggest that there could indeed be very different astrocyte populations within these subregions. For example, in every comparative statistical measure conducted in this study assessing differences between EtOH naïve animals (i.e., control animals only) in different subregions, we were able to demonstrate that the ACC has significantly higher astrocyte volume

with less PAP-synaptic coupling, a higher ratio of mature spines, and higher levels of neurexin-neuroligin co-localization than all other subregions, particularly when compared to the VO-OFC. While there were a variety of differences across the various subregions at baseline, the most pronounced differences were seen when comparing ACC and VO-OFC. Interestingly, these two regions were also the most vulnerable to PAP-synaptic decoupling. Why the loss of PAP-synaptic proximity occurred specifically within the VO-OFC and the ACC requires further investigation, as does the mechanism underlying the delayed occurrence of this phenomenon (i.e., not present at the acute timepoint but emerges during prolonged abstinence, in adulthood). Understanding astrocyte heterogeneity across PFC subregions and the unique neuronal populations that these astrocytes serve will be necessary moving forward.

Due to the AIE-induced loss of PAP-synaptic co-localization in ACC and VO-OFC we investigated the impact that the loss of proximity would have on dendritic spine number and morphology. Previous work by Witcher et al. (2007) using serial section electron microscopy of mature rat hippocampal slices demonstrated that synapses are larger when PAPs are present. This is consistent with the findings in the current study in which we demonstrated a shift towards a less mature dendritic spine phenotype that only occurred in the VO-OFC where there was a significant loss of PAP-synaptic proximity, suggesting a strong relationship between dendritic spine maturity and PAP proximity. The current finding that AIE increased the presence of intermediate dendritic spines in the VO-OFC is consistent with McGuier et al. (2015) who previously showed that the more immature phenotype is present after a 7-day abstinence period but not during peak withdrawal. However, here we showed that even after a prolonged period (26 days) of abstinence, the changes in dendritic spine phenotype persist.

An interesting finding that emerged from the dendritic spine analysis was that, following EtOH exposure, when the % of mature dendritic spines decreased in the VO-OFC, they increased in the LO-OFC. When the % of intermediate dendritic spines increased in the VO-OFC, they decreased in the LO-OFC without affecting overall spine density. It is possible that the increase in mature spines within the LO-OFC was due to an increase in PAP-synaptic proximity without impacting the overall number of colocalized puncta, though this is difficult to determine due to the limitations of the analysis in which we used a threshold of 0.5 µM to define proximity (due to resolution limits). We are currently unable to determine with any accuracy whether PAPs are in fact getting closer to the synapses as a result of AIE exposure. Further analysis using super-resolution and/or electron microscopy would be beneficial to further define changes in proximity across PFC subregions. In summary, there were clear differences in sensitivity to AIE-induced loss of PAP-synaptic proximity and corresponding dendritic spine morphology across OFC subregions, despite no change in overall spine density.

Previous work in mice has shown that proteins responsible for bridging the tripartite synapse, such as neurexin-neuroligin and eph-ephrin, are critical for dendritic spine stabilization and maturation (Nishida & Okabe, 2007), synaptic function, and even astrocyte complexity (Stogsdill et al., 2017). Since AIE resulted in a sub-region dependent shift towards a less mature dendritic spine phenotype, we investigated if a loss of neurexin and neuroligin expression could be driving the changes in dendritic spine phenotype. Following AIE, there were no changes in expression of neurexin, neuroligin 1, or neuroligin 3. However, work by Ko et al. (2009) previously showed that using mutational disruption of neurexin-neuroligin binding prevents normal increases in pre- and post-synaptic size. Based on this finding, we next assessed colocalization of neurexin-neuroligin 1 and neurexin-neuroligin 3, hypothesizing that the loss of

PAP-synaptic proximity may prevent appropriate localization of neurexin-neuroligins and therefore impede normal synaptic enlargement. In the current study, we were able to confirm that, despite no change in the expression of either neurexin or neuroligins 1 or 3 following AIE, there was a decrease in co-localization of neurexin-neuroligin 1 and 3 specifically in the ACC and VO-OFC (where a change in dendritic spine phenotype was also observed). However, this finding is inconclusive since it is possible that AIE directly disrupts neurexin-neuroligin binding sites or drives the generation of alternate splice variants, thereby disrupting the ability of neurexin-neuroligin to interact. Another possibility is that leucine-rich repeat transmembrane neuronal proteins (LRRTM2), which bind to neurexins and work synergistically with neuroligin 1 are impacted by AIE, thus modulating neurexin-neuroligin 1 interactions (Siddiqui et al., 2010). However, based on the pro-synaptogenic properties of LRRTM2 (Dagar & Gottmann, 2019; de Wit et al., 2009) we would likely see changes in PSD-95 puncta or changes in dendritic spine density, indicative of pro or anti-synaptogenic signaling, depending on the type of AIE-induced protein modulation that occurs. Further work is necessary to determine whether neurexin-neuroligin binding is impaired and if so, precedes PAP-synaptic decoupling.

Changes in astrocyte morphology and increased protein expression at the level of GFAP antibody staining are considered to be signs of astrocyte reactivity/activation and correlated with the induction of neuroinflammation (Norden et al., 2016; Pelinka et al., 2004; Reilly et al., 1998) and injury. GFAP upregulation and immune activation have also been demonstrated to occur following EtOH exposure in rats and mice (Grifasi et al., 2019; Nwachukwu et al., 2021; Nwachukwu et al., 2022). However, GFAP antibody staining only captures the backbone of the astrocyte and not the fine processes that interact with blood vessels, other astrocytes, or synapses. Moreover, we have previously demonstrated that hippocampal astrocytes begin

releasing factors associated with reactivity much earlier than the appearance of increased GFAP expression (Risher, Sexton, et al., 2015) in an identical model, suggesting that GFAP expression is not the most sensitive measure for astrocyte reactivity. However, there is no doubt that astrocytes become reactive and can drive neuroinflammation or the response to neuroinflammation (Liddelow et al., 2017; Mrak et al., 1995; Wyss-Coray, 2006). The questions that remain are whether changes in GFAP expression are reflective of changes at the PAPs, and whether GFAP expression can be correlated with a loss of PAP-synaptic coupling. Furthermore, it has yet to be demonstrated that neuroimmune activation can directly drive PAP-synaptic decoupling.

We have demonstrated that AIE-induced loss of PAP-synaptic coupling is PFC subregion-dependent. Based on astrocyte volumetric measures, it is quite possible that we are comparing two different astrocyte populations that are likely providing support for different types of neurons. This raises questions of whether all synapses are equally dependent on astrocyte support for spine morphology, and whether all tripartite synapses are equally dependent on the presence of these particular NLGN-NRXN interactions.

However, the implications of AIE-induced loss of PAP-synaptic coupling go beyond the health of dendritic spines and could significantly impact the glymphatic system and astrocyte-astrocyte communication, both of which are critical for maintaining the movement of cerebrospinal fluid and ion homeostasis. Previous work demonstrates that even chronic 30-day exposure to 1.5 g/kg EtOH (i.p.) can significantly diminish glymphatic function in the mouse (Lundgaard et al., 2018) and has been associated with the development of dementia in humans (Reeves et al., 2020), particularly in heavy drinkers (Xu et al., 2009).

Conclusions

These data provide novel insight into the selective vulnerability of astrocyte-synaptic interactions and dendritic spine morphology within PFC subregions following AIE. Interestingly, many of these effects occur well after the acute effects of EtOH have dissipated, suggesting delayed and enduring changes to astrocyte-synaptic interactions that persist into adulthood. Given the importance of astrocytes in regulating synaptic activity and their emerging role in behavioral regulation, further work is necessary to determine the molecular mechanisms that drive the loss of PAP-synaptic coupling and to understand why some PFC subregions display increased vulnerability to the effects of AIE. How changes in PAP-synaptic proximity and dendritic spine morphology contribute to the neuronal and behavioral changes observed following repeated AIE will be an important step moving forward and may provide novel non-neuronal targets for future pharmacological interventions.

Chapter 5

The Effects of Adolescent Ethanol Exposure on Hippocampal Astrocyte Morphology, Synaptic Interactions, and Astrocyte Responsivity to Neuronal Signaling in Female Rats

C.D Walker[1,2], H.G. Sexton[1,2], H. Hylton[1], I. Parsons[1], L. Reasor[1], D. Prasad[1], L. Titus[1], T Carter[1], O. Coulter[1], B.J. Henderson[1], and M-L Risher[1,2]

[1]Department of Biomedical Research, Joan C. Edwards School of Medicine, Marshall University, Huntington, WV 25701, USA

[2]Neurobiology Research Laboratory, Hershel 'Woody' Williams Veterans Affairs Medical Center, Huntington, WV 25704, USA

Women are especially vulnerable to the effects of alcohol as biological differences between males and females result in higher rates of absorption and longer time to metabolize alcohol resulting in higher blood alcohol concentrations in females compared to males when consuming identical amounts of alcohol (see (Erol & Karpyak, 2015) for review). These differences in alcohol absorption and metabolism make women more susceptible to the long-term adverse effects of alcohol consumption.

Traditionally, it has been reported that males consume more alcohol than females. However, more recent studies have shown that this gap in consumption is narrowing. A national survey revealed that in 2019, 32% of female high school students consumed alcohol compared to 26% of male students (Jones et al., 2020). Alcohol consumption in the form of binge drinking has also increased among females, with 15% of female high school students reporting binge drinking compared to 13% of male students (Jones et al., 2020). This increased incidence of binge drinking coincides with critical late-stage adolescent maturation of key brain regions such as the hippocampus, which is particularly vulnerable to the detrimental effects of early alcohol use (see Walker et al. (2021) for additional information). More recently, during the COVID-19 pandemic has been a rise in the number of females reporting an increase in alcohol consumption. A recent survey found that 1 in 5 females reported a rise in alcohol consumption after the onset of the COVID-19 pandemic (Campbell et al., 2023; Devoto et al., 2022). While these studies did not separate their data to isolate female adolescents, their findings support the continued increasing trend in alcohol consumption among females reported in other studies.

In previous chapters, we discussed the prevalence of alcohol use among adolescents (Chapter 1) and the effects of alcohol use on the developing hippocampus (Chapter 3).

In this chapter, we have sought to investigate the acute and chronic effects of AIE on astrocyte morphology and function in the CA1 of the dhipp in female rats. In this study, we use viral vectors and immunohistochemistry and collect physiological recordings to determine and analyze astrocyte morphology, PAP-synaptic proximity, and astrocyte responsivity to neuronal signaling. We hypothesize that AIE changes astrocyte morphology that coincides with changes in PAP-synaptic proximity in adulthood. Furthermore, we hypothesize that AIE results in deficits in astrocyte responsivity to neuronal signaling.

Materials and Methods

All procedures used in this study were conducted in accordance with the guidelines of the Institutional Animal Care and Use Committee and were approved by the Hershel 'Woody' Williams Veterans Affairs Medical Center and Marshall University, Huntington, WV.

Animals and Surgical Procedures

A total of 36 female Sprague Dawley rats (Hilltop, Scottdale, PA, USA) were received, double-housed, and maintained in a temperature- and humidity-controlled environment with ad libitum access to food and water on postnatal day (PND) 24. Animals were kept on a 12-hour:12-hour reverse light:dark cycle (lights on at 6:00 pm and off at 6:00 am). Surgical procedures were performed as previously described in Testen et al. (2019) and Walker et al. (2022) with minor modifications. Animals were allowed to habituate for two days prior to handling and surgical procedures. On PND 26-27 rats (n=6/treatment group) received 0.3 mg/kg intraperitoneal injection (i.p.) of 25% w/v mannitol (Carty et al., 2013, Testen et al., 2019, Walker et al., 2022) and were anesthetized with a cocktail of ketamine (30 mg/kg), xylazine (2.5 mg/kg), and acepromazine (0.5 mg/kg). The depth of anesthesia was closely monitored throughout the procedure. After shaving the area where the incision would be made, animals were secured into a

stereotaxic frame via nose clip and blunt ear bars. The surgical site was cleaned three times with 70% ethanol and 10% iodine. A burr hole was drilled into the skull allowing for unilateral injection of virus suspension into the dorsal hippocampus at the following coordinates, −3.2mm anterior/posterior, +/− 2.6mm medial/lateral, +3.0mm dorsal/ventral. Animals received either 1 μL AAV1/5 gfaABC1D Lck-GFP diluted in 1:1 H_2O (3.26 x 10^{12} gc/mL; Addgene plasmid # 105598; http://n2t.net/addgene:105598; Shigetomi et al. (2013)), 1 uL AAV5 gfaABC1D GCamp6f (7.3 x 10^{12} gc/mL; Addgene plasmid # 52925; http://n2t.net/addgene:52925; Haustein et al. (2014)), or AAV5.GFAP.iGluSnFr.WPRE.SV40 (1 x 10^{13} gc/mL; Addgene plasmid # 98930; http://n2t.net/addgene:98930; Marvin et al. (2013)) administered by microinjection using a syringe pump and 26-gauge needle with a dwell time of 10 minutes. The burr whole was closed with bone cement, then bupivacaine was administered to the site, and the surgical incision was closed with dissolvable external sutures. Antibiotic ointment was applied to the incision, saline was administered via subcutaneous injection to prevent dehydration, and the animal was allowed to recover on a heating pad. Once the animal was fully awake and mobile, it was returned to its home cage with its original cagemate.

Intermittent Binge EtOH Exposure

Beginning on PND 30, animals received 10 doses of 5 g/kg EtOH (35% v/v in H_2O) or H_2O via intragastric gavage (i.g.) using a two days on, one day off, two days on, two days off intermittent schedule over 16 days (Figure 10), as previously described (Walker et al., 2022). The individual administering the EtOH was responsible for observing animals after EtOH administration to ensure full recovery from intoxication. The individual administering the EtOH was responsible for ensuring that everyone involved in the subsequent experiments remained blinded to treatments until the completion of the study. Animals were euthanized and brain tissue

was collected on PND 72-76 following a 26- to 30-day forced abstinence period. The EtOH

dosage was selected to produce blood EtOH concentrations (BECs) consistent with those of

adolescent humans during binge drinking episodes (Donovan, 2009) and consistent with our

previous studies where BECs reached 172-199 mg/dL (Risher, Sexton, et al., 2015; Walker et al.,

2022) All animals undergoing behavioral testing underwent the 26-day forced abstinence period.

Figure 10
Experimental Timeline.
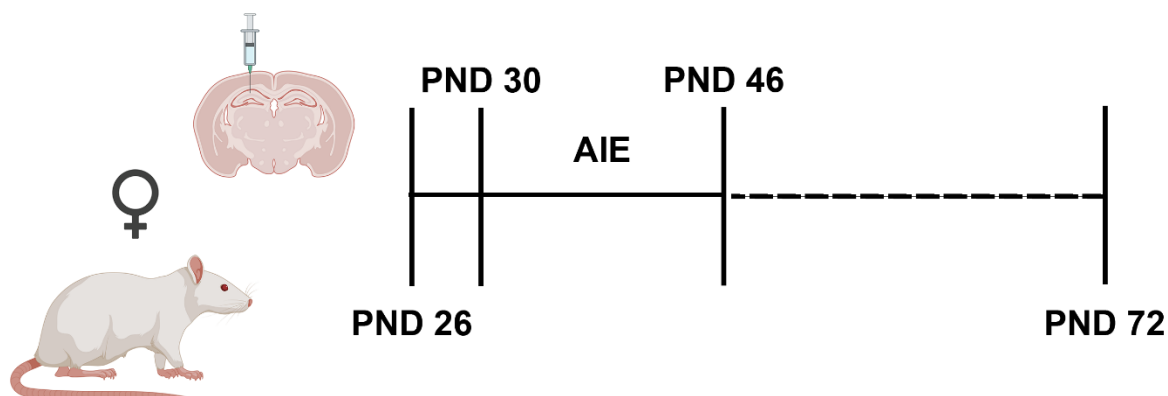
Animals received an intracranial injection of an astrocyte-specific adeno-associated virus with a
GFP on PND 26. Animals underwent AIE and received 5 g/kg EtOH (35% v/v in H_2O) or H_2O
via intragastric gavage (i.g.) intermittently over 16 days. Animals underwent a period of forced
abstinence from PND 46 to PND 72. Tissue was harvested for immunohistochemistry on PND
72 or physiological recordings began on PND 72. Created with Biorender.

Immunohistochemistry (IHC)

Brain Section Preparation. At PND 72, animals were deeply anesthetized with

isoflurane (6 animals/treatment group/experiment; total n = 24). Animals were transcardially

perfused with phosphate buffered saline (PBS; pH 7.4; cat# P5368, Sigma-Aldrich, St. Louis,

MO, USA) for 5 minutes, followed by 4% paraformaldehyde (PFA; cat# 19210, Electron

Microscopy Solutions, Hatfield, PA, USA) for 12 minutes (20 mL/min). Brains were extracted

and post-fixed in 4% PFA at 4°C overnight followed by 30% glycerol (cat# G5516-1L, Sigma-

Aldrich, St. Louis, MO, USA) in PBS at 4°C for 1-2 days. Brains were then placed in a 2:1

solution of 30% sucrose to OTC freezing compound (Electron Microscopy Sciences, Hatfield, PA, USA) and stored at -80 °C. Using a cryostat (CM 1950, Leica Biosystems, Richmond, IL, USA), fixed tissue was sliced into 80 µm or 40 µm sections, depending on the experiment.

PSD-95 and GFAP. 80 µm sections underwent antigen retrieval as previously described in (Jiao et al., 1999; Testen et al., 2019; Walker et al., 2022). Free-floating slices were briefly rinsed three times (5 minutes each) in 0.1 M phosphate buffer (PB; 3.1 g/L NaH_2PO_4, 10.9 g/l Na_2HPO_4, pH 7.4), then transferred to a 10 mM sodium citrate buffer preheated to 80 °C for 30 minutes, shaking every 10 minutes. Slices were then allowed to cool to room temperature followed by three additional washes (5 minutes each) in 0.1 M PB (pH 7.4). Slices were blocked with 5% normal goat serum (NGS, cat# 005-000-121, Jackson Immunolabs, West Grove, PA, USA) in phosphate-buffer in saline (PBS) with triton (PBST; 0.2% triton 100-X; cat# 13134900, Roche,) for one hour at room temperature. Sections were then incubated for four days in mouse anti-PSD-95 (1:450; cat# MA1-045, ThermoFisher Scientific, Waltham, MA, USA) and rabbit anti-GFAP (1:500 cat# Z0334, Agilent Technologies, Santa Clara, CA, USA) in PBST (0.2% triton 100-X) and 5% NGS at 4 °C on shaker. Sections were then washed three times (5 minutes each) in PBST (0.2% triton 100-X) and incubated for 6 hours at room temperature in Alexa Fluor goat anti-mouse 594 (1:200; cat# A-11032, Molecular Probes, Eugene, OR, USA) and Alexa Fluor goat anti-rabbit 647 (1:200, cat# A-21245 ThermoFisher Scientific, Waltham, MA, USA) in PBST (0.2% triton 100-X) and 5% NGS. Sections were then washed three times (5 minutes each in PBST (0.2% triton 100-X) and once in PBS. The sections were then mounted with Vectashield with DAPI (cat# H-1200, Vector Laboratories West Grove, PA, USA), coverslipped, and sealed with nail varnish.

Neuroligin 1, Neurexin, and Hevin. 40 µm sections were rinsed three times (10 minutes each) with PBST (0.2% triton 100-X) then blocked at room temperature for 1 hour in 5% normal donkey serum (NDS) and PBST (0.2% triton 100-X). Sections were then incubated overnight in mouse anti-neuroligin 1 (1:500, cat# 129111, Synaptic Systems) or mouse anti-neuroligin 3 (1:500, cat# 129311, Synaptic Systems, Goettingen, Germany), with goat anti-hevin (1:500, cat# AF2836, Synaptic Systems), and with rabbit anti-neurexin 1/2/3 (1: 500, cat# 175003, Synaptic Systems, Goettingen, Germany), 5% NDS and PBST (0.2% triton 100-X) at 4 °C. Slices were then washed three times (5 minutes each) in PBST (0.2% triton 100-X) then incubated for 2 hours at room temperature in donkey Alexa Fluor 594 anti-mouse (1:200 Alexa Fluor cat# A11029, Lifetech), Alexa Fluor 488 donkey anti goat (1:200, cat# A11055, Lifetech), and Alexa Fluor 647 donkey anti rabbit (1:200, cat# A21245, Lifetech) in 5% NDS and PBST (0.2% triton 100-X). Slices were washed three more times in PBST (0.2% triton 100-X) then mounted with Vectashield with DAPI (cat# H-1200Vector Laboratories West Grove, PA, USA), coverslipped, and sealed with nail varnish.

Data Acquisition and Processing

Astrocyte Volume and Astrocyte-Synaptic Co-Localization. A Leica SP5 laser-scanning confocal microscope with 63× oil-immersive objective, NA 1.45 (Leica, Wetzlar, Germany) was used for image acquisition. Acquisition parameters for AAV[+] astrocyte-PSD-95 imaging were set at 1024 × 1024 pixels frame size, 16-bit depths, 4× lines averaging, 1 µm z-step size. Lck-GFP expression pattern is diffuse, aiding in the acquisition of single, isolated astrocytes. Individual, whole GFP[+] astrocytes were randomly selected by the experimenter. GFP[+], GFAP, and PSD-95 were then imaged within the CA1 dorsal hippocampus (dhipp) and 4-6 individual astrocytes were captured from each (2-3 brains/treatment group).

Astrocyte-PSD-95 co-localization was performed as previously described in Testen et al. (2019) and Walker et al. (2022), with modifications. AutoQuant X3.1.2 software (Media Cypernetics, Rockville, MD, USA) was used to deconvolve raw images before digitally reconstructing z-stacks. AutoQuant's algorithm for blind deconvolution with 10 iterations was run on each z-stack prior to reconstruction. Parameters for blind deconvolution are automatically optimized by the software based on confocal, objective, and imaging specifications. Output files were directly imported to Imaris x64 version 9.0 (Bitplane, Santa Barbara, CA, USA) for 3-dimensional reconstruction. Using Imaris, each individual astrocyte was first isolated from a Lck-GFP background signal using a surface building feature. Surface rendering enables the extraction of morphometric values, including surface area and volume, and generates a new Lck-GFP channel devoid of background noise, revealing only a signal from a single isolated astrocyte. Close attention was paid to verify that collected Lck-GFP signal accounted for a single astrocyte, in its entirety. Co-localization of the Lck-GFP and GFAP signals was used to confirm astrocyte identity for quantification. Only confirmed astrocytes that were captured in their entirety were used for quantification and analysis. The isolated Lck-GFP channel (surface mask) was used, in conjunction with the PSD-95 channel, to perform colocalization analysis to determine the proximity between the astrocytes and post-synaptic neuronal terminals. Before co-localization analysis, the threshold for the PSD-95 signal was manually determined by measuring the fluorescence intensity of unambiguous PSD-95 positive puncta on multiple optical planes by a blinded experimenter. This was achieved by rotating the reconstructed astrocyte image in 3D space while adjusting voxels to ensure that PSD-95 expression could be observed without the interference of background noise. An average of these measurements was used as a final PSD-95

signal threshold value. Co-localization was reported as % of astrocyte volume (identified as Lck-GFP$^+$ surface reconstruction) co-localized with the PSD-95 channel.

Neuroligin 1, Neurexin, and Hevin. Confocal z-stacks (5 µm thick, optical section depth 0.33 µm, and 1024 × 1024 image size) of the dhipp were imaged on a Leica SP5 laser-scanning confocal microscope with 63× oil-immersive objective, NA 1.45 (Leica, Wetzlar, Germany). A total of 3 randomly selected image stacks from 3 randomly selected hemispheres were captured from 3 separate brain slices per animal (4-6 brains/treatment group).

Images were analyzed based on Risher, Fleming, et al. (2015) with slight modification. Z-stacks were uploaded into ImageJ 1.53t (NIH, USA) and converted to RGB files to allow for analysis of expression of all proteins and the colocalization of two proteins (neuroligins 1 or 3 with neurexin) and three proteins (neuroligin 1, hevin, and neurexin). Maximum projections of 3 consecutive optical sections (corresponding to 1 µm total depth) were generated from the original *z*-stack. The Puncta Analyzer plugin (available upon request from c.eroglu@cellbio.duke.edu) for ImageJ was used to count the individual number of proteins of interest and co-localized proteins (Ippolito & Eroglu, 2010).

Physiological Recordings

Glutamate and Calcium Signaling and Recording. Prior to EtOH or H$_2$O administration, animals received intracranial injection of one of the following astrocyte-specific AAVs: AAV5.gfaABC$_1$D.GCamp6f or AAV5.GFAP.iGluSnFr.WPRE.SV40 at PND 26. At PND72-76, animals were deeply anesthetized with isoflurane and transcardially perfused with *N*-methyl-D-glucamine – HEPES (NMDG-HEPES) recovery solution consisting of (in mM) 93 mg NMDG, 2.5 mg KCl, 1.2 NaH$_2$PO$_4$, 30 mg NaHCO$_3$, 20 mg HEPES, 25 mg D-glucose, 5 mg sodium ascorbate, 2 mg thiourea, 3 mg MgSO$_4$•7H$_2$O, 0.5 mg CaCl$_2$•2H$_2$O that had been

bubbled with a carbogen (95% O_2 and 5% CO_2). Whole brain tissue was embedded in agar and 250 µm coronal sections were obtained using a Comprestome (Precisionary Instruments, Natick, MA, USA) and incubated in NMDG-HEPES recovery solution at 32 °C for 12 minutes while bubbling with carbogen. Slices were then transferred to an artificial cerebrospinal fluid (ACSF) consisting of (in mM) 125 mg NaCl, 1.6 mg KCl, 1.2 mg NaH_2PO_4, 2.4 mg $CaCl_2$, 1.2 mg $MgCl_2$, 18 mg $NaHCO_3$, 11 mg glucose that was bubbling in carbogen and incubated in a water bath at 32 °C for 1 hour. Individual slices were transferred to the recording stage equipped with a Zeiss Axicam 702 mono camera and perfused with ACSF at a constant flow rate of 4 ml/min maintained at 32 °C. Astrocytes of interest were identified by expression of GFP (GCamp6f) or mCherry (iGluSnFr). Physiological recordings were collected using methods as previously described in Haustein et al. (2014) with slight modification. The tip of a 0.254 mm carbon-fiber bipolar microelectrode (MS303-1-B-SPCL, Plastics One, Roanoke, VA, USA) was placed at the CA3 Schaffer Collateral being careful as to not come into direct contact with tissue. The electrode should be approximately 30-80 µm above the tissue (Haustein et al., 2014) to prevent stimulation artifacts. Baseline fluorescence was recorded from the astrocyte of interest in the CA1 for 5 seconds prior to Schaffer Collateral stimulation with an A.M.P.I. Master 9 Stimulator (A.M.P.I., Jerusalem, Israel). Individual 1 ms pulses were delivered at 40 µA with 15 pulses per second at a rate of 15 Hz. Recording continued for an additional 15 seconds following stimulation.

Analysis. Video recordings of changes in fluorescent activity were captured using Zeiss ZEN Pro (Blue edition) version 3.7.97.04000 (Zeiss, White Plains, NY, USA). A region of interest was created to isolated GFP (GCaMP6f) or mCherry (iGluSnFr) positive astrocytes in the field of view of the CA1 dhipp. Individual fluorescent values were transferred to an Excel

spreadsheet. Values were isolated to 2 seconds prior to neuronal stimulation and continued for an additional 10 seconds to capture fluorescent response. A linear equation was extrapolated from the fluorescence recordings across the 2 seconds prior to Schaffer Collateral stimulation. This equation was then used to normalize the fluorescence recording to account for loss of fluorescence intensity due to exposure to the mercury lamp during recording. Then, $\Delta F/F$ was used to determine changes in fluorescent intensity following Schaffer Collateral stimulation.

Statistical Analysis

Data were compiled using Excel 365 (Microsoft, Redmond, WA, USA) and analyzed using GraphPad Prism version 9.4.1 (GraphPad Software, San Diego, CA, USA). A Student's t-test was performed for analysis of each dataset. Statistical significance was assessed using an alpha level of 0.05. Data are presented as violin plots with individual plot points and with median displayed.

Figure 11

AIE Results in an Increase in CA1 Hippocampal Astrocyte Volume and PAP-Synaptic Colocalization in Adulthood.
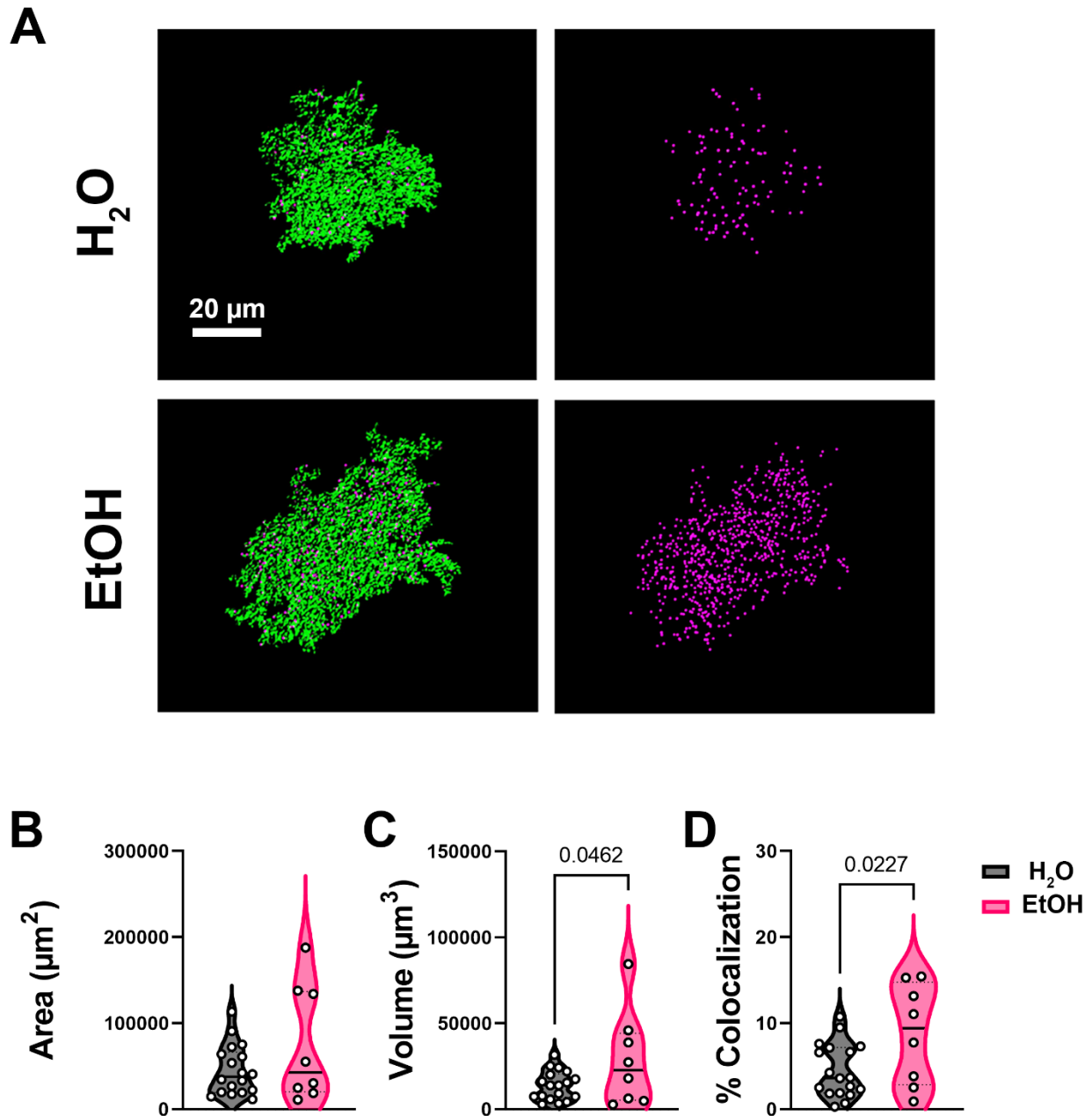
A) Single cell representative images of surface renderings of astrocytes following the 26-Day forced abstinence period in green in panels on the left. PSD-95 that is within 0.5 µm of PAPs are represented as individual magenta points in panels on the right. B) Quantification of astrocyte area shows no change in astrocyte area. C) Quantification of astrocyte volume revealed a significant increase in astrocyte volume in animals that received EtOH. D) Quantification of PAP-synaptic colocalization, reported as a percentage of astrocyte volume colocalized with PSD-95. Analysis revealed a significant increase in PAP-synaptic colocalization in animals that

received EtOH during AIE. Analysis: Student's t-test, n = 3-7 astrocytes/animal (2-3 animals/treatment group).

Results

Astrocyte Morphology and PAP-Synaptic Proximity

First, we wanted to see if AIE resulted in changes in astrocyte morphology in the form of changes in astrocyte volume. After acquiring images of GFP^+ astrocytes from the CA1 dhipp, astrocytes were reconstructed (Figure 11A), and cell surface areas and volumes were quantified (Figure 11B and C). We observed no change in astrocyte area (t(24) = 1.589, p = 0.1251). However, we observed a significant increase in astrocyte volumes of AIE animals compared to H_2O age-matched controls (t(24) = 2.102, p = 0.0462). Next, we wanted to see if AIE-induced changes in astrocyte morphology corresponded to a change in PAP-synaptic interactions (Figure 1C). Analysis revealed a significant increase in PAP-synaptic colocalization in AIE animals compared to H_2O age-matched controls (t(24) = 2.434, p = 0.0227).

Figure 12

AIE Results in an Increase in the Expression of Proteins Necessary for Synaptic Stabilization But Has No Impact on Protein-Protein Interactions.
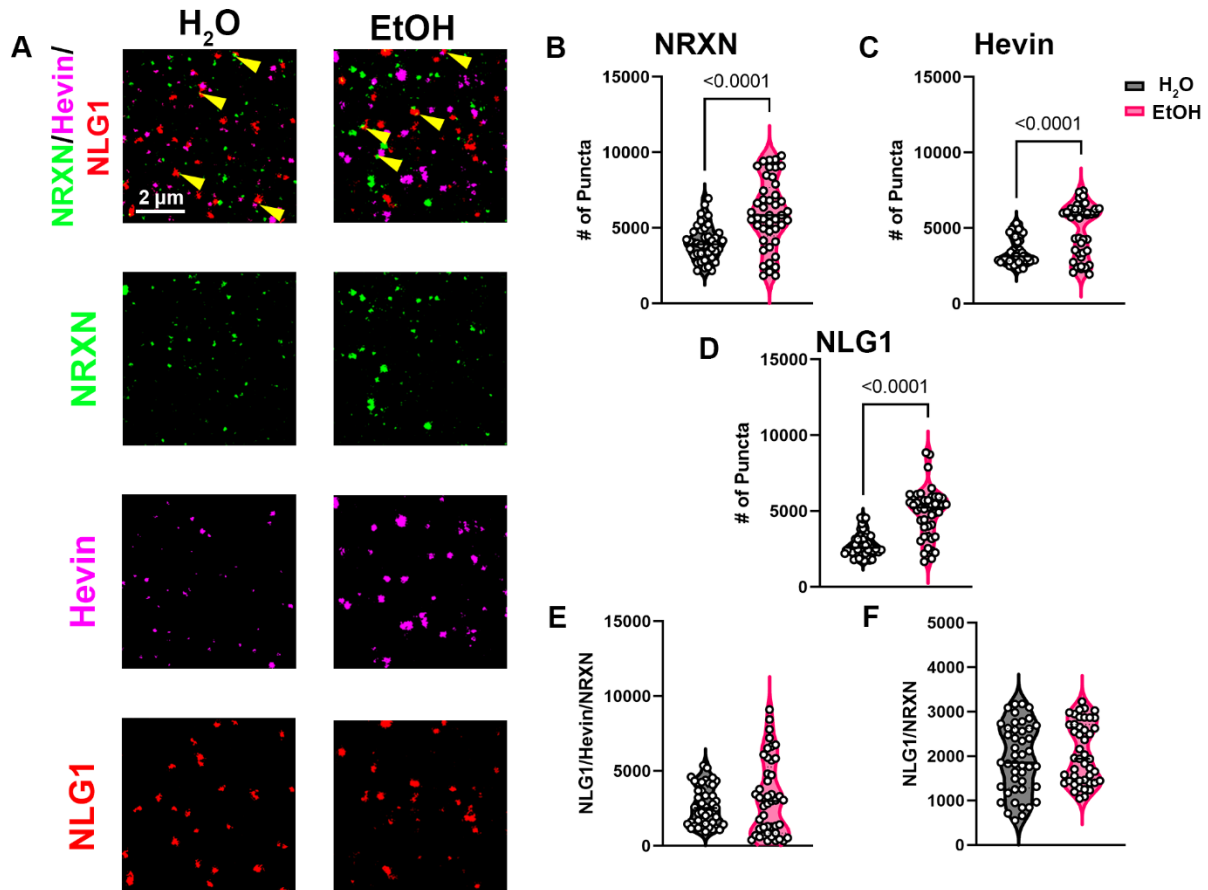
A) Representative images of the colocalization of synaptic bridging proteins neurexin (NRXN), Hevin, and neurolin-1 (NLG1) as well as representative images of individual protein expression in H_2O and EtOH treated animals. Yellow arrows indicate where all three briding proteins are coming into contact. B) There was a significant increase in presynaptic neurexin expression following AIE, C) Quantification revealed that there was a significant increase in the neuroligin 1-neurexin bridging protein, Hevin. D) There was also a significant increase in neuroligin 1 expression, found on the postsynaptic dendrite and ensheathing PAPs. There was no change in the colocalization of the bridging proteins neuroligin1-Hevin-neurexin (E; (t(88) = 1.203, p = 0.2321) or neuroligin 1-neurexin (F; (t(88) 0.8052), p = 0.4229). Analysis: Student's t-test, n = 4-5 images per animal (5 animals/treatment group).

AIE Results in Increased Expression of Synaptic Proteins But Has No Effect On Their

Interactions

Next, we wanted to test whether AIE-induced loss of PAP-synaptic proximity was driven

by changes in structural protein expression and interactions that are necessary for the

stabilization of the tripartite synapse. IHC imaging and analysis revealed a significant increase in

presynaptic neurexin expression in AIE animals compared to H_2O age-matched controls (Figure

12B; t(88) = 5.109, $p < 0.0001$). Furthermore, there was a significant increase in the neuroligin

1-neurexin bridging protein, Hevin, in AIE animals compared to H_2O age-matched controls

(Figure 12C; t(88) = 4.633, $p < 0.0001$). We also observed a significant increase in neuroligin 1

expression, compared to H_2O age-matched controls (Figure 12D; t(88) = 7.334, $p < 0.0001$).

Lastly, we observed no change in the colocalization of the synaptic proteins neuroligin1-Hevin-

neurexin (12; (t(88) = 1.203, $p = 0.2321$) or neuroligin 1-neurexin (F; (t(88) 0.8052), $p =$

0.4229), that are essential for excitatory synapse stabilization.

Figure 13

AIE Results in a Decrease in Astrocyte Responsivity to Neuronal Stimulation in Adulthood.

A) Experimental timeline showing that female rats received intracranial injections of an astrocyte specific Ca^{2+} sensor (GCamp6f) at PND 26 to record changes in Ca^{2+} activity following Schaffer Collateral stimulation. Animals received 5 g/kg EtOH (35% v/v in H_2O) or H_2O via intragastric gavage (i.g.) intermittently over 16 days. Animals underwent a period of forced abstinence from PND 46 to PND 72. Tissue was collected and physiological recordings were collected on PND 72 – 76. B) Diagram showing electrode placement in the CA3 along the Schaffer Collateral and recording from astrocytes in the CA1 dhipp. C) Representative traces from astrocytes in animals that received H_2O or EtOH. D) Representative images of fluorescent activity pre stimulation of the Schaffer Collateral and following Schaffer Collateral Stimulation. E) There was a significant decrease in fluorescent activity corresponding to astrocyte Ca^{2+} activity in AIE animals compared to H_2O age matched controls. Figure was in part created with Biorender. Analysis: Student's t-test, n = 6-10 astrocytes per animal (5 animals/treatment group).

AIE Results in Decreased Astrocyte Ca^{2+} Responsivity to Neuronal Stimulation

We wanted to test whether AIE-induced increases in PAP-synaptic proximity resulted in an increase in astrocyte response to neuronal stimulation. To do this, we used an astrocyte specific Ca^{2+} sensor (GCamp6f). Following the abstinence period, we recorded changes in fluorescent activity in GCamp6f$^+$ astrocytes in the CA1 dhipp. We found a significant decrease in astrocyte Ca^{2+} activity following Schaffer Collateral stimulation in AIE animals compared to H_2O age-matched controls. (Figure 13E; t(95) = 4.323, $p < 0.0001$).

AIE Results in Increased Synaptic Glutamate Concentrations

We saw a decrease in astrocyte Ca^{2+} response to neuronal stimulation, and wanted to determine whether this was due to a decrease in glutamate interactions with proximal astrocytes. To do this, we used an astrocyte-specific glutamate sensor (iGluSnFr) targeted to astrocytes. We recorded changes in fluorescence in response to glutamate in the CA1 dhipp following Schaffer Collateral stimulation. We found a significant increase in glutamate reaching the astrocyte membrane in AIE animals compared to H_2O age-matched controls (Figure 14E; t(88) = 11.34, $p < 0.0001$).

Figure 14

AIE Results in an Increase in Synaptic Glutamate Concentrations in Adulthood. an Astrocyte Specific Glutamate Sensor (IGluSnFr) Was Used to Observe Glutamate at CA1 dHipp Astrocyte Membranes Following Schaffer Collateral Stimulation.

A) Experimental timeline showing that female rats received intracranial injections of an astrocyte specific glutamate sensor (iGluSnFr) at PND 26 to record changes glutamate at the astrocyte membrane following Schaffer Collateral stimulation. Animals received 5 g/kg EtOH (35% v/v in H_2O) or H_2O via intragastric gavage (i.g.) intermittently over 16 days. Animals underwent a period of forced abstinence from PND 46 to PND 72. Tissue was collected and physiological recordings were collected on PND 72 – 76. B) Diagram showing electrode placement in the CA3 along the Schaffer Collateral and recording from astrocytes in the CA1 dhipp. C) Representative traces from astrocytes in animals that received H_2O or EtOH. D) Representative images of fluorescent activity pre stimulation of the Schaffer Collateral and following Schaffer Collateral Stimulation. E) There was a significant increase in fluorescent intensity corresponding to glutamate reaching the PAPs of AIE animals compared to H_2O age matched controls. Figure was in part created with Biorender. Analysis: Student's t-test, n = 6-10 astrocytes per animal (5 animals/treatment group).

Discussion

This study aimed to investigate the impact of adolescent binge EtOH exposure, or AIE, on astrocyte morphology, PAP-synaptic proximity, and astrocyte responsivity to neuronal signaling in the CA1 dhipp of adult female rats. Furthermore, we sought to determine whether changes in expression and interaction of the structural proteins neuroligin 1 and neurexin and their bridging protein Hevin may facilitate increases in the PAP-synaptic interactions observed in this study. Overall, we found that AIE resulted in an increase in astrocyte volume and PAP-synaptic proximity in adulthood. Although we found an increase in the expression of neuroligin, neurexin, and hevin in AIE animals compared to age-matched controls, there were no changes in the interactions of these proteins. Physiological recordings revealed an increase in the neurotransmitter glutamate reaching the PAPs. We anticipated that increased PAP-synaptic proximity and glutamate-astrocyte interactions would increase astrocyte Ca^{2+} activity. However, our analysis revealed a significant decrease in astrocyte Ca2+ responsivity to neuronal stimulation in AIE animals compared to age-matched controls. Our data reveal unique astrocyte morphology and function changes that may contribute to AIE-induced changes in neuronal function and behaviors.

The tripartite synapse's structural integrity relies on synaptic proteins with contact-mediated functions. Our current study focused on neurexin, found on the presynaptic terminal of excitatory and inhibitory synapses and one of its counterparts, neuroligin 1. Neuroligin 1 is found exclusively at excitatory synapses, where it is expressed on the membrane of the postsynaptic dendritic spine and the membrane of ensheathing astrocyte. Together these interactions play an essential role in synaptic stabilization and contact-mediated signaling to promote synaptic maturation during development (Octeau et al., 2018; Stogsdill et al., 2017). While we were unable to investigate specific subtypes of neuroligin 1 in this study, we do know that there are subtypes of neuroligin 1 that require a bridging protein, hevin, for appropriate indirect contact with the presynaptic neuroligin (Singh et al., 2016). Neuroligin 1 participates in the recruitment of receptors, channels, and signal-transduction of molecules to the excitatory synapse (Song et al., 1999). Disruption of the neuroligin–neurexin relationship has been associated with autism disorder and other neurological diseases, leading some groups to speculate whether these interactions are perturbed in the pathology of addiction (Sudhof, 2008). While our current study does not examine the effect of disruption of these bridging proteins on reward-seeking behaviors, we have found that AIE results in an increase in the expression of neuroligin 1, neurexin, and hevin with no effect on their interactions at the tripartite synapse. However, based on our data, we can speculate that AIE-induced increases in neurexin, neuroligin 1, and hevin are occurring to recruit other proteins to the synapse necessary for normal neuronal function. It has been previously shown that neurexin-neuroligin 1 interactions trigger the recruitment of NMDA and AMPA receptors to the synapse. Neurexin interactions with LRRTM2 (Leucine Rich Repeat Transmembrane Neuronal 2) have also been shown to recruit PSD-95 to the apex of the dendritic spine, which is one of the hallmarks of a mature dendritic spine phenotype. Further investigation

to determine how AIE affects dendritic spine phenotypes in the female hippocampus would be pertinent to understand better how protein expression changes may be driving synapse maturation.

Astrocytes respond to glutamatergic signaling, releasing Ca^{2+} stores and driving signal propagation that can impact individual PAPs and overall astrocyte function (Yu et al., 2021). Astrocyte Ca^{2+} signaling occurs through various events necessary to balance and regulate synaptic ion homeostasis and neuronal excitability. The intricate crosstalk between astrocytes and neurons through this complex mechanism is crucial for neuronal function, meaning that dysregulation of this process could have significant consequences for synaptic and neuronal function and subsequent behaviors (Durkee et al., 2019). Our current study shows an increase in PAP-synaptic coupling and glutamate reaching the PAP in animals that underwent AIE compared to age-matched controls. However, these data demonstrate a significant decrease in astrocyte Ca^{2+} responsivity to neuronal signaling. Together these data suggest that AIE may be affecting other intracellular astrocyte mechanisms critical for appropriate astrocyte response to neuronal signaling. One of the primary sources of intrinsic Ca^{2+} signaling in astrocytes is the IP3 signaling cascade. After glutamate is released from the presynaptic terminal, it enters the tripartite synapse, where it binds to receptors on the postsynaptic terminals and the membrane of the ensheathing astrocyte. Glutamate binds to the metabotropic glutamate receptors (mGluRs; mGluR2, mGluR3, and mGluR5) on the astrocytes. This triggers the release of internal IP3 from these G-coupled proteins (GPCs) on the astrocyte. IP3 binds to IP3 receptors, ligand-gated Ca^{2+} channels on the endoplasmic reticulum. As a result, Ca^{2+} is released into the cytosol of the astrocyte, activating a variety of processes, including the release of neuromodulators. However, we have been limited in this study and need to investigate whether AIE affects glutamate

receptors, transports (i.e., GLAST and GLT1), IP3, or IP3 receptors contributing to astrocyte Ca^{2+} activity.

Conclusions

These data provide a novel insight into an understudied area of adolescent alcohol use. Most interesting is that these changes in astrocyte morphology, PAP-synaptic interactions, and astrocyte function are shown in adulthood following forced abstinence. Further research is necessary to understand better how AIE affects mechanisms that lead to the increase in astrocyte-synaptic proximity and the disruption of astrocyte Ca2+ activity in the female rat hippocampus. However, the present study is an essential step in understanding how AIE affects astrocytes in a female rodent model and may lead to novel-non neuronal targets for future pharmacological treatments for patients with EtOH-induced neuronal dysfunction.

Chapter 6

Adolescent Alcohol Exposure Results in Disrupted Astrocyte-Synaptic Proximity, Function, and Behavior in The Male Dorsal Hippocampus

C.D. Walker[1,2], O. Coulter[1], T. Carter[1], H.G. Sexton[1,2], H. Hylton, L. Reasor[1], I. Parsons[1], B.J. Henderson[1], and M-L Risher[1,2]

[1]Department of Biomedical Research, Joan C. Edwards School of Medicine, Marshall University, Huntington, WV 25701, USA

[2]Neurobiology Research Laboratory, Hershel 'Woody' Williams Veterans Affairs Medical Center, Huntington, WV 25704, USA

In Chapter 4, we demonstrated that adolescent intermittent binge ethanol (EtOH) exposure (AIE) exposure results in a loss of PAP-synaptic proximity (i.e., loss of synaptic ensheathment by astrocytes) and a loss of neurexin-neuroligin interactions in the male rat PFC in a subregion dependent manner that persists into adulthood (Walker et al., 2022). In Chapter 5, we demonstrated that AIE increases PAP-synaptic proximity and deficits in Ca^{2+} activity in adult female rats. These findings are significant because 1) they show that AIE has long-term consequences on PAP-synaptic proximity and synaptic bridging proteins that may contribute to long-term neuronal dysfunction, 2) AIE affects astrocyte morphology and PAP-synaptic interactions differently across brain regions, and 3) AIE has long-term effects on astrocyte function. Together, these studies, in conjunction with the growing appreciation for the roles that astrocytes play in synaptic maturation, regulation, and cognition, reveal a potential role for astrocytes in EtOH-induced neuronal disruption. However, the male hippocampus has yet to be investigated in this manner. Previous work from our lab has demonstrated that AIE results in a shift towards a more immature dendritic spine phenotype in the CA1 dorsal hippocampus (dhipp; (Risher, Fleming, et al., 2015)) that could be indicative of a loss of astrocyte ensheathment of synapses (Witcher et al., 2007). Risher and colleagues (2015) also showed a corresponding reduction in the threshold to induce long-term potentiation following AIE, suggesting long-term changes in dhipp neuronal excitability that persisted beyond a period of forced abstinence into adulthood. Therefore, the current study sought to determine the effects of AIE on astrocyte morphology, PAP-synaptic proximity, the integrity of synaptic structural proteins, and neuronal-astrocyte communication in the male CA1 dhipp. We hypothesize that AIE disrupts astrocyte morphology, PAP-synaptic proximity, and astrocyte responsivity to neuronal communication in adulthood. We further hypothesize that AIE-induced disruption of freezing behavior in the

hippocampal-dependent contextual fear conditioning paradigm would be attenuated by using designer by exclusively activated by designer drugs (DREADDs) to activate astrocyte-specific Ca^{2+} activity, which has downstream effects on neuronal activity.

Materials and Methods

All procedures used in this study were conducted in accordance with the guidelines of the Institutional Animal Care and Use Committee and were approved by the Hershel 'Woody' Williams Veterans Affairs Medical Center and Marshall University, Huntington, WV.

Animals and Surgical Procedures

A total of 118 male Sprague Dawley rats (Hilltop, Scottdale, PA, USA) were received, double-housed, and maintained in a temperature- and humidity-controlled environment with ad libitum access to food and water on postnatal day (PND) 24. Animals were kept on a 12-hour:12-hour reverse light:dark cycle (lights on at 6:00 pm and off at 6:00 am). Surgical procedures were performed as previously described in Testen et al. (2019) and Walker et al. (2022) with minor modifications. Animals were allowed to habituate for two days prior to handling and/or surgical procedures. On PND 26-27 rats (n=6/treatment group) received 0.3 mg/kg intraperitoneal injection (i.p.) of 25% w/v mannitol (Carty et al., 2013; Testen et al., 2019; Walker et al., 2022) and anesthetized with a cocktail of ketamine (30 mg/kg), xylazine (2.5 mg/kg), and acepromazine (0.5 mg/kg). The depth of anesthesia was closely monitored throughout the procedure. After shaving the area where the incision would be made, animals were secured into a stereotaxic frame via nose clip and blunt ear bars. The surgical site was cleaned three times with 70% ethanol and 10% iodine. A burr hole was drilled into the skull allowing for unilateral injection of virus into the dorsal hippocampus at the following coordinates, −3.2 mm anterior/posterior, +/− 2.6 mm medial/lateral, +3.0 mm dorsal/ventral. Animals received either 1

μL AAV1/5 gfaABC$_1$D Lck-GFP diluted in 1:1 H_2O (3.26 x 10^{12} gc/mL; Addgene plasmid # 105598; http://n2t.net/addgene:105598; Shigetomi et al. (2013)), 1 uL AAV5.GfaABC1D.GCamp6f (7.3 x 10^{12} gc/mL; Addgene plasmid # 52925; http://n2t.net/addgene:52925; Haustein et al. (2014)), AAV5.GFAP.iGluSnFr.WPRE.SV40 (1 x 10^{13} gc/mL; Addgene plasmid # 98930; http://n2t.net/addgene:98930; Marvin et al. (2013)), or 1 μL AAV5.GFAP.hM3D(Gq).mCherry (7 x 10^{12} gc/mL; Addgene plasmid # 50478; http://n2t.net/addgene:50478) which were administered by microinjection using a syringe pump and 26-gauge needle with a dwell time of 10 minutes. The burr whole was closed with bone cement, bupivacaine was administered to the site, and the surgical incision was closed with dissolvable external sutures. Antibiotic ointment was applied to the incision, saline was administered via subcutaneous injection to prevent dehydration, and the animal was allowed to recover on a heating pad. Once the animal was fully awake and mobile, it was returned to the home cage with the original cagemate.

Intermittent Binge EtOH Exposure

Animals were habituated to handling prior to EtOH/water (H_2O) administration. Beginning on PND 30, animals received 10 doses of 5 g/kg EtOH (35% v/v in H_2O) or H_2O via intragastric gavage (i.g.) using a two day on, one day off, two day on, two day off intermittent schedule over 16 days (Figure 15), as previously described in (Walker et al., 2022). The individual administering the EtOH was responsible for observing animals after EtOH administration to ensure full recovery from intoxication and for ensuring that everyone involved in the subsequent experiments remained blinded to treatments until the completion of the study. Animals were euthanized and brain tissue was collected on PND 46 (24 h following the last dose of EtOH) or following a 26-day forced abstinence period on PND 72-76. The EtOH dosage was

selected to produce blood EtOH concentrations (BECs) consistent with those of adolescent humans during binge drinking episodes (Donovan, 2009) and consistent with our previous studies (Risher, Sexton, et al., 2015; Walker et al., 2022). All animals undergoing behavioral testing underwent the 26-day forced abstinence period.

Figure 15
Experimental Timeline.
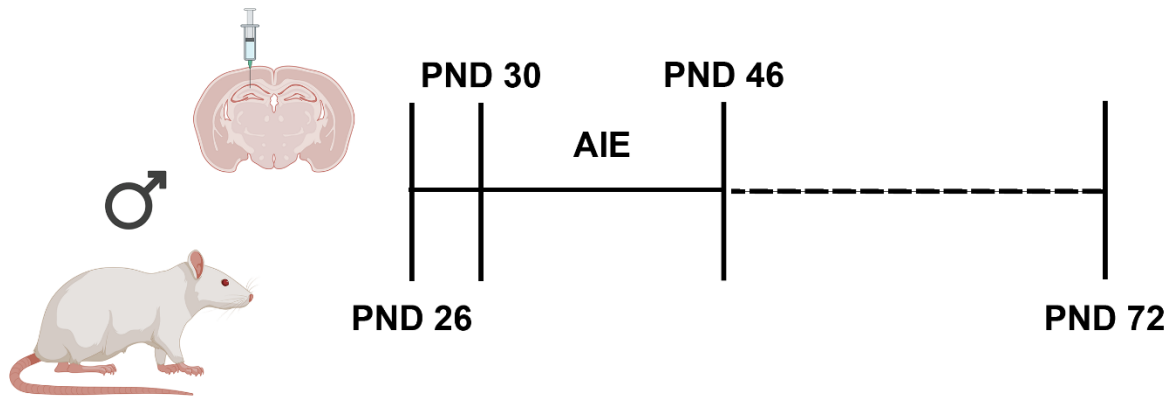
Male rats received an intracranial injection of an astrocyte-specific adeno-associated virus with a GFP on PND 26. Animals then underwent AIE and received 5 g/kg EtOH (35% v/v in H_2O) or H_2O via intragastric gavage (i.g.) intermittently over 16 days. A cohort of animals were sacrificed at PND 46, during peak withdrawal, while another cohort underwent a period of forced abstinence from PND 46 to PND 72. Tissue was harvested for immunohistochemistry on PND 46 or PND 72. Physiological recordings and behavior assays began on PND 72. Created with Biorender.

Immunohistochemistry (IHC)

Brain Section Preparation. At PND 46 or 72 animals were deeply anesthetized with isoflurane (6 animals/treatment group/experiment; total n = 24). Animals were transcardially perfused with phosphate buffered saline (PBS; pH 7.4; cat# P5368, Sigma-Aldrich, St. Louis, MO, USA) for 5 minutes, followed by 4% paraformaldehyde (PFA; cat# 19210, Electron Microscopy Solutions, Hatfield, PA, USA) for 12 minutes (20 mL/min). Brains were extracted and post-fixed in 4% PFA at 4 °C overnight followed by 30% glycerol (cat# G5516-1L, Sigma-

Aldrich, St. Louis, MO, USA) in PBS at 4C for 1-2 days. Brains were then placed in a 2:1 solution of 30% sucrose to OTC freezing compound (Electron Microscopy Sciences, Hatfield, PA, USA) and stored at -80 °C. Using a cryostat (CM 1950, Leica Biosystems, Richmond, IL, USA), tissue was sliced into either 80 µm or 40 µm sections depending on the experiment.

PSD-95 and GFAP Immunohistochemistry. 80 µm sections underwent antigen retrieval as previously described in (Jiao et al., 1999; Testen et al., 2019; Walker et al., 2022). Free-floating slices were briefly rinsed three times (5 minutes each) in 0.1 M phosphate buffer (PB; 3.1 g/L NaH_2PO_4, 10.9 g/l Na_2HPO_4, pH 7.4), then transferred to a 10 mM sodium citrate buffer preheated to 80 °C for 30 minutes, shaking every 10 minutes. Slices were then allowed to cool to room temperature followed by three additional washes (5 minutes each) in 0.1 M PB (pH 7.4). Slices were blocked with 5% normal goat serum (NGS, cat# 005-000-121, Jackson Immunolabs, West Grove, PA, USA) in phosphate-buffer in saline (PBS; pH 7.4; cat# P5368, Sigma-Aldrich, St. Louis, MO, USA) with triton (PBST; 0.2% triton 100-X; cat# 13134900, Roche,) for one hour at room temperature. Slices were then incubated for four days in mouse anti-PSD-95 (1:450; cat# MA1-045, ThermoFisher Scientific, Waltham, MA, USA) and rabbit anti-GFAP (1:500 cat# Z0334, Agilent Technologies, Santa Clara, CA, USA) in PBST (0.2% triton 100-X) and 5% NGS at 4 °C on shaker. Slices were then washed three times (5 minutes each) in PBST (0.2% triton 100-X) and incubated for 6 hours at room temperature in Alexa Fluor goat anti-mouse 594 (1:200; cat# A-11032, Molecular Probes, Eugene, OR, USA) and Alexa Fluor goat anti-rabbit 647 (1:200 ThermoFisher Scientific cat# A-21245) in PBST (0.2% triton 100-X) and 5% NGS. Slices were then washed three times (5 minutes each in PBST (0.2% triton 100-X) and once in PBS. The slices were then mounted with Vectashield with DAPI (cat# H-1200, Vector Laboratories West Grove, PA, USA), coverslipped, and sealed with nail varnish.

Neuroligin 1, 3, and Neurexin. 40 μm slices were rinsed three times (10 minutes each) with PBST (0.2% triton 100-X) then blocked at room temperature for 1 hour in 5% NGS and PBST (0.2% triton 100-X). Slices were then incubated overnight in mouse anti-neuroligin 1 (1:500, cat# 129111, Synaptic Systems) or mouse anti-neuroligin 3 (1:500, cat# 129311, Synaptic Systems) with rabbit anti-neurexin 1/2/3 (1: 500, cat# 175003, Synaptic Systems), 5% NGS and PBST (0.2% triton 100-X) at 4^OC. Slices were then washed three times (5 minutes each) in PBST (0.2% triton 100-X) then incubated for 2 hours at room temperature in goat anti-mouse 488 (1:200 Alexa Fluor cat# A11029, Lifetech) and goat anti rabbit 647 (1:200, cat# A21245, Lifetech) in 5% NGS and PBST (0.2% triton 100-X). Slices were washed three more times in PBST (0.2% triton 100-X) then mounted with Vectashield with DAPI (cat# H-1200, Vector Laboratories West Grove, PA, USA,), coverslipped, and sealed with nail varnish.

Eph A3 and Ephrin A4. 40 μm slices were rinsed three times (10 minutes each) with PBST (0.2% triton 100-X) then blocked at room temperature for 1 hour in 5% NGS and PBST (0.2% triton 100-X). Slices were then incubated overnight in mouse anti-ephrin A3 (1:500, cat# OTI4A4, Novus Biologicals) and rabbit anti-eph A4 (1: 500, cat# BS-1764R, ThermoFisher) 5% NGS and PBST (0.2% triton 100-X) at 4^OC. Slices were then washed three times (5 minutes each) in PBST (0.2% triton 100-X) then incubated for 2 hours at room temperature in goat anti-mouse 488 (1:200 Alexa Fluor cat# A11029, Lifetech) and goat anti rabbit 647 (1:200, cat# A21245, Lifetech) in 5% NGS and PBST (0.2% triton 100-X). Slices were washed three more times in PBST (0.2% triton 100-X) then mounted with Vectashield with DAPI (cat# H-1200, Vector Laboratories West Grove, PA, USA), coverslipped, and sealed with nail varnish.

Data Acquisition and Processing

Astrocyte Volume and Astrocyte-Synaptic Co-Localization. A Leica SP5 laser-scanning confocal microscope with 63× oil-immersive objective, NA 1.45 (Leica, Wetzlar, Germany) was used for image acquisition. Acquisition parameters for AAV+ astrocyte-PSD-95 imaging were set at 1024 × 1024 pixels frame size, 16-bit depths, 4× lines averaging, 1 μm z-step size. Lck-GFP expression pattern is diffuse, aiding in the acquisition of single, isolated astrocytes. Individual, whole GFP$^+$ astrocytes were randomly selected by the experimenter. GFP$^+$, GFAP, and PSD-95 were then imaged within the CA1 dorsal hippocampus (dhipp) and 8–11 individual astrocytes were captured per animal. A total of 5 brains were used per treatment group.

Co-localization was performed as previously described in Testen et al. (2019) and Walker et al. (2022), with modifications. AutoQuant X3.1.2 software (Media Cypernetics, Rockville, MD, USA) was used to deconvolve raw images before digitally reconstructing z-stacks. AutoQuant's algorithm for blind deconvolution with 10 iterations was run on each z-stack prior to reconstruction. Parameters for blind deconvolution are automatically optimized by the software based on confocal, objective, and imaging specifications. Output files were directly imported to Imaris x64 version 9.0 (Bitplane, Santa Barbara, CA, USA) for 3-dimensional reconstruction. Using Imaris, each individual astrocyte was first isolated from a Lck-GFP background signal using a surface building feature. Surface rendering enables the extraction of morphometric values, including surface area and volume, and generates a new Lck-GFP channel devoid of background noise, revealing only a signal from a single isolated astrocyte. Close attention was paid to verify that collected Lck-GFP signal accounted for a single astrocyte, in its entirety. Co-localization of the Lck-GFP and GFAP signals was used to confirm astrocyte identity for quantification. Only confirmed astrocytes that were captured in their entirety were

used for quantification and analysis. The isolated Lck-GFP channel (surface mask) was used, in conjunction with the PSD-95 channel, for perform colocalization analysis to determine the proximity between the astrocytes and post-synaptic neuronal terminals. Before co-localization analysis, the threshold for the PSD-95 signal was manually set by measuring the fluorescence intensity of unambiguous PSD-95 positive puncta on multiple optical planes by a blinded experimenter. This was achieved by rotating the reconstructed astrocyte image in 3D space while adjusting voxels to ensure that PSD-95 expression could be observed without the interference of background noise. An average of these measurements was used as a final PSD-95 signal threshold value. Co-localization is reported as a % of astrocyte volume (identified as Lck-GFP^{+} surface reconstruction) co-localized with the PSD-95 channel.

Neuroligin 1, 3, Neurexin, Ephrin A3, and EphA4. Confocal z-stacks (5 µm thick, optical section depth 0.33 µm, and 1024 × 1024 image size) of the dhipp were imaged on a Leica SP5 laser-scanning confocal microscope with 63× oil-immersive objective, NA 1.45 (Leica, Wetzlar, Germany). A total of 3 randomly selected image stacks from a randomly selected hemisphere were captured from 3 separate brain slices per animal (4-6 brains/treatment group).

Images were analyzed based on Risher, Fleming, et al. (2015) with slight modification. Z-stacks were uploaded into ImageJ 1.53t (NIH, USA). Maximum projections of 3 consecutive optical sections (corresponding to 1 µm total depth) were generated from the original *z*-stack. The Puncta Analyzer plugin (available upon request from c.eroglu@cellbio.duke.edu) for ImageJ was used to count the individual number of proteins of interest and co-localized proteins (Ippolito & Eroglu, 2010).

Physiological Recordings

Glutamate and Calcium Signaling and Recording. Prior to EtOH or H_2O

administration, animals received intracranial injection of one of the following astrocyte-specific

AAVs: AAV5.gfaABC$_1$D.GCamp6f or AAV.GFAP.iGluSnFr.WPRE.SV40 at PNDXX. At

PND72-76, animals were deeply anesthetized with isoflurane and transcardially perfused with *N*-

methyl-D-glucamine – HEPES (NMDG-HEPES) recovery solution consisting of (in mM) 93 mg

NMDG, 2.5 mg KCl, 1.2 NaH$_2$PO$_4$, 30 mg NaHCO$_3$, 20 mg HEPES, 25 mg D-glucose, 5 mg

sodium ascorbate, 2 mg thiourea, 3 mg MgSO$_4$·7H$_2$O, 0.5 mg CaCl$_2$·2H$_2$O that had been bubbled

with a carbogen (95% O_2 and 5% CO_2). Whole brain tissue was embedded in agar and 250 µm

coronal sections were obtained using a Comprestome (Precisionary Instruments, Natick, MA,

USA) and incubated in NMDG-HEPES recovery solution at 32 °C for 12 minutes while bubbling

with carbogen. Slices were then transferred to an artificial cerebral spinal fluid (ACSF)

consisting of (in mM) 125 mg NaCl, 1.6 mg KCl, 1.2 mg NaH$_2$PO$_4$, 2.4 mg CaCl$_2$, 1.2 mg

MgCl$_2$, 18 mg NaHCO$_3$, 11 mg glucose that was bubbling in carbogen and incubated in a water

bath at 32 °C for 1 hour. Individual slices were transferred to the recording stage equipped with a

Zeiss Axicam 702 mono camera and perfused with ACSF at a constant flow rate of 4 ml/min

maintained at 32 °C. Astrocytes of interest were identified by expression of GFP (GCamp6f) or

mCherry (iGluSnFr). Physiological recordings were collected using methods as previously

described in Haustein et al. (2014) with slight modification. The tip of a 0.254 mm carbon-fiber

bipolar microelectrode (MS303-1-B-SPCL, Plastics One, Roanoke, VA, USA) was placed at the

CA3 Schaffer Collateral being careful as to not come into direct contact with tissue. The

electrode was placed approximately 30-80 µm above the tissue (Haustein et al., 2014) to prevent

stimulation artifacts. Baseline fluorescence was recorded from the astrocyte of interest in the

CA1 for 5 s prior to Schaffer Collateral stimulation with an A.M.P.I. Master 9 Stimulator

(A.M.P.I., Jerusalem, Israel). Individual 1 ms pulses were delivered at 40 μA with 15 pulses per second at a rate of 15 Hz. Recording continued for an additional 15 s following stimulation.

Analysis. Video recordings of changes in fluorescent activity were captured using Zeiss ZEN Pro (Blue edition) version 3.7.97.04000 (Zeiss, White Plains, NY, USA). A region of interest was created to isolated GFP (GCaMP6f) or mCherry (iGluSnFr) positive astrocytes in the field of view of the CA1 dhipp. Individual fluorescence intensities were transferred to an Excel spreadsheet. Values were isolated to 2 seconds prior to neuronal stimulation and continued through 10 seconds following fluorescent response. A linear equation was extrapolated from the fluorescence recordings across the 2 s prior to Schaffer Collateral stimulation. This equation was then used to normalize the fluorescence recordings to account for loss of fluorescence intensity due to exposure to the mercury lamp during recording. Then, $\Delta F/F$ was used to determine changes in fluorescent intensity following Schaffer Collateral stimulation.

Contextual Fear Conditioning

Following the 26-day forced abstinence period, animals underwent a 3-day contextual fear conditioning paradigm. Five animal groups underwent the behavioral testing with or without clozapine-N-oxide (CNO) administration (2 mg/kg in 0.5% DMSO/saline, i.p.): H_2O+ Lck GFAP AAV + CNO, H_2O + Lck GFAP + saline, H_2O+ hM3D(Gq)+saline, EtOH+ hM3D(Gq)+saline, and EtOH + hM3D(Gq)+CNO. Animals were habituated to the testing room for 30 minutes, in their home cages, 24 hours prior to the first testing day. CNO or saline was administered 30 minutes prior to testing on Day 1. Animals were habituated in the room for 30 minutes prior to testing followed by 2-minute habituation into fear conditioning chamber (18x18x30 cm), with a grid floor wired to a shock generator surrounded by an acoustic chamber, and a high-quality factory installed camera on the door (Med Associates). After the 2-minute habituation the animal

received a 2s foot shock (0.5 mA) followed by a delay period of 120 sec. This was repeated two times for a total of three foot shocks. Freezing behavior was recorded during the 120 sec delay times and 120 sec following the final foot shock. On test day 2, fear retention day, the animal was allowed to habituate to the room for 30 minutes. The animal was then placed in the fear conditioning chamber for 12 minutes recording freezing behavior in 120 sec bins. On day 3, extinction day, the animals were again allowed to habituate to the room for 30 minutes. Then the animal was placed in the chamber for 12 minutes and freezing behavior was recorded in 120 sec bins.

Analysis. *All* Video Freeze software (Med Associates) was used to analyze freezing behavior. Freezing below a motion index threshold of 18 for 30 seconds was considered to be a fear response to the contextual fear conditioning paradigm (Kol et al., 2020). The number of freezing responses for each animal was recorded and exported to an Excel spreadsheet. H_2O+ Lck GFAP AAV + CNO, H_2O + Lck GFAP + saline, and H_2O+ hM3D(Gq)+saline controls were analyzed to confirm that the behavioral outcomes were not driven by surgical procedures, CNO administration, or hM3D(Gq) DREADDs injection independently of CNO activation. After confirming that there were no off-target effects, H_2O+ hM3D(Gq)+saline, EtOH+ hM3D(Gq)+saline, and EtOH + hM3D(Gq)+CNO groups were compared to determine the effects of AIE on freezing behavior during acquisition, retention, and extinction, and to determine if astrocyte activation via hM3D(Gq)+ could attenuate the effects of AIE on behavior.

Statistical Analysis

Data were compiled using Excel 365 (Microsoft, Redmond, WA, USA) and analyzed using GraphPad Prism Version 9.4.1 (GraphPad Software, San Diego, CA, USA). Mixed-effects ANOVA was performed (timepoint x treatment) with a Tukey's *post hoc* or Student's t-test was

performed, where indicated. Statistical significance was assessed using an alpha level of 0.05.

Data are presented as violin plots with individual data points and medians.

Figure 16

Single Cell Imaging and Analysis of Astrocyte Volumes 24 hrs After Final Dose of EtOH During Peak Withdrawal (PND 46) and Following a 26-Day Forced Abstinence Period (PND 72).
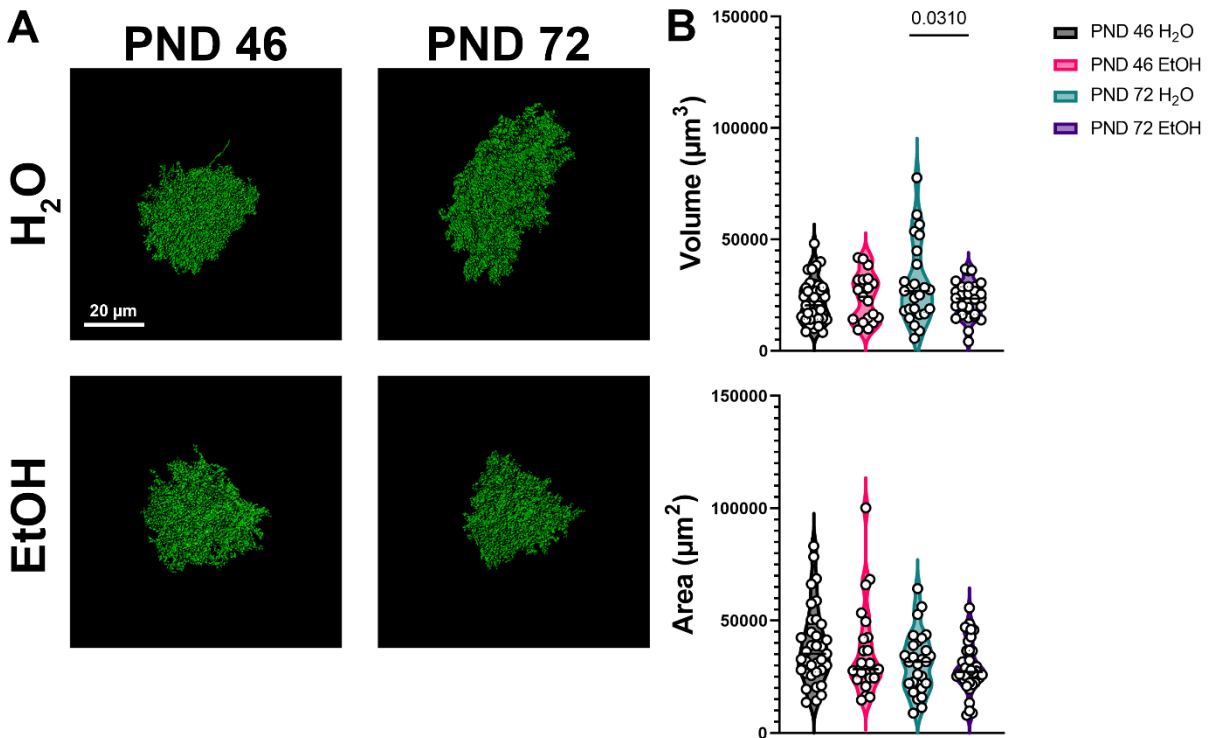
A) Representative images of astrocyte surface rendering from the CA1 dhipp during peak withdrawal (PND46) and following a 26-day forced abstinence period (PND72). Scale bars, 20 μm. B) Quantification of astrocyte volumes 24 hrs after the final dose during peak withdrawal and following the 26-day forced abstinence period. There was no significant treatment effect (H_2O vs AIE). There was a significant decrease in astrocyte volume at PND72 when comparing H_2O vs AIE groups. Analysis: Mixed-effects ANOVA was performed (timepoint x treatment) with a Tukey's *post hoc* comparison, n = 8-11 astrocytes/animal (5 animals/treatment group).

Results

AIE Induced Changes in Astrocyte Morphology and PAPs-Synaptic Proximity

Following 3D reconstruction of individual GFP[+] astrocytes, we measured changes in whole-cell astrocyte volume 24 h after the 10th dose (PND 46) and following a 26-day forced abstinence period (PND 72). We observed an overall treatment effect on astrocyte volume (F (3,

113

68) = 3.084); $p = 0.0333$). Interestingly, *post hoc* analysis revealed that there was no treatment (AIE) effect on astrocyte volume 24 h after the final dose, during peak withdrawal ($p = 0.9984$; Figure 16A,B). However, there was a significant decrease in astrocyte volume following AIE after the 26-day forced abstinence period ($p = 0.0310$); Figure 16A,B).

When determining the effects of AIE on PAP-synaptic colocalization, we quantified the localization of individual GFP$^+$ astrocytes with the postsynaptic density marker, PSD-95 (Figure 2A,B). There was a significant overall treatment effect (F (2.252, 53.29) = 31.58), $p < 0.0001$). *Post hoc* analysis revealed a significant increase in PAP-synaptic colocalization from PND 46 to PND 72 when compared to EtOH naïve animals ($p < 0.0001$), suggesting ongoing colocalization throughout this developmental period. AIE resulted in a significant loss of PAP-synaptic colocalization during peak withdrawal (PND 46), this loss of colocalization became more robust following a 26-day forced abstinence period (PND 72; ($p = 0.0243$; Figure 17A,B) and ($p = 0.0370$; Figure 1B), respectively).

Figure 17
Single Astrocyte Co-Localization With PSD-95 and Analysis 24 hrs After the Last Dose (PND 46) And Following a 26-Day Forced Abstinence Period (PND 72).
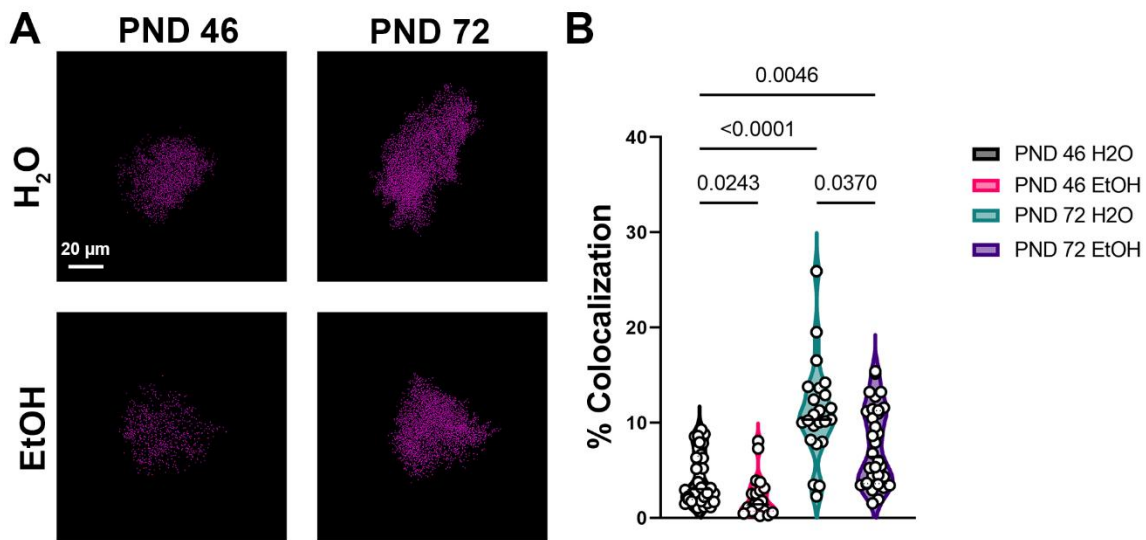
A) Representative images of PSD-95 colocalized within 0.5 µm of a Lck-GFP$^+$ astrocyte in the CA1 dhipp during peak withdrawal (PND 46) and following a 26-day forced abstinence period

(PND 72). Scale bars, 20 µm. B) Quantification of PSD-95/astrocyte volumes at PND46 and PND72 following AIE. There was an overall treatment effect (p < 0.0001). When comparing treatment (H_2O vs AIE) there was a significant decrease in PSD-95/astrocyte volume during peak withdrawal (PND 46) and following the 26-day forced abstinence period (PND 72). *Post hoc* comparisons also revealed a significant increase in PSD-95/astrocyte when comparing naïve animals at PND 46 and PND 72 as well as AIE animals at PND 46 and 72. Analysis: Mixed-effects ANOVA was performed (timepoint x treatment) with a Tukey's *post hoc* comparison, n = 8-11 astrocytes/animal (5 animals/treatment group).

Loss of PAP-Synaptic Proximity Corresponds to Loss of Synaptic Stabilization Proteins

To determine if the loss of PAP-synaptic proximity in adulthood was driven by a loss of synaptic proteins critical for the stabilization tripartite synapse we stained for critical synaptic bridging proteins and their bridging partners. Furthermore, we analyzed whether there were changes in the colocalization of these bridging partners that may indicate disruption of protein-protein interactions. Using IHC, we probed for neuroligins 1 and 3 and the presynaptic partner, neurexin (Figure 18) as well as Ephrin A3 and the postsynaptic partner Eph A4 (Figure 19).

There was no AIE-induced change in neurexin protein expression following the 26-day forced abstinence (t(93) = 1.733; *p* = 0.0864; Figure 18B). However, there was a significant decrease in neuroligin 1 expression in AIE treated animals following a 26-day forced abstinence period (t(93) = 2.080; *p* = 0.0403; Figure 18C). Furthermore, we found that AIE resulted in a loss of neuroligin 1-neurexin colocalization (t(93) = 16.40; *p* < 0.0001; Figure 18D). Next we analyzed the effects of AIE on neuroligin 3 protein expression and found a significant decrease in neuroligin 3 expression following the 26-day forced abstinence period (t(78) = 5.110; *p* < 0.0001; Figure 18E). Once again, the loss of neuroligin 3 expression coincided with a loss of colocalization of neuroligin 3-neurexin (t(78) = 2.359; *p* = 0.0208; Figure 18G) following forced abstinence.

Next, we analyzed expression and interactions of Ephrin A3 and EphA4 (Figure 4A,B)
and observed no AIE-induced changes in expression of Ephrin A3 ($t(158) = 1.005$; $p = 0.3165$;
Figure 19C or Eph A4 ($t(158) = 1.247$; $p = 0.2142$; Figure 19D) following the forced abstinence
period. Interestingly, despite no change in protein expression, there was an increase in Ephrin
A3-E.

Figure 18
The Effects of AIE On Neuroligins 1, Neuroligin 3, and Neurexin Expression and Neuroligin 1-
Neurexin and Neuroligin 3-Neurexin Colocalization Following a 26-Day Forced Abstinence
Period.
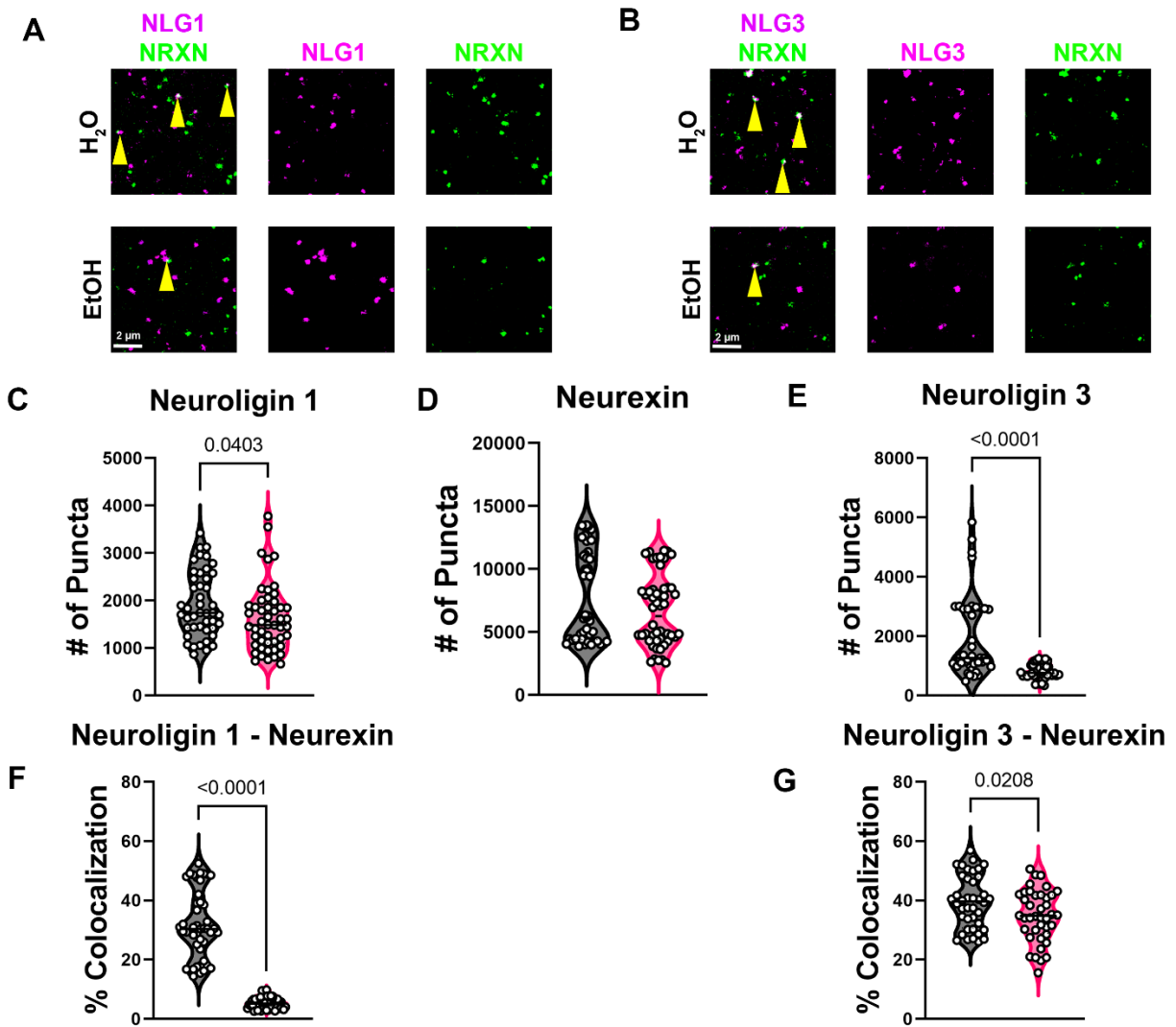
A) Representative images of colocalization (indicated by yellow arrows) of neurexin (NRXN) and neuroligin 1 (NLG1) and representative images of individual protein expression in control animals and animals that underwent AIE. B) Representative images of colocalization (indicated by yellow arrows) of neurexin (NRXN) and neuroligin 3 (NLG3) and representative images of individual protein expression of control animals and animals that underwent AIE. C) There was a significant decrease in neuroligin 1 expression in animals that underwent AIE. D) There were no AIE-induced changes in neurexin expression. E) There was a significant decrease in the expression of neuroligin 3 expression following animals that underwent AIE compared to age-matched H_2O controls. F,G) There was a significant decrease in neuroligin 1-neurexin colocalization and neuroligin 3-neurexin colocalization in animals that underwent AIE compared to age matched H_2O controls. Analysis: Student's t-test, n=6/treatment group.

Figure 19

The Effects of AIE on Ephrin A3 and Eph A4 Expression and Colocalization.
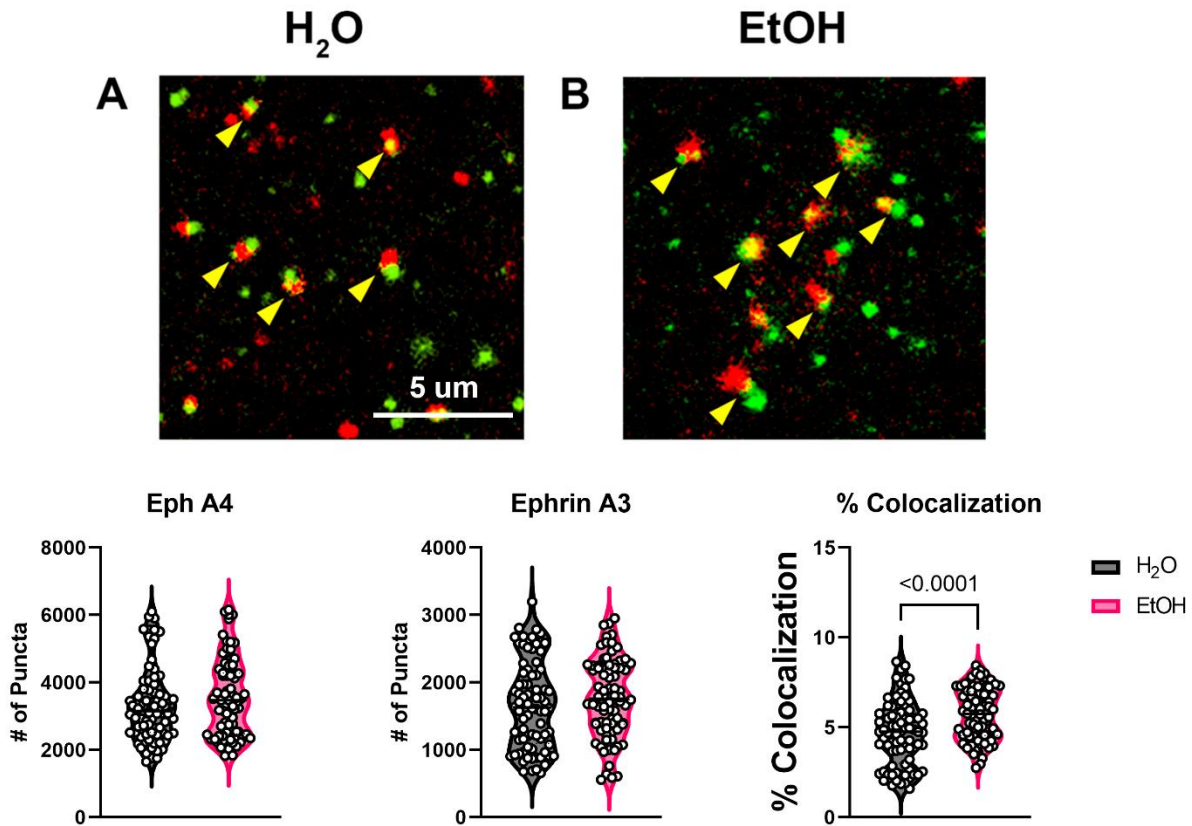
A,B) Representative images of Ephrin A3 (red) and EphA4 (green) expression in control H_2O and AIE animals. Yellow arrows indicate where these proteins are interacting. Analysis revealed no AIE-induced change in Eph A4 (C) or Ephrin A3 (D) expression. There was a significant decrease in Ephrin A3 and Eph A4 colocalization (E) in AIE compared to age matched H_2O controls. Analysis: Student's t-test n = 4-5 images/animal (6 animals/treatment group).

AIE Disrupts Astrocyte Ca²⁺ Responsivity to Neuronal Stimulation in Adulthood

To assess whether disruption of PAP-synaptic colocalization would impede neuronal-to-astrocyte communication we assessed astrocyte Ca^{2+} responsivity to Schaffer Collateral neuronal stimulation using the Ca^{2+} GCamp6f sensor specifically targeted to astrocytes (Figure 20A-D). In AIE treated animals, there was a decrease in astrocyte-specific Ca^{2+} responsivity to neuronal stimulation following abstinence ($t(104) = 5.368$; $p < 0.0001$; Figure 20E).

AIE Increases Synaptic Glutamate Availability in Adulthood

To assess whether the loss of astrocyte Ca^{2+} responsivity to neuronal stimulation was due to the loss of PAP-synaptic colocalization/proximity resulting in inefficient diffusion of glutamate towards the PAP membranes, we investigated how AIE influences glutamate reaching the PAP membrane. We used the iGluSnFr sensor targeted to astrocytes to record glutamate availability at the astrocyte membrane following Schaffer Collateral stimulation (Figure 21A-D). Despite the loss of AIE-induced PAP-synaptic co-localization, there was an increase in glutamate interactions with the astrocytes ($t(156) = 4.972$; $p < 0.0001$; Figure 21E) following abstinence, suggesting that the loss of astrocyte Ca^{2+} responsivity to neuronal stimulation is not due to an AIE-induced loss of glutamate-PAP interactions.

Figure 20

AIE Results in a Decrease in Astrocyte Responsivity to Neuronal Stimulation.

A) Experimental timeline showing that female rats received intracranial injections of an astrocyte-specific Ca^{2+} sensor (GCamp6f) at PND 26 to record changes in Ca^{2+} activity following Schaffer Collateral stimulation. Animals received 5 g/kg EtOH (35% v/v in H_2O) or H_2O via intragastric gavage (i.g.) intermittently over 16 days. Animals underwent a period of forced abstinence from PND 46 to PND 72. Tissue was collected and physiological recordings were collected on PND 72 – 76. B) Diagram showing electrode placement in the CA3 along the Schaffer Collateral and recording from astrocytes in the CA1 dhipp. C) Representative traces from astrocytes in animals that received H_2O or EtOH. D) Representative images of fluorescent activity before and after stimulation of the Schaffer Collateral. E) There was a significant decrease in fluorescent activity corresponding to astrocyte Ca^{2+} activity in AIE animals compared to H_2O age matched controls. Figure was in part created with Biorender. Analysis: Student's t-test, n = 6-10 astrocytes per animal (5 animals/treatment group).

Figure 21

AIE Results in an Increase in Synaptic Glutamate Concentrations.
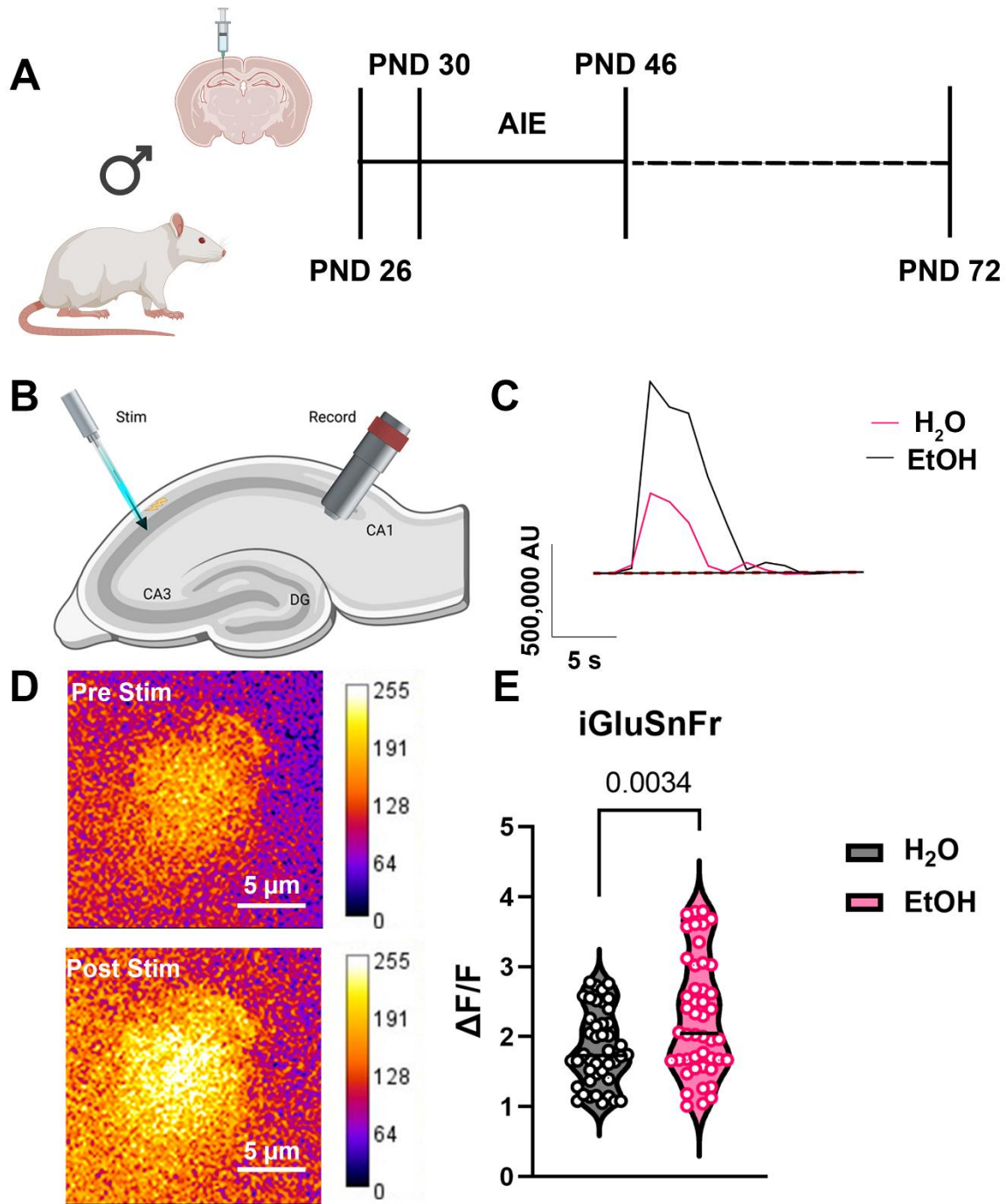
A) Experimental timeline showing that male rats received intracranial injections of an astrocyte specific glutamate sensor (iGluSnFr) at PND 26 to record changes glutamate at the astrocyte membrane following Schaffer Collateral stimulation. Animals received 5 g/kg EtOH (35% v/v in H_2O) or H_2O via intragastric gavage (i.g.) intermittently over 16 days. Animals underwent a period of forced abstinence from PND 46 to PND 72. Tissue was collected and physiological recordings were collected on PND 72 – 76. B) Diagram showing electrode placement in the CA3 along the Schaffer Collateral and recording from astrocytes in the CA1 dhipp. C) Representative traces from astrocytes in animals that received H_2O or EtOH. D) Representative images of fluorescent activity pre stimulation of the Schaffer Collateral and following Schaffer Collateral Stimulation. E) There was a significant increase in fluorescent intensity corresponding to glutamate reaching the PAPs of AIE animals compared to H_2O age matched controls. Figure was in part created with Biorender. Analysis: Student's t-test, n = 6-10 astrocytes per animal (5 animals/treatment group).

Astrocyte-Targeted GqDREADDs Attenuates AIE-Induced Behavior Deficits in a Contextual Fear Conditioning Paradigm

To determine if AIE-induced behavioral deficits in the hippocampal-dependent contextual fear conditioning paradigm can be attenuated through the recovery of astrocyte Ca^{2+} signaling, we used GqDREADDs targeted to astrocytes. Prior to behavioral testing, we confirmed localization of GqDREADDs to the CA1 dhipp (Figure 22A-C). We then tested a cohort of control animals to confirm that behavioral outcomes would not be confounded by surgery, CNO, or inactivated GqDREADDs (Figure 22D). On Day 1 of behavioral testing, during the acquisition phase, (Figure 22E), there was an overall treatment effect ($(F(2.313, 74.01) = 83.37$; $p < 0.0001$), timepoint effect ($F(2, 32) = 3.271$; $p = 0.0510$), and interaction (treatment x timepoint: ($F(8, 128) = 4.398$; $p = 0.0001$)). *Post hoc* analysis revealed a significant decrease in freezing behavior in EtOH/GqDREADDs saline group compared to the control group H_2O/GqDREADDs saline, during the 3rd foot shock period ($p = 0.0326$), and post-shock period ($p = 0.0402$). Upon activation of GqDREADDs with CNO we were able to attenuate the effects of EtOH on freezing behavior (EtOH/GqDREADDs CNO vs. H_2O/GqDREADDs saline ($p = 0451$), EtOH/GqDREADDs CNO vs. EtOH/GqDREADDs saline ($p = 0333$). During Day 2 of

testing (Figure 22F), the fear retention day, there was a significant timepoint effect $(F(2.162, 69.20) = 7.940; p = 0.0006)$. However, p*ost hoc* analysis revealed no significant differences. There was no overall treatment effect or treatment x timepoint interaction $(F(2, 32) = 2.508; p = 0.0973)$ and $(F(10, 160) = 0.4768; p = 0.9032)$, respectively). During Day 3 of testing (Figure 22G), extinction day, we found no overall treatment effect, timepoint effect, or treatment x timepoint interaction $((F(2, 32) = 0.8393; p = 0.2259), (F(3.519, 112.6) = 0.8398; p = 0.4903), (F(10, 160) = 1.316' p = 0.0.2259)$ respectively). These data indicate that EtOH-induced deficits in freezing behavior in the contextual fear conditioning task can be attenuated through the recovery of astrocyte activity.

Figure 22

The Use of GqDREADDs Attenuates Freezing Behavior in a Fear Conditioning Paradigm.
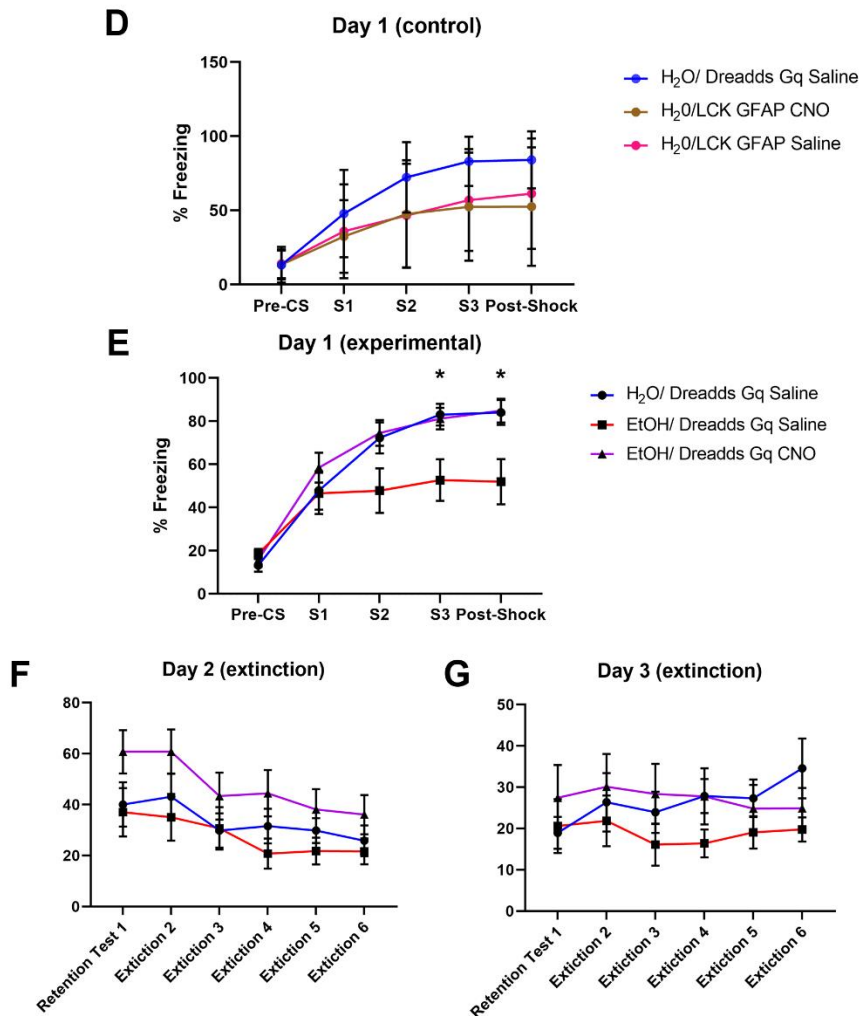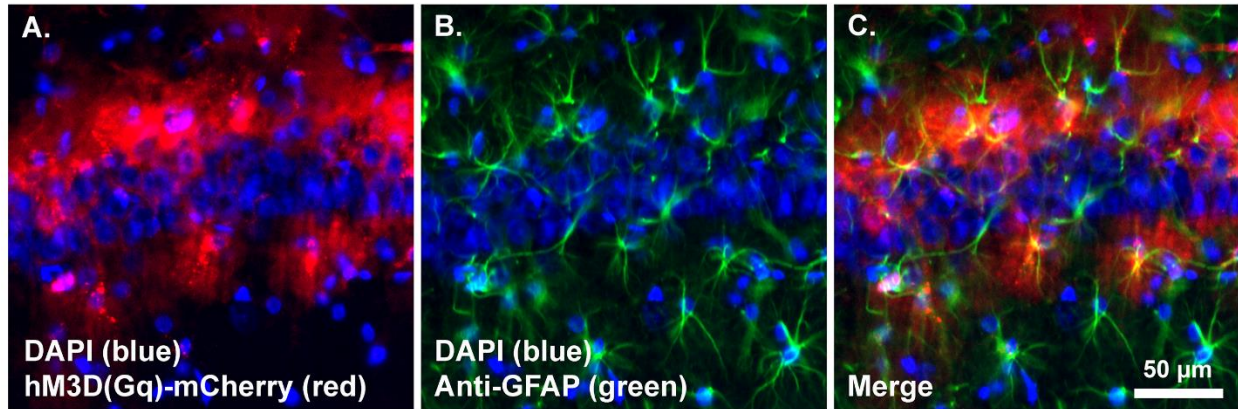
A) Representative image showing DAPI in Blue and GqDREADDs in red in the CA1 dhipp. B) Representative image showing colocalization of GFAP in green and GqDREADDs in red, confirming DREADDs targeted astrocytes in the CA1 dhipp. C) Representative image showing DAPI (blue), GFAP (green) and GqDREADDs (red) in the CA1 dhipp. D) Analysis of control animals in the fear conditioning paradigm. There was no effect of surgery, DREADDs, or Lck GFAP injection. E) Analysis of Day 1 (experimental). There was a significant decrease in freezing behaviors in animals that did not receive CNO activation compared to H_2O/DREADDs saline and EtOH/DREADDs saline groups following foot shock 3. There was a significant decrease in freezing behaviors in animals that did not receive CNO activation compared to H_2O/DREADDs saline and EtOH/DREADDs saline groups during the Post-Shock period (p = 0.0402 and p = 0.0333 respectively). F) Analysis during Day 2 (extinction) showed no changes between groups however there was significant treatment effect (F(2.162, 69.20) = 7.940; p = 0.0006). G) Analysis during Day 3 (extinction) showed no changes between groups. Figure was in part created with Biorender. Analysis: 2-way ANOVA with a Tukey's post hoc comparison, n = 12/treatment group.

Discussion

This study aimed to investigate the impact of AIE on astrocyte morphology, PAP-synaptic proximity, the integrity of synaptic structural proteins, and neuronal-astrocyte communication in the male CA1 dhipp. Due to the more robust AIE-induced loss of PAP-synaptic proximity and astrocyte volume in adulthood, we decided to move forward with the subsequent experiments focusing exclusively on the 26-day forced abstinence period (adulthood; PND 72). We observed a decrease in astrocyte responsivity to neuronal activity in the form of astrocyte-specific Ca^{2+} activity, despite an increase in synaptic glutamate. Therefore, we decided to see if we could attenuate AIE-induced deficits in a hippocampal-dependent fear conditioning paradigm if we used GqDREADDs to activate astrocyte-specific Ca^{2+} signaling cascades. These data suggest that AIE induces changes in astrocyte morphology and impairs neuronal-astrocyte bidirectional communication.

The human and rodent hippocampus continues to undergo structural and functional neuronal refinement throughout adolescence and into early adulthood (see (Walker et al., 2021) for review. Interestingly, we did not observe a change in astrocyte volume when comparing PND

46 and PND 72 naïve animals, suggesting that these astrocytes may already be in a morphologically mature state at PND 46 despite ongoing maturation of the hippocampus itself. However, we did see an increase in astrocyte-synaptic interactions over this period. These data suggest that colocalization of astrocytes and synapses may indicate ongoing CA1 dhipp synaptic maturation that continues throughout adolescence and into early adulthood that has never been reported before.

Astrocytes can modulate neuronal function and subsequent behaviors via the uptake of neurotransmitters, such as glutamate, from the synaptic cleft, the release of gliotransmitters, and through-contact mediated and astrocyte-secreted signaling (see reviews (Allen, 2014a; Allen & Eroglu, 2017; Blanco-Suarez et al., 2017)). As these processes are highly dependent on astrocyte-synaptic proximity, the findings in this study prove critical to our understanding of how AIE-induced changes in PAP-synaptic interactions contribute to deficits in neuronal functions. Stabilization of the tripartite synapse relies on various factors, including appropriate expression and interactions of synaptic bridging proteins. Previous work has shown that synaptic bridging proteins, neuroligins-neurexins, and eph-ephrins, are critical for synaptic function and astrocyte complexity (Stogsdill et al., 2017). Our data shows a loss of neuroligin 1 and 3 expression corresponding to a loss of neuroligin interactions with their presynaptic neurexin counterpart. It suggests that AIE results in a loss of PAP-synaptic proximity and a loss of mature synapses in adulthood. While we found that there was no change in Ephrin A3 or EphA4 expression in our model, we did find that there was an increase in Ephrin A3-EphA4 interactions. While the implications of the increase in Ephrin A3-EphA4 interaction have not been studied in a rodent model of AIE, this could result from an AIE-induced effect on other functions of Ephrin-Eph signaling. Previous work in mice has shown that Ephrin A2-EphA4 signaling can modulate

glutamate uptake by glial cells (Carmona et al., 2009; Filosa et al., 2009). Interestingly, our experiments assessing glutamate interactions with the proximal astrocyte processes show an increase in glutamate reaching the PAP. However, we found a significant decrease in astrocyte-Ca^{2+} responsivity, suggesting that AIE may impair glutamate transporters or receptors on the PAP. This is further supported by our data showing AIE increases Ephrin A3-EphA4 interactions in adulthood, as activation of the Ephrin A3-EphaA4 signaling cascade inhibits glutamate transport into the cell. Therefore, further research is needed to determine whether there is a loss of Ephrin A3 or EphA4 function or a loss of glutamate transporters or receptors in adulthood following AIE.

It has been well-established that adolescent alcohol use has lasting effects on some but not all hippocampal-dependent behaviors. In humans, chronic excessive alcohol use during adolescence has been associated with cognitive deficits manifesting in adulthood (Brown et al., 2000; Hanson et al., 2011). Multiple studies have demonstrated long-term, selective, hippocampal-dependent changes in response to chronic intermittent EtOH exposure that have been observed in humans ((Crews et al., 2016; Silvers et al., 2003) for review). These laboratory studies are consistent with human clinical studies that have revealed deficits in cognitive domains that rely heavily on hippocampal function, such as visuospatial construction (Hanson et al., 2011; Tomlinson et al., 2004), verbal learning and working memory (Hanson et al., 2011), and executive function (Giancola et al., 1998; Parada et al., 2012) in adolescents with AUD. However, the mechanisms underlying these deficits in cognition are not fully understood. Here in this study, we reveal a novel mechanism that could occur, mediated by long-term induced disruption of astrocyte morphology and function.

Astrocytes respond to neuronal signaling, releasing Ca^{2+} stores and driving signal propagation that can impact individual PAPs and overall astrocyte function (Yu et al., 2021). Astrocyte Ca^{2+} signaling occurs through various events necessary to balance and regulate synaptic ion homeostasis and neuronal excitability. The intricate crosstalk between astrocytes and neurons through this complex mechanism is crucial for neuronal function, meaning that dysregulation of this process could have significant consequences for synaptic and neuronal function and subsequent behaviors (Durkee et al., 2019). Our data reveal a loss of PAP-synaptic proximity corresponding to a loss of astrocyte responsivity in the form of Ca^{2+} signaling. Despite the loss of PAP-synaptic proximity, there was an increase in glutamate activity at the PAP. This was surprising because it has been established that when glutamate signaling increases at the PAPs, there is a downstream increase in astrocyte-Ca^{2+} signaling (Khakh & McCarthy, 2015). Further research is necessary to determine if this inconsistency is due to a loss of expression or function of glutamate transport or receptor expression at the PAP or to AIE-induced changes in intracellular Ca^{2+} signaling pathways.

One of the downstream consequences of astrocyte Ca^{2+} response to neuronal signaling is the release of gliotransmitters (e.g., adenosine) that can modulate neuronal function. The resulting gliotransmitter-neuronal receptor interaction can increase or inhibit neuronal signaling and subsequent downstream synaptic events. Therefore, we hypothesized that we could restore the astrocyte's ability to modulate neuronal signaling and subsequent behaviors through GqDREADDs. DREADD-based chemogenetic technologies are a relatively new technology that can be used to manipulate astrocyte iCa^{2+} signaling (Roth, 2016). The first DREADDs were the G_q-coupled DREADDs (G_q-DREADDs or excitatory DREADDs), including hM1D, hM3Dq, and hM5Dq and are activated by the administration of the pharmacologically inert designer drug,

CNO (Armbruster et al., 2007). CNO is a prototypical chemical actuator with drug-like properties resulting in rapid CNS penetration and distribution (Roth, 2016). G_q-DREADDs have repeatedly been shown to mobilize Ca^{2+} signaling in neurons and astrocytes through Gαq/11 g-protein, which stimulates phospholipase C, releasing Ca^{2+} stores (Armbruster et al., 2007). Using GqDREADDs in our contextual fear conditioning experiments, we found that activation of astrocyte-specific Ca^{2+} signaling following the 26-day forced abstinence period attenuated AIE-induced reduction in freezing behavior. This may suggest that AIE results in a loss of astrocyte Ca^{2+} signaling that typically drives the downstream release of gliotransmitters and the regulation of neuronal activity. By recovering the astrocyte Ca^{2+} signaling pathway, we can restore gliotransmitter-dependent neuronal regulation of behavior. Further investigation is necessary to confirm the involvement of downstream gliotransmitter release and neuronal regulation and the possible perturbation of adenosine receptors and transporters at this timepoint.

Conclusions

These data provide novel insight into how EtOH exposure during adolescence disrupts astrocyte morphology, astrocyte-synaptic interactions, glutamatergic signaling, and astrocyte responsivity to neuronal signaling in the form of astrocyte-Ca^{2+} activity. Furthermore, we have shown that activation of astrocyte-specific Ca^{2+} activity by activating GqDREADDs rescues freezing behavior in a contextual fear conditioning test. Given the importance of astrocyte regulation of synaptic activity during critical periods of development, further work is necessary to understand better the molecular mechanisms that drive the loss of PAP-synaptic coupling that contribute to the loss of astrocyte response to neuronal activity. The rescue of AIE-induced freezing behaviors by activating astrocyte-specific Ca^{2+} signaling suggests that AIE may disrupt gliotransmitter release, which could contribute to aberrant neuronal signaling. Future plans in our

lab are to test this hypothesis by investigating the effects of AIE on adenosine release, adenosine transporters, and receptor expression that are critical for the modulation of neuronal signaling. Further understanding of the molecular mechanisms contributing to the disruption of neuronal signaling may provide novel non-neuronal targets for future pharmacological interventions for individuals suffering from the chronic effects of alcohol use.

Chapter 7

Discussion and Future Directions

Discussion

Over the last few decades, alcohol use has been on the decline. However, alcohol in the form of binge drinking remains highly prevalent among adolescents and young adults. This excessive alcohol consumption coincides with late-stage brain development and increased vulnerability to the cytotoxic effects of alcohol and other drugs. Early alcohol use is associated with an increased likelihood of developing an alcohol use disorder and long-term cognitive deficits, including memory and learning, in which the prefrontal cortex and hippocampus play a significant role. Over the last decade, a growing field of research has focused on bettering our understanding of the long-term consequences of adolescent alcohol use on neuronal structure, function, and subsequent cognitive changes that may be associated with neuropsychiatric disorders, neurodegeneration, and addictive behavior. However, the impact of alcohol on astrocyte dysfunction and its contribution to these observed changes in neuronal function and cognition are just beginning to be elucidated.

Astrocytes continue to undergo maturation throughout adolescence and into early adulthood in the mPFC (IL and PL). Astrocyte maturation was identified by changes in astrocyte morphology (i.e., increases in astrocyte volume) and increases in PAP-synaptic interactions across adolescent development. Therefore, we sought to investigate how AIE would impact astrocyte morphology and PAP-synaptic interactions across multiple subregions of the PFC. We observed no effects on astrocyte volumes or PAP-synaptic interactions immediately following AIE (Chapter 4). Interestingly, despite no AIE-induced changes following a 26-day forced abstinence period, we did see a significant reduction in PAP-synaptic interactions in the ACC

and VO-OFC. This loss of PAP-synaptic interaction in the VO-OFC also correlated to a loss of mature dendric spine phenotypes in this region. This is important as there are previous studies that have shown that early EtOH exposure results in long-term cognitive impairment that is mediated by these subregions of the PFC. Preclinical studies such as these can help us understand how AIE disrupts synapses and contributes to AIE-induced neuronal dysfunction, which can aid in developing clinical treatments to treat individuals suffering from AUD.

It has previously been demonstrated that within the hipp, mature dendritic spines are found within closer proximity to PAPs than immature spines (Witcher et al., 2007) and combined with evidence that AIE results in a shift toward an immature dendritic spine phenotype in male rats (Risher et al., 2015) we sought to determine whether AIE disrupts PAP-synaptic interactions and astrocyte morphology in the dorsal CA1 in both female and male rats, respectively. As predicted, AIE decreased PAP-synaptic interactions in male rats; however increased PAP-synaptic interactions in females (Chapters 5 and 6). These findings demonstrate opposing sex-dependent responses to AIE in the context of PAP-synaptic decoupling. While these manuscripts do not directly compare male and female findings in our AIE studies, additional analysis reveals exciting sex differences in our models of AIE. As shown in Figure 23, astrocytes in EtOH naïve adult males have significantly larger volumes than age-matched EtOH naïve females ($p = 0.0080$). Even more interesting, astrocytes for males that underwent AIE have significantly larger volumes than naïve adult females ($p = 0.0156$). Additional analysis of PAP-synaptic proximity revealed similar findings. As shown in Figure 24, astrocytes from EtOH naïve adult males (PND 72) come into proximity to more PSD-95 markers than astrocytes from EtOH naïve age-matched females ($p = 0.0004$) and astrocytes from adult males that underwent AIE are near more PSD-95 markers than age-matched EtOH naïve females ($p = 0.0259$). This data suggests

that hippocampal astrocytes differ in morphology and (volume) and PAP-synaptic interactions

across adolescent development in males and females. This additional analysis further highlights

the importance of including females in studies of astrocyte maturation and the effects of AIE on

astrocyte morphology and PAP-synaptic interactions.

Figure 23
Astrocyte Volumes Differ in a Sex-Dependent Manner.
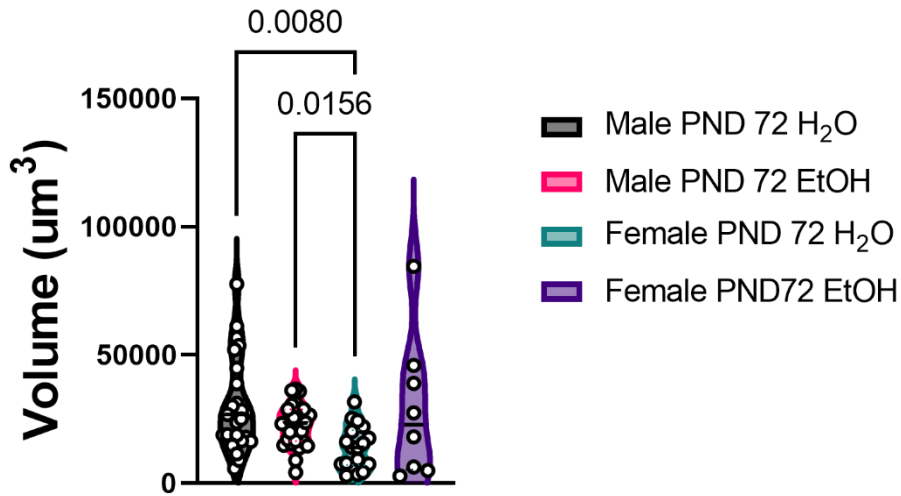
Quantifying astrocyte volumes revealed that astrocytes from EtOH naïve adult males (PND 72) are significantly larger than astrocytes from EtOH naïve age-matched females ($p = 0.0080$). There was no significant astrocyte volume when comparing astrocytes from males and females that underwent AIE. However, this could be due to the small n from the female study. Interestingly, astrocytes from adult males that underwent AIE were significantly larger than age-matched EtOH naïve females ($p = 0.0156$). Analysis: One-way ANOVA with a Tukey's post hoc comparison, n = 3-11 astrocytes/animal (3-11 animals/treatment group).

Figure 24

Astrocyte-Synaptic Proximity Differs in a Sex-Dependent Manner.
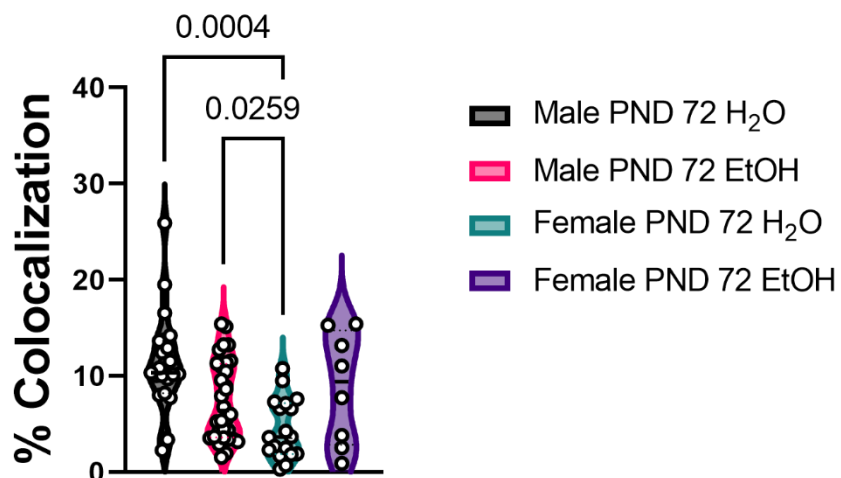
Quantification of PAP-synaptic proximity revealed that astrocytes from EtOH naïve adult males (PND 72) come into close proximity to more PSD-95 markers than astrocytes from EtOH naïve age-matched females ($p = 0.0004$). There were no significant differences in PAP-synaptic proximity when comparing astrocytes from males and females that underwent AIE. Astrocytes from adult males that underwent AIE are near more PSD-95 markers than age-matched EtOH naïve females ($p = 0.0259$). Analysis: One-way ANOVA with a Tukey's post hoc comparison, n = 3-11 astrocytes/animal (3-11 animals/treatment group).

Based on previous findings that AIE results in a reactive astrocyte response based on GFAP expression following a forced abstinence period in male rats, not during withdrawal, we have begun ancillary experiments to determine the extent to which this occurs in males versus females. While still preliminary, we are beginning to see that AIE induces atypical astrocyte function in males (Appendices B and C). These data and the previous suggest that there may be a correlation between astrocyte reactivity and PAP-synaptic interactions in males. However, further investigation is required to make a direct correlation between reactive astrocyte phenotypes and synaptic proximity. Since we found increases in astrocyte volumes and PAP-synaptic proximity in females, it would be interesting to investigate reactive astrocyte phenotypes in female models of AIE. We may be observing a different type of reactive astrocyte

response in females contributing to the increase in PAP-synaptic proximity. These experiments will improve our understanding of the long-term effects of AIE on astrocyte function that can influence PAP-synaptic interactions and subsequent neuronal function in males and females.

Despite differences in AIE-induced changes in PAP-synaptic interactions between the male and female groups, we observed that AIE followed by a 26-day forced abstinence period resulted in a loss of Ca^{2+} activity and an increase in glutamate reaching the PAPs of these proximal hippocampal astrocytes in the dorsal CA1 of both male and female rats. These findings suggest that while AIE has sex-dependent effects on astrocyte morphology and tripartite integrity, there may be an overarching mechanism that mediates increased glutamate availability in the tripartite synapse and loss of astrocyte iCa^{2+} activity. This could occur in several ways, including AIE-induced disruption of expression, function, or internalization of glutamate transporters or receptors on the PAPs.

Astrocytes respond to glutamatergic signaling as glutamate interacts with these G-protein coupled receptors (GPCRs) located at the PAP, which then induces multiple downstream events, including activation of the inositol 1,4,5-trisphosphate (IP3) pathway and phospholipase C (PLC) pathway. IP3 receptor activation induces the mobilization of astrocytic Ca^{2+} signaling from the endoplasmic reticulum (ER) that then propagates throughout the cell. This also reveals a possible mechanism by which AIE decreases astrocyte Ca^{2+} responsivity to glutamate signaling. Previous work has demonstrated that the deletion of IP3R2 in astrocytes disrupts IP3R-mediated astrocyte Ca^{2+} signaling (Li et al., 2015). While preliminary work from our lab has shown that AIE induces an increase in IP3 expression in males (Appendix D), we have yet to investigate whether AIE impacts IP3 receptors.

Our physiological recordings have allowed us to observe Ca^{2+} activity in the astrocyte

cell body. However, using electrophysiology and hippocampal iCa^{2+} imaging, it has been

demonstrated that IP3R subtypes contribute to astrocyte Ca^{2+} activity in distinct ways (Sherwood

et al., 2017). Specifically, IP3R2 induces more global Ca^{2+} release within the cell body and

major branches of the astrocyte. At the same time, IP3R1 and IP3R3 are responsible for more

localized Ca^{2+} signaling within the microdomains of the PAPs. However, more studies are

needed to demonstrate the full functionality of these different IP3R subtypes in astrocytes and

their roles in AIE-induced loss of Ca^{2+} signaling.

Lastly, we investigated AIE-induced deficits in freezing behaviors using a contextual fear

conditioning behavioral paradigm. Contextual fear conditioning requires a concerted network of

brain regions, including the mPFC, the hippocampus, and the amygdala. The mPFC, specifically

the IL and PL, are strongly associated with suppressing fear circuits. Our current studies found

no changes in astrocyte morphology or PAP-synaptic interactions in the mPFC (IL or PL).

However, we did see changes in astrocyte-synaptic interactions and astrocyte function in the

dorsal CA1.

Furthermore, we could attenuate AIE-induced deficits in freezing behaviors by activating

astrocyte-specific Ca^{2+} activity in the CA1 dhipp using GqDREADDs. Therefore, AIE disruption

of PAP-synaptic interactions in the CA1 dhipp may contribute to the loss of mPFC regulation of

amygdala activation because we know that projections originating in the CA1 hippocampus

innervate the IL-mPFC, leading us to speculate that AIE-induced disruption of PAP-synaptic

interactions in the CA1 may contribute to AIE-induced disruptions in our contextual fear

conditioning experiment. However, further work to better understand how disruption of astrocyte

function in the CA1 hippocampus influences these projections to the mPFC is necessary and

would strengthen the field's understanding of how AIE-induced changes in one brain region influence neuronal activity in others. Furthermore, this would help us better understand the circuitry involved in contextual fear conditioning experiments and how brain region-specific disruption of astrocytes contributes to deficits in freezing behaviors in these experiments.

These findings contribute to the overall knowledge of how AIE impacts astrocyte morphology and PAP-synaptic interactions in a region- and sex-specific manner. Furthermore, we identify ways in which AIE influences astrocyte function, which may be contributing to overall neuronal dysfunction that has been previously observed. Together, the studies presented in this dissertation reveal an essential role for astrocytes in AIE-induced dysfunction and provide a new target for therapeutic interventions for treated AUD.

Limitations

Despite the novelty of this work and the importance of the findings in identifying non-neuronal consequences of AIE that may influence known neuronal disruption in models of adolescent EtOH use, our model could be modified to be more translatable. For obvious ethical reasons, examining adolescent alcohol consumption in human models is prohibited. Therefore, we need to use laboratory rat models. Our studies focus on EtOH exposure during early adolescence (PND 30 to PND 46) because alcohol exposure during early adolescence is largely correlated to an increased risk of AUD in humans. However, in humans, peak alcohol consumption, both binge and non-binge consumption, occurs around 20 years of age. Based on rat developmental models, this would likely be more closely related to PND 55-60 in our rat model. Further studies that continue EtOH exposure throughout adolescent development would transform our model into one that more closely depicts human alcohol consumption and assess

the possible contributions of astrocytes in AIE-induced cognitive dysfunction observed in humans.

Our studies use an astrocyte-specific AAV with GFP to visualize the more complete astrocyte morphology, which is typical in a rat model where genetic modification is impossible. Even with this advanced technique, we still fail to capture some finer peripheral astrocyte processes. While this is a limitation in our current study, our lab is acquiring serial EM sections that would allow for the reconstruction of these finer PAPs that are ensheathing the synapse. Not only will this allow for better visualization of the PAPs, but it will also allow us to collect precise measurements of how AIE influences changes in PAP-synaptic distances.

Lastly, we were limited in our GCaMP6f studies when observing how AIE-induced changes in astrocyte-synaptic interactions influence astrocyte Ca^{2+} responsivity by using a microscope equipped with a mercury lamp. While we can observe and acquire data corresponding to changes in Ca^{2+} activity within the entire cell's body, we cannot isolate differences in the PAP microdomains that influence whole astrocyte Ca^{2+} activity. Also, we are limited in our physiological recordings of astrocyte Ca^{2+} activity by the sporadic expression of GCaMP6f in these hippocampal astrocytes. Ca^{2+} response in the astrocyte within proximity to the synapse triggers Ca^{2+} waves that spread throughout the network of surrounding astrocytes via astrocyte-astrocyte interactions. Sporadic uptake of the AAV containing GCaMP6f is typical, and being that we used a rat model for these studies, the use of AAV is unavoidable. There would be a need to use genetically modified mice to allow a uniform expression of GCaMP6f in astrocytes. For example, Ye et al. 2017 use a cre recombinase conditional GCaMP6f crossed with a *GLAST-CreEr* to allow astrocyte expression. Unfortunately, this would not allow for a direct correlation of results to the model described in these studies. However, using cultured

hippocampal rat astrocytes as a parallel study, a goal of this lab, that can be transfected with a GCaMP may allow for a better understanding of how EtOH may affect astrocyte-astrocyte communication and astrocyte Ca^{2+} waves across a network of astrocytes.

Future Directions

This dissertation highlights the non-neuronal effects of AIE on astrocytes in the female and male dhipp (Chapters 5 and 6, respectively) and subsequent behaviors. A logical follow-up to the physiology studies discussed in this dissertation would be determining whether AIE-induced disruption of PAP-synaptic interaction and astrocyte responsivity impeded astrocyte-neuronal communication. Astrocytes can modulate neuronal signaling by releasing gliotransmitters such as adenosine. Preliminary data collected by our lab (Appendix E) has revealed a significant increase in the expression of equilibrative nucleoside transporter 2 (ENT2) in the dhipp following AIE and a period of forced abstinence. ENT2 is a bidirectional transporter capable of shuttling adenosine across the cell membrane of neurons and glial cells. While the preliminary study was not cell-specific, the data suggest that AIE may have long-term effects on adenosine transport. Further studies to determine how AIE impacts astrocyte-neuronal communication would help us better understand the role of astrocyte-mediated neuronal modulation in AIE-induced behaviors.

The hippocampus regulates top-down fear processing and is required to learn about the degrees of danger of an object or situation. We have shown that AIE-induced deficits in freezing behaviors in a contextual fear conditioning test can be attenuated using GqDREADDs to activate Ca^{2+} activity in astrocytes of the male dhipp (Chapter 6). The hippocampus has projections to the amygdala, and hippocampal-amygdala circuitry has been identified as central to acquiring short-term contextual conditioned fear response. Our study found an AIE-induced conditioned fear

response during the acquisition phase of the fear conditioning paradigm that was not observed during the extinction phases. Therefore, further study of how AIE impacts hippocampus-to-amygdala communications would be necessary.

Lastly, while we use a widely accepted model of AIE, it would be essential to conduct longitudinal studies that continue past the onset of adulthood. Emerging roles of astrocyte dysfunction are being identified in psychiatric disease and neurodegeneration. While several psychiatric disorders manifest shortly after the onset of adulthood, it would be necessary to understand if these effects subside over time or have lasting consequences that contribute to neurodegenerative disease in mature and late-stage adults. Therefore, it would further our understanding of how AIE's impact on astrocyte function and PAP-synaptic interactions contribute to cognitive function later in life.

References

Abernathy, K., Chandler, L. J., & Woodward, J. J. (2010). Alcohol and the prefrontal cortex. *Int Rev Neurobiol*, *91*, 289-320. https://doi.org/10.1016/S0074-7742(10)91009-X

Abrahao, K. P., Salinas, A. G., & Lovinger, D. M. (2017). Alcohol and the Brain: Neuronal Molecular Targets, Synapses, and Circuits. *Neuron*, *96*(6), 1223-1238. https://doi.org/10.1016/j.neuron.2017.10.032

Acheson, S. K., Bearison, C., Risher, M. L., Abdelwahab, S. H., Wilson, W. A., & Swartzwelder, H. S. (2013). Effects of acute or chronic ethanol exposure during adolescence on behavioral inhibition and efficiency in a modified water maze task. *PLoS One*, *8*(10), e77768. https://doi.org/10.1371/journal.pone.0077768

Acheson, S. K., Stein, R. M., & Swartzwelder, H. S. (1998). Impairment of semantic and figural memory by acute ethanol: age-dependent effects. *Alcohol Clin Exp Res*, *22*(7), 1437-1442. https://doi.org/10.1111/j.1530-0277.1998.tb03932.x

Adriani, W., Chiarotti, F., & Laviola, G. (1998). Elevated novelty seeking and peculiar d-amphetamine sensitization in periadolescent mice compared with adult mice. *Behav Neurosci*, *112*(5), 1152-1166. https://doi.org/10.1037//0735-7044.112.5.1152

Agartz, I., Momenan, R., Rawlings, R. R., Kerich, M. J., & Hommer, D. W. (1999). Hippocampal volume in patients with alcohol dependence. *Arch Gen Psychiatry*, *56*(4), 356-363. https://doi.org/10.1001/archpsyc.56.4.356

Akkoc, R., & Ogeturk, M. (2017). M. The Prefrontal Cortex: A Basic Embryological, Histological, Anatomical, and Functional Guideline. *Journal of Human Anatomy & Physiology*, *1*(4), 1-4.

Alaux-Cantin, S., Warnault, V., Legastelois, R., Botia, B., Pierrefiche, O., Vilpoux, C., & Naassila, M. (2013). Alcohol intoxications during adolescence increase motivation for alcohol in adult rats and induce neuroadaptations in the nucleus accumbens. *Neuropharmacology*, *67*, 521-531. https://doi.org/10.1016/j.neuropharm.2012.12.007

Allen, N. J. (2014a). Astrocyte regulation of synaptic behavior. *Annu Rev Cell Dev Biol*, *30*, 439-463. https://doi.org/10.1146/annurev-cellbio-100913-013053

Allen, N. J. (2014b). Synaptic plasticity: Astrocytes wrap it up. *Curr Biol*, *24*(15), R697-699. https://doi.org/10.1016/j.cub.2014.06.030

Allen, N. J., & Eroglu, C. (2017). Cell Biology of Astrocyte-Synapse Interactions. *Neuron*, *96*(3), 697-708. https://doi.org/10.1016/j.neuron.2017.09.056

Amodeo, L. R., Wills, D. N., Sanchez-Alavez, M., Nguyen, W., Conti, B., & Ehlers, C. L. (2018). Intermittent voluntary ethanol consumption combined with ethanol vapor exposure during adolescence increases drinking and alters other behaviors in adulthood in female and male rats. *Alcohol*, *73*, 57-66. https://doi.org/10.1016/j.alcohol.2018.04.003

Arantius, G. (1587). *De humano foetu…Ejusdem anatomicorum observationum liber*.

Armbruster, B. N., Li, X., Pausch, M. H., Herlitze, S., & Roth, B. L. (2007). Evolving the lock to fit the key to create a family of G protein-coupled receptors potently activated by an inert ligand. *Proc Natl Acad Sci U S A*, *104*(12), 5163-5168. https://doi.org/10.1073/pnas.0700293104

Asato, M. R., Terwilliger, R., Woo, J., & Luna, B. (2010). White matter development in adolescence: a DTI study. *Cereb Cortex*, *20*(9), 2122-2131. https://doi.org/10.1093/cercor/bhp282

Barres, B. A. (2008). The mystery and magic of glia: a perspective on their roles in health and disease. *Neuron*, *60*(3), 430-440. https://doi.org/10.1016/j.neuron.2008.10.013

Beaulieu, C. (2002). The basis of anisotropic water diffusion in the nervous system - a technical review. *NMR Biomed*, *15*(7-8), 435-455. https://doi.org/10.1002/nbm.782

Bell, H. C., Pellis, S. M., & Kolb, B. (2010). Juvenile peer play experience and the development of the orbitofrontal and medial prefrontal cortices. *Behav Brain Res*, *207*(1), 7-13. https://doi.org/10.1016/j.bbr.2009.09.029

Benediktsson, A. M., Schachtele, S. J., Green, S. H., & Dailey, M. E. (2005). Ballistic labeling and dynamic imaging of astrocytes in organotypic hippocampal slice cultures. *J Neurosci Methods*, *141*(1), 41-53. https://doi.org/10.1016/j.jneumeth.2004.05.013

Beresford, T. P., Arciniegas, D. B., Alfers, J., Clapp, L., Martin, B., Du, Y., Liu, D., Shen, D., & Davatzikos, C. (2006). Hippocampus volume loss due to chronic heavy drinking. *Alcohol Clin Exp Res*, *30*(11), 1866-1870. https://doi.org/10.1111/j.1530-0277.2006.00223.x

Bian, X. L., Qin, C., Cai, C. Y., Zhou, Y., Tao, Y., Lin, Y. H., Wu, H. Y., Chang, L., Luo, C. X., & Zhu, D. Y. (2019). Anterior Cingulate Cortex to Ventral Hippocampus Circuit Mediates Contextual Fear Generalization. *J Neurosci*, *39*(29), 5728-5739. https://doi.org/10.1523/JNEUROSCI.2739-18.2019

Blakemore, S. J., & Mills, K. L. (2014). Is adolescence a sensitive period for sociocultural processing? *Annu Rev Psychol*, *65*, 187-207. https://doi.org/10.1146/annurev-psych-010213-115202

Blanco-Suarez, E., Caldwell, A. L., & Allen, N. J. (2017). Role of astrocyte-synapse interactions in CNS disorders. *J Physiol*, *595*(6), 1903-1916. https://doi.org/10.1113/JP270988

Blitzer, R. D., Gil, O., & Landau, E. M. (1990). Long-term potentiation in rat hippocampus is inhibited by low concentrations of ethanol. *Brain Res*, *537*(1-2), 203-208. https://doi.org/10.1016/0006-8993(90)90359-j

Boettiger, C. A., Mitchell, J. M., Tavares, V. C., Robertson, M., Joslyn, G., D'Esposito, M., & Fields, H. L. (2007). Immediate reward bias in humans: fronto-parietal networks and a role for the catechol-O-methyltransferase 158(Val/Val) genotype. *J Neurosci*, *27*(52), 14383-14391. https://doi.org/10.1523/JNEUROSCI.2551-07.2007

Bohm, M. K., Liu, Y., Esser, M. B., Mesnick, J. B., Lu, H., Pan, Y., & Greenlund, K. J. (2021). Binge Drinking Among Adults, by Select Characteristics and State - United States, 2018. *MMWR Morb Mortal Wkly Rep*, *70*(41), 1441-1446. https://doi.org/10.15585/mmwr.mm7041a2

Bourgeois, J. P., Goldman-Rakic, P. S., & Rakic, P. (1994). Synaptogenesis in the prefrontal cortex of rhesus monkeys. *Cereb Cortex*, *4*(1), 78-96. https://doi.org/10.1093/cercor/4.1.78

Bourne, J. N., & Harris, K. M. (2008). Balancing structure and function at hippocampal dendritic spines. *Annu Rev Neurosci*, *31*, 47-67. https://doi.org/10.1146/annurev.neuro.31.060407.125646

Broadwater, M., Varlinskaya, E. I., & Spear, L. P. (2013). Effects of voluntary access to sweetened ethanol during adolescence on intake in adulthood. *Alcohol Clin Exp Res*, *37*(6), 1048-1055. https://doi.org/10.1111/acer.12049

Broadwater, M. A., Lee, S. H., Yu, Y., Zhu, H., Crews, F. T., Robinson, D. L., & Shih, Y. I. (2018). Adolescent alcohol exposure decreases frontostriatal resting-state functional connectivity in adulthood. *Addict Biol*, *23*(2), 810-823. https://doi.org/10.1111/adb.12530

Brown, S. A., Tapert, S. F., Granholm, E., & Delis, D. C. (2000). Neurocognitive functioning of adolescents: effects of protracted alcohol use. *Alcohol Clin Exp Res*, *24*(2), 164-171. https://www.ncbi.nlm.nih.gov/pubmed/10698367

Bush, G., Luu, P., & Posner, M. I. (2000). Cognitive and emotional influences in anterior cingulate cortex. *Trends Cogn Sci*, *4*(6), 215-222. https://doi.org/10.1016/s1364-6613(00)01483-2

Bushong, E. A., Martone, M. E., Jones, Y. Z., & Ellisman, M. H. (2002). Protoplasmic astrocytes in CA1 stratum radiatum occupy separate anatomical domains. *J Neurosci*, *22*(1), 183-192. https://doi.org/10.1523/JNEUROSCI.22-01-00183.2002

Caine, S. B., Geyer, M. A., & Swerdlow, N. R. (1992). Hippocampal modulation of acoustic startle and prepulse inhibition in the rat. *Pharmacol Biochem Behav*, *43*(4), 1201-1208. https://doi.org/10.1016/0091-3057(92)90503-8

Camchong, J., Stenger, A., & Fein, G. (2013). Resting-state synchrony during early alcohol abstinence can predict subsequent relapse. *Cereb Cortex*, *23*(9), 2086-2099. https://doi.org/10.1093/cercor/bhs190

Campbell, J. P., Jahagirdar, V., Muhanna, A., Kennedy, K. F., & Helzberg, J. H. (2023). Hospitalizations for alcoholic liver disease during the COVID-19 pandemic increased more for women, especially young women, compared to men. *World J Hepatol*, *15*(2), 282-288. https://doi.org/10.4254/wjh.v15.i2.282

Carmona, M. A., Murai, K. K., Wang, L., Roberts, A. J., & Pasquale, E. B. (2009). Glial ephrin-A3 regulates hippocampal dendritic spine morphology and glutamate transport. *Proc Natl Acad Sci U S A*, *106*(30), 12524-12529. https://doi.org/10.1073/pnas.0903328106

Carty, N., Nash, K. R., Brownlow, M., Cruite, D., Wilcock, D., Selenica, M. L., Lee, D. C., Gordon, M. N., & Morgan, D. (2013). Intracranial injection of AAV expressing NEP but not IDE reduces amyloid pathology in APP+PS1 transgenic mice. *PLoS One*, *8*(3), e59626. https://doi.org/10.1371/journal.pone.0059626

Caspi, A., McClay, J., Moffitt, T. E., Mill, J., Martin, J., Craig, I. W., Taylor, A., & Poulton, R. (2002). Role of genotype in the cycle of violence in maltreated children. *Science*, *297*(5582), 851-854. https://doi.org/10.1126/science.1072290

Choenni, V., Hammink, A., & van de Mheen, D. (2017). Association Between Substance Use and the Perpetration of Family Violence in Industrialized Countries: A Systematic Review. *Trauma Violence Abuse*, *18*(1), 37-50. https://doi.org/10.1177/1524838015589253

Choudhury, S. (2010). Culturing the adolescent brain: what can neuroscience learn from anthropology? *Soc Cogn Affect Neurosci*, *5*(2-3), 159-167. https://doi.org/10.1093/scan/nsp030

Christopherson, K. S., Ullian, E. M., Stokes, C. C., Mullowney, C. E., Hell, J. W., Agah, A., Lawler, J., Mosher, D. F., Bornstein, P., & Barres, B. A. (2005). Thrombospondins are astrocyte-secreted proteins that promote CNS synaptogenesis. *Cell*, *120*(3), 421-433. https://doi.org/10.1016/j.cell.2004.12.020

Chung, T., Creswell, K. G., Bachrach, R., Clark, D. B., & Martin, C. S. (2018). Adolescent Binge Drinking. *Alcohol Res*, *39*(1), 5-15. https://www.ncbi.nlm.nih.gov/pubmed/30557142

Chung, W. S., Clarke, L. E., Wang, G. X., Stafford, B. K., Sher, A., Chakraborty, C., Joung, J., Foo, L. C., Thompson, A., Chen, C., Smith, S. J., & Barres, B. A. (2013). Astrocytes

mediate synapse elimination through MEGF10 and MERTK pathways. *Nature*, *504*(7480), 394-400. https://doi.org/10.1038/nature12776

Clarke, L. E., Liddelow, S. A., Chakraborty, C., Munch, A. E., Heiman, M., & Barres, B. A. (2018). Normal aging induces A1-like astrocyte reactivity. *Proc Natl Acad Sci U S A*, *115*(8), E1896-E1905. https://doi.org/10.1073/pnas.1800165115

Coleman, L. G., Jr., He, J., Lee, J., Styner, M., & Crews, F. T. (2011). Adolescent binge drinking alters adult brain neurotransmitter gene expression, behavior, brain regional volumes, and neurochemistry in mice. *Alcohol Clin Exp Res*, *35*(4), 671-688. https://doi.org/10.1111/j.1530-0277.2010.01385.x

Coleman, L. G., Jr., Liu, W., Oguz, I., Styner, M., & Crews, F. T. (2014). Adolescent binge ethanol treatment alters adult brain regional volumes, cortical extracellular matrix protein and behavioral flexibility. *Pharmacol Biochem Behav*, *116*, 142-151. https://doi.org/10.1016/j.pbb.2013.11.021

Cressman, V. L., Balaban, J., Steinfeld, S., Shemyakin, A., Graham, P., Parisot, N., & Moore, H. (2010). Prefrontal cortical inputs to the basal amygdala undergo pruning during late adolescence in the rat. *J Comp Neurol*, *518*(14), 2693-2709. https://doi.org/10.1002/cne.22359

Crews, F. T., Braun, C. J., Hoplight, B., Switzer, R. C., 3rd, & Knapp, D. J. (2000). Binge ethanol consumption causes differential brain damage in young adolescent rats compared with adult rats. *Alcohol Clin Exp Res*, *24*(11), 1712-1723. https://www.ncbi.nlm.nih.gov/pubmed/11104119

Crews, F. T., Robinson, D. L., Chandler, L. J., Ehlers, C. L., Mulholland, P. J., Pandey, S. C., Rodd, Z. A., Spear, L. P., Swartzwelder, H. S., & Vetreno, R. P. (2019). Mechanisms of Persistent Neurobiological Changes Following Adolescent Alcohol Exposure: NADIA Consortium Findings. *Alcohol Clin Exp Res*, *43*(9), 1806-1822. https://doi.org/10.1111/acer.14154

Crews, F. T., Vetreno, R. P., Broadwater, M. A., & Robinson, D. L. (2016). Adolescent Alcohol Exposure Persistently Impacts Adult Neurobiology and Behavior. *Pharmacol Rev*, *68*(4), 1074-1109. https://doi.org/10.1124/pr.115.012138

Crone, E. A., & Dahl, R. E. (2012). Understanding adolescence as a period of social-affective engagement and goal flexibility. *Nat Rev Neurosci*, *13*(9), 636-650. https://doi.org/10.1038/nrn3313

Csikszentmihalyi, M., Larson, R., & Prescott, S. (1977). The ecology of adolescent activity and experience. *J Youth Adolesc*, *6*(3), 281-294. https://doi.org/10.1007/bf02138940

Cunningham, M. G., Bhattacharyya, S., & Benes, F. M. (2002). Amygdalo-cortical sprouting continues into early adulthood: implications for the development of normal and abnormal function during adolescence. *J Comp Neurol*, *453*(2), 116-130. https://doi.org/10.1002/cne.10376

Dagar, S., & Gottmann, K. (2019). Differential Properties of the Synaptogenic Activities of the Neurexin Ligands Neuroligin1 and LRRTM2. *Front Mol Neurosci*, *12*, 269. https://doi.org/10.3389/fnmol.2019.00269

Dahl, R. E. (2004). Adolescent brain development: a period of vulnerabilities and opportunities. Keynote address. *Ann N Y Acad Sci*, *1021*, 1-22. https://doi.org/10.1196/annals.1308.001

Das, S., Sasaki, Y. F., Rothe, T., Premkumar, L. S., Takasu, M., Crandall, J. E., Dikkes, P., Conner, D. A., Rayudu, P. V., Cheung, W., Chen, H. S., Lipton, S. A., & Nakanishi, N.

(1998). Increased NMDA current and spine density in mice lacking the NMDA receptor subunit NR3A. *Nature*, *393*(6683), 377-381. https://doi.org/10.1038/30748

Davey, C. G., Yucel, M., & Allen, N. B. (2008). The emergence of depression in adolescence: development of the prefrontal cortex and the representation of reward. *Neurosci Biobehav Rev*, *32*(1), 1-19. https://doi.org/10.1016/j.neubiorev.2007.04.016

Davydov, D. M., Stewart, R., Ritchie, K., & Chaudieu, I. (2010). Resilience and mental health. *Clin Psychol Rev*, *30*(5), 479-495. https://doi.org/10.1016/j.cpr.2010.03.003

De Bellis, M. D., Clark, D. B., Beers, S. R., Soloff, P. H., Boring, A. M., Hall, J., Kersh, A., & Keshavan, M. S. (2000). Hippocampal volume in adolescent-onset alcohol use disorders. *Am J Psychiatry*, *157*(5), 737-744. https://doi.org/10.1176/appi.ajp.157.5.737

de Wit, J., Sylwestrak, E., O'Sullivan, M. L., Otto, S., Tiglio, K., Savas, J. N., Yates, J. R., 3rd, Comoletti, D., Taylor, P., & Ghosh, A. (2009). LRRTM2 interacts with Neurexin1 and regulates excitatory synapse formation. *Neuron*, *64*(6), 799-806. https://doi.org/10.1016/j.neuron.2009.12.019

Demyttenaere, K., Bruffaerts, R., Posada-Villa, J., Gasquet, I., Kovess, V., Lepine, J. P., Angermeyer, M. C., Bernert, S., de Girolamo, G., Morosini, P., Polidori, G., Kikkawa, T., Kawakami, N., Ono, Y., Takeshima, T., Uda, H., Karam, E. G., Fayyad, J. A., Karam, A. N., . . . Consortium, W. H. O. W. M. H. S. (2004). Prevalence, severity, and unmet need for treatment of mental disorders in the World Health Organization World Mental Health Surveys. *JAMA*, *291*(21), 2581-2590. https://doi.org/10.1001/jama.291.21.2581

Devoto, A., Himelein-Wachowiak, M., Liu, T., & Curtis, B. (2022). Women's Substance Use and Mental Health During the COVID-19 Pandemic. *Womens Health Issues*, *32*(3), 235-240. https://doi.org/10.1016/j.whi.2022.01.004

DeWit, D. J., Adlaf, E. M., Offord, D. R., & Ogborne, A. C. (2000). Age at first alcohol use: a risk factor for the development of alcohol disorders. *Am J Psychiatry*, *157*(5), 745-750. https://doi.org/10.1176/appi.ajp.157.5.745

Dickson, B. J. (2002). Molecular mechanisms of axon guidance. *Science*, *298*(5600), 1959-1964. https://doi.org/10.1126/science.1072165

Dong, Z., Bai, Y., Wu, X., Li, H., Gong, B., Howland, J. G., Huang, Y., He, W., Li, T., & Wang, Y. T. (2013). Hippocampal long-term depression mediates spatial reversal learning in the Morris water maze. *Neuropharmacology*, *64*, 65-73. https://doi.org/10.1016/j.neuropharm.2012.06.027

Dong, Z., Gong, B., Li, H., Bai, Y., Wu, X., Huang, Y., He, W., Li, T., & Wang, Y. T. (2012). Mechanisms of hippocampal long-term depression are required for memory enhancement by novelty exploration. *J Neurosci*, *32*(35), 11980-11990. https://doi.org/10.1523/JNEUROSCI.0984-12.2012

Donovan, J. E. (2009). Estimated blood alcohol concentrations for child and adolescent drinking and their implications for screening instruments. *Pediatrics*, *123*(6), e975-981. https://doi.org/10.1542/peds.2008-0027

Doremus, T. L., Brunell, S. C., Rajendran, P., & Spear, L. P. (2005). Factors influencing elevated ethanol consumption in adolescent relative to adult rats. *Alcohol Clin Exp Res*, *29*(10), 1796-1808. https://doi.org/10.1097/01.alc.0000183007.65998.aa

Durkee, C. A., Covelo, A., Lines, J., Kofuji, P., Aguilar, J., & Araque, A. (2019). G(i/o) protein-coupled receptors inhibit neurons but activate astrocytes and stimulate gliotransmission. *Glia*, *67*(6), 1076-1093. https://doi.org/10.1002/glia.23589

Ehlers, C. L., Oguz, I., Budin, F., Wills, D. N., & Crews, F. T. (2013). Peri-adolescent ethanol vapor exposure produces reductions in hippocampal volume that are correlated with deficits in prepulse inhibition of the startle. *Alcohol Clin Exp Res*, *37*(9), 1466-1475. https://doi.org/10.1111/acer.12125

Erickson, E. K., DaCosta, A. J., Mason, S. C., Blednov, Y. A., Mayfield, R. D., & Harris, R. A. (2021). Cortical astrocytes regulate ethanol consumption and intoxication in mice. *Neuropsychopharmacology*, *46*(3), 500-508. https://doi.org/10.1038/s41386-020-0721-0

Eroglu, C., Allen, N. J., Susman, M. W., O'Rourke, N. A., Park, C. Y., Ozkan, E., Chakraborty, C., Mulinyawe, S. B., Annis, D. S., Huberman, A. D., Green, E. M., Lawler, J., Dolmetsch, R., Garcia, K. C., Smith, S. J., Luo, Z. D., Rosenthal, A., Mosher, D. F., & Barres, B. A. (2009). Gabapentin receptor alpha2delta-1 is a neuronal thrombospondin receptor responsible for excitatory CNS synaptogenesis. *Cell*, *139*(2), 380-392. https://doi.org/10.1016/j.cell.2009.09.025

Eroglu, C., & Barres, B. A. (2010). Regulation of synaptic connectivity by glia. *Nature*, *468*(7321), 223-231. https://doi.org/10.1038/nature09612

Erol, A., & Karpyak, V. M. (2015). Sex and gender-related differences in alcohol use and its consequences: Contemporary knowledge and future research considerations. *Drug Alcohol Depend*, *156*, 1-13. https://doi.org/10.1016/j.drugalcdep.2015.08.023

Esser, M. B., Sherk, A., Liu, Y., Naimi, T. S., Stockwell, T., Stahre, M., Kanny, D., Landen, M., Saitz, R., & Brewer, R. D. (2020). Deaths and Years of Potential Life Lost From Excessive Alcohol Use - United States, 2011-2015. *MMWR Morb Mortal Wkly Rep*, *69*(30), 981-987. https://doi.org/10.15585/mmwr.mm6930a1

Fair, D. A., Cohen, A. L., Dosenbach, N. U., Church, J. A., Miezin, F. M., Barch, D. M., Raichle, M. E., Petersen, S. E., & Schlaggar, B. L. (2008). The maturing architecture of the brain's default network. *Proc Natl Acad Sci U S A*, *105*(10), 4028-4032. https://doi.org/10.1073/pnas.0800376105

Fan, Y., Shen, F., Chen, Y., Hao, Q., Liu, W., Su, H., Young, W. L., & Yang, G. Y. (2008). Overexpression of netrin-1 induces neovascularization in the adult mouse brain. *J Cereb Blood Flow Metab*, *28*(9), 1543-1551. https://doi.org/10.1038/jcbfm.2008.39

Farhy-Tselnicker, I., & Allen, N. J. (2018). Astrocytes, neurons, synapses: a tripartite view on cortical circuit development. *Neural Dev*, *13*(1), 7. https://doi.org/10.1186/s13064-018-0104-y

Filosa, A., Paixao, S., Honsek, S. D., Carmona, M. A., Becker, L., Feddersen, B., Gaitanos, L., Rudhard, Y., Schoepfer, R., Klopstock, T., Kullander, K., Rose, C. R., Pasquale, E. B., & Klein, R. (2009). Neuron-glia communication via EphA4/ephrin-A3 modulates LTP through glial glutamate transport. *Nat Neurosci*, *12*(10), 1285-1292. https://doi.org/10.1038/nn.2394

Flores-Barrera, E., Thomases, D. R., Heng, L. J., Cass, D. K., Caballero, A., & Tseng, K. Y. (2014). Late adolescent expression of GluN2B transmission in the prefrontal cortex is input-specific and requires postsynaptic protein kinase A and D1 dopamine receptor signaling. *Biol Psychiatry*, *75*(6), 508-516. https://doi.org/10.1016/j.biopsych.2013.07.033

Fujii, S., Yamazaki, Y., Sugihara, T., & Wakabayashi, I. (2008). Acute and chronic ethanol exposure differentially affect induction of hippocampal LTP. *Brain Res*, *1211*, 13-21. https://doi.org/10.1016/j.brainres.2008.02.052

Gass, J. T., Glen, W. B., Jr., McGonigal, J. T., Trantham-Davidson, H., Lopez, M. F., Randall, P. K., Yaxley, R., Floresco, S. B., & Chandler, L. J. (2014). Adolescent alcohol exposure reduces behavioral flexibility, promotes disinhibition, and increases resistance to extinction of ethanol self-administration in adulthood. *Neuropsychopharmacology*, *39*(11), 2570-2583. https://doi.org/10.1038/npp.2014.109

Gavrilov, N., Golyagina, I., Brazhe, A., Scimemi, A., Turlapov, V., & Semyanov, A. (2018). Astrocytic Coverage of Dendritic Spines, Dendritic Shafts, and Axonal Boutons in Hippocampal Neuropil. *Front Cell Neurosci*, *12*, 248. https://doi.org/10.3389/fncel.2018.00248

Ge, Y., Dong, Z., Bagot, R. C., Howland, J. G., Phillips, A. G., Wong, T. P., & Wang, Y. T. (2010). Hippocampal long-term depression is required for the consolidation of spatial memory. *Proc Natl Acad Sci U S A*, *107*(38), 16697-16702. https://doi.org/10.1073/pnas.1008200107

Giancola, P. R., Mezzich, A. C., & Tarter, R. E. (1998). Disruptive, delinquent and aggressive behavior in female adolescents with a psychoactive substance use disorder: relation to executive cognitive functioning. *J Stud Alcohol*, *59*(5), 560-567. https://doi.org/10.15288/jsa.1998.59.560

Gianoulakis, C., Dai, X., & Brown, T. (2003). Effect of Chronic Alcohol Consumption on the Activity of the Hypothalamic-Pituitary-Adrenal Axis and Pituitary β-Endorphin as a Function of Alcohol Intake, Age, and Gender. *Alcoholism: Clinical and Experimental Research*, *27*(3), 410-423. https://doi.org/https://doi.org/10.1097/01.ALC.0000056614.96137.B8

Gilpin, N. W., Karanikas, C. A., & Richardson, H. N. (2012). Adolescent binge drinking leads to changes in alcohol drinking, anxiety, and amygdalar corticotropin releasing factor cells in adulthood in male rats. *PLoS One*, *7*(2), e31466. https://doi.org/10.1371/journal.pone.0031466

Glasper, E. R., LaMarca, E. A., Bocarsly, M. E., Fasolino, M., Opendak, M., & Gould, E. (2015). Sexual experience enhances cognitive flexibility and dendritic spine density in the medial prefrontal cortex. *Neurobiol Learn Mem*, *125*, 73-79. https://doi.org/10.1016/j.nlm.2015.07.007

Gogtay, N., Giedd, J. N., Lusk, L., Hayashi, K. M., Greenstein, D., Vaituzis, A. C., Nugent, T. F., 3rd, Herman, D. H., Clasen, L. S., Toga, A. W., Rapoport, J. L., & Thompson, P. M. (2004). Dynamic mapping of human cortical development during childhood through early adulthood. *Proc Natl Acad Sci U S A*, *101*(21), 8174-8179. https://doi.org/10.1073/pnas.0402680101

Gomez, R. L., & Edgin, J. O. (2016). The extended trajectory of hippocampal development: Implications for early memory development and disorder. *Dev Cogn Neurosci*, *18*, 57-69. https://doi.org/10.1016/j.dcn.2015.08.009

Grieve, S. M., Williams, L. M., Paul, R. H., Clark, C. R., & Gordon, E. (2007). Cognitive aging, executive function, and fractional anisotropy: a diffusion tensor MR imaging study. *AJNR Am J Neuroradiol*, *28*(2), 226-235. https://www.ncbi.nlm.nih.gov/pubmed/17296985

Grifasi, I. R., McIntosh, S. E., Thomas, R. D., Lysle, D. T., Thiele, T. E., & Marshall, S. A. (2019). Characterization of the Hippocampal Neuroimmune Response to Binge-Like Ethanol Consumption in the Drinking in the Dark Model. *Neuroimmunomodulation*, *26*(1), 19-32. https://doi.org/10.1159/000495210

Griffin, A. (2017). Adolescent Neurological Development and Implications for Health and Well-Being. *Healthcare (Basel)*, *5*(4). https://doi.org/10.3390/healthcare5040062

Guirado, R., Umemori, J., Sipila, P., & Castren, E. (2016). Evidence for Competition for Target Innervation in the Medial Prefrontal Cortex. *Cereb Cortex*, *26*(3), 1287-1294. https://doi.org/10.1093/cercor/bhv280

Hanson, K. L., Medina, K. L., Padula, C. B., Tapert, S. F., & Brown, S. A. (2011). Impact of Adolescent Alcohol and Drug Use on Neuropsychological Functioning in Young Adulthood: 10-Year Outcomes. *J Child Adolesc Subst Abuse*, *20*(2), 135-154. https://doi.org/10.1080/1067828X.2011.555272

Harper, C. (1998). The neuropathology of alcohol-specific brain damage, or does alcohol damage the brain? *J Neuropathol Exp Neurol*, *57*(2), 101-110. https://doi.org/10.1097/00005072-199802000-00001

Harris, K. M., Fiala, J. C., & Ostroff, L. (2003). Structural changes at dendritic spine synapses during long-term potentiation. *Philos Trans R Soc Lond B Biol Sci*, *358*(1432), 745-748. https://doi.org/10.1098/rstb.2002.1254

Haustein, M. D., Kracun, S., Lu, X. H., Shih, T., Jackson-Weaver, O., Tong, X., Xu, J., Yang, X. W., O'Dell, T. J., Marvin, J. S., Ellisman, M. H., Bushong, E. A., Looger, L. L., & Khakh, B. S. (2014). Conditions and constraints for astrocyte calcium signaling in the hippocampal mossy fiber pathway. *Neuron*, *82*(2), 413-429. https://doi.org/10.1016/j.neuron.2014.02.041

Healey, K. L., Kibble, S., Hodges, S., Reissner, K. J., Testen, A., Wills, T. A., Acheson, S. K., Siemsen, B. M., McFaddin, J. A., Scofield, M. D., & Swartzwelder, H. S. (2020). Enduring alterations in hippocampal astrocytesynaptic proximity following adolescent alcohol exposure: reversal by gabapentin. *Neural Regen Res*, *15*(8), 1496-1501. https://doi.org/10.4103/1673-5374.274339

Henson, M. A., Roberts, A. C., Salimi, K., Vadlamudi, S., Hamer, R. M., Gilmore, J. H., Jarskog, L. F., & Philpot, B. D. (2008). Developmental regulation of the NMDA receptor subunits, NR3A and NR1, in human prefrontal cortex. *Cereb Cortex*, *18*(11), 2560-2573. https://doi.org/10.1093/cercor/bhn017

Himmler, B. T., Pellis, S. M., & Kolb, B. (2013). Juvenile play experience primes neurons in the medial prefrontal cortex to be more responsive to later experiences. *Neurosci Lett*, *556*, 42-45. https://doi.org/10.1016/j.neulet.2013.09.061

Hingson, R., & White, A. (2014). New research findings since the 2007 Surgeon General's Call to Action to Prevent and Reduce Underage Drinking: a review. *J Stud Alcohol Drugs*, *75*(1), 158-169. https://doi.org/10.15288/jsad.2014.75.158

Hogarth, L., Balleine, B. W., Corbit, L. H., & Killcross, S. (2013). Associative learning mechanisms underpinning the transition from recreational drug use to addiction. *Ann N Y Acad Sci*, *1282*, 12-24. https://doi.org/10.1111/j.1749-6632.2012.06768.x

Holder, M. K., & Blaustein, J. D. (2014). Puberty and adolescence as a time of vulnerability to stressors that alter neurobehavioral processes. *Front Neuroendocrinol*, *35*(1), 89-110. https://doi.org/10.1016/j.yfrne.2013.10.004

Holroyd, C. B., & McClure, S. M. (2015). Hierarchical control over effortful behavior by rodent medial frontal cortex: A computational model. *Psychol Rev*, *122*(1), 54-83. https://doi.org/10.1037/a0038339

Holroyd, C. B., & Yeung, N. (2012). Motivation of extended behaviors by anterior cingulate cortex. *Trends Cogn Sci*, *16*(2), 122-128. https://doi.org/10.1016/j.tics.2011.12.008

Hunt, D. L., & Castillo, P. E. (2012). Synaptic plasticity of NMDA receptors: mechanisms and functional implications. *Curr Opin Neurobiol*, *22*(3), 496-508. https://doi.org/10.1016/j.conb.2012.01.007

Huttenlocher, P. R. (1990). Morphometric study of human cerebral cortex development. *Neuropsychologia*, *28*(6), 517-527. https://doi.org/10.1016/0028-3932(90)90031-i

Huttenlocher, P. R., & Dabholkar, A. S. (1997). Regional differences in synaptogenesis in human cerebral cortex. *J Comp Neurol*, *387*(2), 167-178. https://doi.org/10.1002/(sici)1096-9861(19971020)387:2<167::aid-cne1>3.0.co;2-z

Hwang, S. N., Lee, J. S., Seo, K., & Lee, H. (2021). Astrocytic Regulation of Neural Circuits Underlying Behaviors. *Cells*, *10*(2). https://doi.org/10.3390/cells10020296

Ippolito, D. M., & Eroglu, C. (2010). Quantifying synapses: an immunocytochemistry-based assay to quantify synapse number. *J Vis Exp*(45). https://doi.org/10.3791/2270

Iwai, Y., Ozawa, K., Yahagi, K., Mishima, T., Akther, S., Vo, C. T., Lee, A. B., Tanaka, M., Itohara, S., & Hirase, H. (2021). Transient Astrocytic Gq Signaling Underlies Remote Memory Enhancement. *Front Neural Circuits*, *15*, 658343. https://doi.org/10.3389/fncir.2021.658343

Jaaskelainen, E., Juola, P., Hirvonen, N., McGrath, J. J., Saha, S., Isohanni, M., Veijola, J., & Miettunen, J. (2013). A systematic review and meta-analysis of recovery in schizophrenia. *Schizophr Bull*, *39*(6), 1296-1306. https://doi.org/10.1093/schbul/sbs130

Jacobson, R. (1986). The contributions of sex and drinking history to the CT brain scan changes in alcoholics. *Psychol Med*, *16*(3), 547-559. https://doi.org/10.1017/s003329170001031x

Jernigan, T. L., Butters, N., DiTraglia, G., Schafer, K., Smith, T., Irwin, M., Grant, I., Schuckit, M., & Cermak, L. S. (1991). Reduced cerebral grey matter observed in alcoholics using magnetic resonance imaging. *Alcohol Clin Exp Res*, *15*(3), 418-427. https://doi.org/10.1111/j.1530-0277.1991.tb00540.x

Jiao, Y., Sun, Z., Lee, T., Fusco, F. R., Kimble, T. D., Meade, C. A., Cuthbertson, S., & Reiner, A. (1999). A simple and sensitive antigen retrieval method for free-floating and slide-mounted tissue sections. *J Neurosci Methods*, *93*(2), 149-162. https://doi.org/10.1016/s0165-0270(99)00142-9

Jobson, D. D., Hase, Y., Clarkson, A. N., & Kalaria, R. N. (2021). The role of the medial prefrontal cortex in cognition, ageing and dementia. *Brain Commun*, *3*(3), fcab125. https://doi.org/10.1093/braincomms/fcab125

Johnson, M. H. (2001). Functional brain development in humans. *Nat Rev Neurosci*, *2*(7), 475-483. https://doi.org/10.1038/35081509

Jones, C. M., Clayton, H. B., Deputy, N. P., Roehler, D. R., Ko, J. Y., Esser, M. B., Brookmeyer, K. A., & Hertz, M. F. (2020). Prescription Opioid Misuse and Use of Alcohol and Other Substances Among High School Students - Youth Risk Behavior Survey, United States, 2019. *MMWR Suppl*, *69*(1), 38-46. https://doi.org/10.15585/mmwr.su6901a5

Kalivas, P. W. (2009). The glutamate homeostasis hypothesis of addiction. *Nat Rev Neurosci*, *10*(8), 561-572. https://doi.org/10.1038/nrn2515

Kandel, D. B., Johnson, J. G., Bird, H. R., Canino, G., Goodman, S. H., Lahey, B. B., Regier, D. A., & Schwab-Stone, M. (1997). Psychiatric disorders associated with substance use among children and adolescents: findings from the Methods for the Epidemiology of Child and Adolescent Mental Disorders (MECA) Study. *J Abnorm Child Psychol*, *25*(2), 121-132. https://doi.org/10.1023/a:1025779412167

Karriker-Jaffe, K. J., Subbaraman, M. S., Greenfield, T. K., & Kerr, W. C. (2018). Contribution of alcohol and drug co-use to substance use problems: Data from a nationally-representative sample of U.S. adults who have never been to treatment. *Nordisk Alkohol Nark*, *35*(6), 428-442. https://doi.org/10.1177/1455072518806122

Karve, I. P., Taylor, J. M., & Crack, P. J. (2016). The contribution of astrocytes and microglia to traumatic brain injury. *Br J Pharmacol*, *173*(4), 692-702. https://doi.org/10.1111/bph.13125

Khakh, B. S., & McCarthy, K. D. (2015). Astrocyte calcium signaling: from observations to functions and the challenges therein. *Cold Spring Harb Perspect Biol*, *7*(4), a020404. https://doi.org/10.1101/cshperspect.a020404

Khakh, B. S., & Sofroniew, M. V. (2015). Diversity of astrocyte functions and phenotypes in neural circuits. *Nat Neurosci*, *18*(7), 942-952. https://doi.org/10.1038/nn.4043

Kim, S. K., Nabekura, J., & Koizumi, S. (2017). Astrocyte-mediated synapse remodeling in the pathological brain. *Glia*, *65*(11), 1719-1727. https://doi.org/10.1002/glia.23169

Kim, Y., Park, J., & Choi, Y. K. (2019). The Role of Astrocytes in the Central Nervous System Focused on BK Channel and Heme Oxygenase Metabolites: A Review. *Antioxidants (Basel)*, *8*(5). https://doi.org/10.3390/antiox8050121

Knudsen, E. I. (2004). Sensitive periods in the development of the brain and behavior. *J Cogn Neurosci*, *16*(8), 1412-1425. https://doi.org/10.1162/0898929042304796

Ko, J., Zhang, C., Arac, D., Boucard, A. A., Brunger, A. T., & Sudhof, T. C. (2009). Neuroligin-1 performs neurexin-dependent and neurexin-independent functions in synapse validation. *EMBO J*, *28*(20), 3244-3255. https://doi.org/10.1038/emboj.2009.249

Kol, A., Adamsky, A., Groysman, M., Kreisel, T., London, M., & Goshen, I. (2020). Astrocytes contribute to remote memory formation by modulating hippocampal-cortical communication during learning. *Nat Neurosci*, *23*(10), 1229-1239. https://doi.org/10.1038/s41593-020-0679-6

Kolling, N., Behrens, T., Wittmann, M. K., & Rushworth, M. (2016). Multiple signals in anterior cingulate cortex. *Curr Opin Neurobiol*, *37*, 36-43. https://doi.org/10.1016/j.conb.2015.12.007

Koob, G. F., & Volkow, N. D. (2016). Neurobiology of addiction: a neurocircuitry analysis. *Lancet Psychiatry*, *3*(8), 760-773. https://doi.org/10.1016/S2215-0366(16)00104-8

Kubotera, H., Ikeshima-Kataoka, H., Hatashita, Y., Allegra Mascaro, A. L., Pavone, F. S., & Inoue, T. (2019). Astrocytic endfeet re-cover blood vessels after removal by laser ablation. *Sci Rep*, *9*(1), 1263. https://doi.org/10.1038/s41598-018-37419-4

Kumar, S., Porcu, P., Werner, D. F., Matthews, D. B., Diaz-Granados, J. L., Helfand, R. S., & Morrow, A. L. (2009). The role of GABA(A) receptors in the acute and chronic effects of ethanol: a decade of progress. *Psychopharmacology (Berl)*, *205*(4), 529-564. https://doi.org/10.1007/s00213-009-1562-z

Kuntsche, E., Kuntsche, S., Thrul, J., & Gmel, G. (2017). Binge drinking: Health impact, prevalence, correlates and interventions. *Psychol Health*, *32*(8), 976-1017. https://doi.org/10.1080/08870446.2017.1325889

Land, C., & Spear, N. E. (2004). Ethanol impairs memory of a simple discrimination in adolescent rats at doses that leave adult memory unaffected. *Neurobiol Learn Mem*, *81*(1), 75-81. https://doi.org/10.1016/j.nlm.2003.08.005

Lasic, E., Lisjak, M., Horvat, A., Bozic, M., Sakanovic, A., Anderluh, G., Verkhratsky, A., Vardjan, N., Jorgacevski, J., Stenovec, M., & Zorec, R. (2019). Astrocyte Specific

Remodeling of Plasmalemmal Cholesterol Composition by Ketamine Indicates a New Mechanism of Antidepressant Action. *Sci Rep*, *9*(1), 10957. https://doi.org/10.1038/s41598-019-47459-z

Laubach, M., Caetano, M. S., & Narayanan, N. S. (2015). Mistakes were made: neural mechanisms for the adaptive control of action initiation by the medial prefrontal cortex. *J Physiol Paris*, *109*(1-3), 104-117. https://doi.org/10.1016/j.jphysparis.2014.12.001

Laurent, V., & Westbrook, R. F. (2009). Inactivation of the infralimbic but not the prelimbic cortex impairs consolidation and retrieval of fear extinction. *Learn Mem*, *16*(9), 520-529. https://doi.org/10.1101/lm.1474609

Lee, C. T., Boeshore, K. L., Wu, C., Becker, K. G., Errico, S. L., Mash, D. C., & Freed, W. J. (2016). Cocaine promotes primary human astrocyte proliferation via JNK-dependent up-regulation of cyclin A2. *Restor Neurol Neurosci*, *34*(6), 965-976. https://doi.org/10.3233/RNN-160676

Lei, H., Lai, J., Sun, X., Xu, Q., & Feng, G. (2019). Lateral orbitofrontal dysfunction in the Sapap3 knockout mouse model of obsessive-compulsive disorder. *J Psychiatry Neurosci*, *44*(2), 120-131. https://doi.org/10.1503/jpn.180032

Li, H., Xie, Y., Zhang, N., Yu, Y., Zhang, Q., & Ding, S. (2015). Disruption of IP(3)R2-mediated Ca(2)(+) signaling pathway in astrocytes ameliorates neuronal death and brain damage while reducing behavioral deficits after focal ischemic stroke. *Cell Calcium*, *58*(6), 565-576. https://doi.org/10.1016/j.ceca.2015.09.004

Liddelow, S. A., Guttenplan, K. A., Clarke, L. E., Bennett, F. C., Bohlen, C. J., Schirmer, L., Bennett, M. L., Munch, A. E., Chung, W. S., Peterson, T. C., Wilton, D. K., Frouin, A., Napier, B. A., Panicker, N., Kumar, M., Buckwalter, M. S., Rowitch, D. H., Dawson, V. L., Dawson, T. M., . . . Barres, B. A. (2017). Neurotoxic reactive astrocytes are induced by activated microglia. *Nature*, *541*(7638), 481-487. https://doi.org/10.1038/nature21029

Liston, C., Watts, R., Tottenham, N., Davidson, M. C., Niogi, S., Ulug, A. M., & Casey, B. J. (2006). Frontostriatal microstructure modulates efficient recruitment of cognitive control. *Cereb Cortex*, *16*(4), 553-560. https://doi.org/10.1093/cercor/bhj003

Little, P. J., Kuhn, C. M., Wilson, W. A., & Swartzwelder, H. S. (1996). Differential effects of ethanol in adolescent and adult rats. *Alcohol Clin Exp Res*, *20*(8), 1346-1351. https://doi.org/10.1111/j.1530-0277.1996.tb01133.x

Lovinger, D. M., White, G., & Weight, F. F. (1989). Ethanol inhibits NMDA-activated ion current in hippocampal neurons. *Science*, *243*(4899), 1721-1724. https://doi.org/10.1126/science.2467382

Lundgaard, I., Wang, W., Eberhardt, A., Vinitsky, H. S., Reeves, B. C., Peng, S., Lou, N., Hussain, R., & Nedergaard, M. (2018). Beneficial effects of low alcohol exposure, but adverse effects of high alcohol intake on glymphatic function. *Sci Rep*, *8*(1), 2246. https://doi.org/10.1038/s41598-018-20424-y

Lyon, K. A., & Allen, N. J. (2021). From Synapses to Circuits, Astrocytes Regulate Behavior. *Front Neural Circuits*, *15*, 786293. https://doi.org/10.3389/fncir.2021.786293

Mann, K., Batra, A., Gunthner, A., & Schroth, G. (1992). Do women develop alcoholic brain damage more readily than men? *Alcohol Clin Exp Res*, *16*(6), 1052-1056. https://doi.org/10.1111/j.1530-0277.1992.tb00698.x

Markham, J. A., Morris, J. R., & Juraska, J. M. (2007). Neuron number decreases in the rat ventral, but not dorsal, medial prefrontal cortex between adolescence and adulthood. *Neuroscience*, *144*(3), 961-968. https://doi.org/10.1016/j.neuroscience.2006.10.015

151

Markwiese, B. J., Acheson, S. K., Levin, E. D., Wilson, W. A., & Swartzwelder, H. S. (1998). Differential effects of ethanol on memory in adolescent and adult rats. *Alcohol Clin Exp Res*, *22*(2), 416-421. https://www.ncbi.nlm.nih.gov/pubmed/9581648

Marvin, J. S., Borghuis, B. G., Tian, L., Cichon, J., Harnett, M. T., Akerboom, J., Gordus, A., Renninger, S. L., Chen, T. W., Bargmann, C. I., Orger, M. B., Schreiter, E. R., Demb, J. B., Gan, W. B., Hires, S. A., & Looger, L. L. (2013). An optimized fluorescent probe for visualizing glutamate neurotransmission. *Nat Methods*, *10*(2), 162-170. https://doi.org/10.1038/nmeth.2333

Mashhoon, Y., Czerkawski, C., Crowley, D. J., Cohen-Gilbert, J. E., Sneider, J. T., & Silveri, M. M. (2014). Binge alcohol consumption in emerging adults: anterior cingulate cortical "thinness" is associated with alcohol use patterns. *Alcohol Clin Exp Res*, *38*(7), 1955-1964. https://doi.org/10.1111/acer.12475

Matias, I., Morgado, J., & Gomes, F. C. A. (2019). Astrocyte Heterogeneity: Impact to Brain Aging and Disease. *Front Aging Neurosci*, *11*, 59. https://doi.org/10.3389/fnagi.2019.00059

Matsuzaki, M. (2007). Factors critical for the plasticity of dendritic spines and memory storage. *Neurosci Res*, *57*(1), 1-9. https://doi.org/10.1016/j.neures.2006.09.017

Maynard, M. E., Barton, E. A., Robinson, C. R., Wooden, J. I., & Leasure, J. L. (2018). Sex differences in hippocampal damage, cognitive impairment, and trophic factor expression in an animal model of an alcohol use disorder. *Brain Struct Funct*, *223*(1), 195-210. https://doi.org/10.1007/s00429-017-1482-3

McBride, W. J., Bell, R. L., Rodd, Z. A., Strother, W. N., & Murphy, J. M. (2005). Adolescent alcohol drinking and its long-range consequences. Studies with animal models. *Recent Dev Alcohol*, *17*, 123-142. https://doi.org/10.1007/0-306-48626-1_6

McCutcheon, J. E., & Marinelli, M. (2009). Age matters. *Eur J Neurosci*, *29*(5), 997-1014. https://doi.org/10.1111/j.1460-9568.2009.06648.x

McGuier, N. S., Padula, A. E., Lopez, M. F., Woodward, J. J., & Mulholland, P. J. (2015). Withdrawal from chronic intermittent alcohol exposure increases dendritic spine density in the lateral orbitofrontal cortex of mice. *Alcohol*, *49*(1), 21-27. https://doi.org/10.1016/j.alcohol.2014.07.017

Medina, K. L., Nagel, B. J., Park, A., McQueeny, T., & Tapert, S. F. (2007). Depressive symptoms in adolescents: associations with white matter volume and marijuana use. *J Child Psychol Psychiatry*, *48*(6), 592-600. https://doi.org/10.1111/j.1469-7610.2007.01728.x

Miguel-Hidalgo, J. J., Overholser, J. C., Meltzer, H. Y., Stockmeier, C. A., & Rajkowska, G. (2006). Reduced glial and neuronal packing density in the orbitofrontal cortex in alcohol dependence and its relationship with suicide and duration of alcohol dependence. *Alcohol Clin Exp Res*, *30*(11), 1845-1855. https://doi.org/10.1111/j.1530-0277.2006.00221.x

Miller, J. W., Naimi, T. S., Brewer, R. D., & Jones, S. E. (2007). Binge drinking and associated health risk behaviors among high school students. *Pediatrics*, *119*(1), 76-85. https://doi.org/10.1542/peds.2006-1517

Mills, K. L., & Tamnes, C. K. (2014). Methods and considerations for longitudinal structural brain imaging analysis across development. *Dev Cogn Neurosci*, *9*, 172-190. https://doi.org/10.1016/j.dcn.2014.04.004

Mira, R. G., Lira, M., Tapia-Rojas, C., Rebolledo, D. L., Quintanilla, R. A., & Cerpa, W. (2019). Effect of Alcohol on Hippocampal-Dependent Plasticity and Behavior: Role of

Glutamatergic Synaptic Transmission. *Front Behav Neurosci*, *13*, 288. https://doi.org/10.3389/fnbeh.2019.00288

Morales, M., & Spear, L. P. (2014). The effects of an acute challenge with the NMDA receptor antagonists, MK-801, PEAQX, and ifenprodil, on social inhibition in adolescent and adult male rats. *Psychopharmacology (Berl)*, *231*(8), 1797-1807. https://doi.org/10.1007/s00213-013-3278-3

Morris, R., Pandya, D. N., & Petrides, M. (1999). Fiber system linking the mid-dorsolateral frontal cortex with the retrosplenial/presubicular region in the rhesus monkey. *J Comp Neurol*, *407*(2), 183-192. https://doi.org/10.1002/(sici)1096-9861(19990503)407:2<183::aid-cne3>3.0.co;2-n

Morrisett, R. A., & Swartzwelder, H. S. (1993). Attenuation of hippocampal long-term potentiation by ethanol: a patch-clamp analysis of glutamatergic and GABAergic mechanisms. *J Neurosci*, *13*(5), 2264-2272. https://www.ncbi.nlm.nih.gov/pubmed/8478698

Mrak, R. E., Sheng, J. G., & Griffin, W. S. (1995). Glial cytokines in Alzheimer's disease: review and pathogenic implications. *Hum Pathol*, *26*(8), 816-823. https://doi.org/10.1016/0046-8177(95)90001-2

Muller, C., & Remy, S. (2018). Septo-hippocampal interaction. *Cell Tissue Res*, *373*(3), 565-575. https://doi.org/10.1007/s00441-017-2745-2

Murray, L., Maurer, J. M., Peechatka, A. L., Frederick, B. B., Kaiser, R. H., & Janes, A. C. (2021). Sex differences in functional network dynamics observed using coactivation pattern analysis. *Cogn Neurosci*, *12*(3-4), 120-130. https://doi.org/10.1080/17588928.2021.1880383

Murty, V. P., Calabro, F., & Luna, B. (2016). The role of experience in adolescent cognitive development: Integration of executive, memory, and mesolimbic systems. *Neurosci Biobehav Rev*, *70*, 46-58. https://doi.org/10.1016/j.neubiorev.2016.07.034

Nagel, B. J., Schweinsburg, A. D., Phan, V., & Tapert, S. F. (2005). Reduced hippocampal volume among adolescents with alcohol use disorders without psychiatric comorbidity. *Psychiatry Res*, *139*(3), 181-190. https://doi.org/10.1016/j.pscychresns.2005.05.008

Nentwig, T. B., Starr, E. M., Chandler, L. J., & Glover, E. J. (2019). Absence of compulsive drinking phenotype in adult male rats exposed to ethanol in a binge-like pattern during adolescence. *Alcohol*, *79*, 93-103. https://doi.org/10.1016/j.alcohol.2019.01.006

Nephew, B. C., Febo, M., Cali, R., Workman, K. P., Payne, L., Moore, C. M., King, J. A., & Lacreuse, A. (2020). Robustness of sex-differences in functional connectivity over time in middle-aged marmosets. *Sci Rep*, *10*(1), 16647. https://doi.org/10.1038/s41598-020-73811-9

Nishida, H., & Okabe, S. (2007). Direct astrocytic contacts regulate local maturation of dendritic spines. *J Neurosci*, *27*(2), 331-340. https://doi.org/10.1523/JNEUROSCI.4466-06.2007

Nogueira, R., Abolafia, J. M., Drugowitsch, J., Balaguer-Ballester, E., Sanchez-Vives, M. V., & Moreno-Bote, R. (2017). Lateral orbitofrontal cortex anticipates choices and integrates prior with current information. *Nat Commun*, *8*, 14823. https://doi.org/10.1038/ncomms14823

Norden, D. M., Trojanowski, P. J., Villanueva, E., Navarro, E., & Godbout, J. P. (2016). Sequential activation of microglia and astrocyte cytokine expression precedes increased Iba-1 or GFAP immunoreactivity following systemic immune challenge. *Glia*, *64*(2), 300-316. https://doi.org/10.1002/glia.22930

Nwachukwu, K. N., Evans, W. A., Sides, T. R., Trevisani, C. P., Davis, A., & Marshall, S. A. (2021). Chemogenetic manipulation of astrocytic signaling in the basolateral amygdala reduces binge-like alcohol consumption in male mice. *J Neurosci Res*, *99*(8), 1957-1972. https://doi.org/10.1002/jnr.24841

Nwachukwu, K. N., King, D. M., Healey, K. L., Swartzwelder, H. S., & Marshall, S. A. (2022). Sex-specific effects of adolescent intermittent ethanol exposure-induced dysregulation of hippocampal glial cells in adulthood. *Alcohol*, *100*, 31-39. https://doi.org/10.1016/j.alcohol.2022.02.002

Oberheim, N. A., Takano, T., Han, X., He, W., Lin, J. H., Wang, F., Xu, Q., Wyatt, J. D., Pilcher, W., Ojemann, J. G., Ransom, B. R., Goldman, S. A., & Nedergaard, M. (2009). Uniquely hominid features of adult human astrocytes. *J Neurosci*, *29*(10), 3276-3287. https://doi.org/10.1523/JNEUROSCI.4707-08.2009

Octeau, J. C., Chai, H., Jiang, R., Bonanno, S. L., Martin, K. C., & Khakh, B. S. (2018). An Optical Neuron-Astrocyte Proximity Assay at Synaptic Distance Scales. *Neuron*, *98*(1), 49-66 e49. https://doi.org/10.1016/j.neuron.2018.03.003

Ongur, D., & Price, J. L. (2000). The organization of networks within the orbital and medial prefrontal cortex of rats, monkeys and humans. *Cereb Cortex*, *10*(3), 206-219. https://doi.org/10.1093/cercor/10.3.206

Oppenheim, R. W. (1991). Cell death during development of the nervous system. *Annu Rev Neurosci*, *14*, 453-501. https://doi.org/10.1146/annurev.ne.14.030191.002321

Panksepp, J. (1981). The ontogeny of play in rats. *Dev Psychobiol*, *14*(4), 327-332. https://doi.org/10.1002/dev.420140405

Parada, M., Corral, M., Caamano-Isorna, F., Mota, N., Crego, A., Holguin, S. R., & Cadaveira, F. (2011). Binge drinking and declarative memory in university students. *Alcohol Clin Exp Res*, *35*(8), 1475-1484. https://doi.org/10.1111/j.1530-0277.2011.01484.x

Parada, M., Corral, M., Mota, N., Crego, A., Rodriguez Holguin, S., & Cadaveira, F. (2012). Executive functioning and alcohol binge drinking in university students. *Addict Behav*, *37*(2), 167-172. https://doi.org/10.1016/j.addbeh.2011.09.015

Pascual, M., Boix, J., Felipo, V., & Guerri, C. (2009). Repeated alcohol administration during adolescence causes changes in the mesolimbic dopaminergic and glutamatergic systems and promotes alcohol intake in the adult rat. *J Neurochem*, *108*(4), 920-931. https://doi.org/10.1111/j.1471-4159.2008.05835.x

Patrick, M. E., & Schulenberg, J. E. (2013). Prevalence and predictors of adolescent alcohol use and binge drinking in the United States. *Alcohol Res*, *35*(2), 193-200. https://www.ncbi.nlm.nih.gov/pubmed/24881328

Paus, T. (2000). Functional anatomy of arousal and attention systems in the human brain. *Prog Brain Res*, *126*, 65-77. https://doi.org/10.1016/S0079-6123(00)26007-X

Paus, T., Keshavan, M., & Giedd, J. N. (2008). Why do many psychiatric disorders emerge during adolescence? *Nat Rev Neurosci*, *9*(12), 947-957. https://doi.org/10.1038/nrn2513

Pautassi, R. M., Myers, M., Spear, L. P., Molina, J. C., & Spear, N. E. (2008). Adolescent but not adult rats exhibit ethanol-mediated appetitive second-order conditioning. *Alcohol Clin Exp Res*, *32*(11), 2016-2027. https://doi.org/10.1111/j.1530-0277.2008.00789.x

Pekny, M., Wilhelmsson, U., & Pekna, M. (2014). The dual role of astrocyte activation and reactive gliosis. *Neurosci Lett*, *565*, 30-38. https://doi.org/10.1016/j.neulet.2013.12.071

Pelinka, L. E., Kroepfl, A., Leixnering, M., Buchinger, W., Raabe, A., & Redl, H. (2004). GFAP versus S100B in serum after traumatic brain injury: relationship to brain damage and outcome. *J Neurotrauma*, *21*(11), 1553-1561. https://doi.org/10.1089/neu.2004.21.1553

Penfield, W., & Roberts, L. (1959). *Speech and brain-mechanisms*. Princeton University Press.

Petanjek, Z., Judas, M., Simic, G., Rasin, M. R., Uylings, H. B., Rakic, P., & Kostovic, I. (2011). Extraordinary neoteny of synaptic spines in the human prefrontal cortex. *Proc Natl Acad Sci U S A*, *108*(32), 13281-13286. https://doi.org/10.1073/pnas.1105108108

Petrides, M., & Pandya, D. N. (1999). Dorsolateral prefrontal cortex: comparative cytoarchitectonic analysis in the human and the macaque brain and corticocortical connection patterns. *Eur J Neurosci*, *11*(3), 1011-1036. https://doi.org/10.1046/j.1460-9568.1999.00518.x

Pfefferbaum, A., Rosenbloom, M., Deshmukh, A., & Sullivan, E. (2001). Sex differences in the effects of alcohol on brain structure. *Am J Psychiatry*, *158*(2), 188-197. https://doi.org/10.1176/appi.ajp.158.2.188

Phillips, R. D., De Bellis, M. D., Brumback, T., Clausen, A. N., Clarke-Rubright, E. K., Haswell, C. C., & Morey, R. A. (2021). Volumetric trajectories of hippocampal subfields and amygdala nuclei influenced by adolescent alcohol use and lifetime trauma. *Transl Psychiatry*, *11*(1), 154. https://doi.org/10.1038/s41398-021-01275-0

Primus, R. J., & Kellogg, C. K. (1989). Pubertal-related changes influence the development of environment-related social interaction in the male rat. *Dev Psychobiol*, *22*(6), 633-643. https://doi.org/10.1002/dev.420220608

Rakic, P., Bourgeois, J., & Goldman-Rakic, P. (1994). The self-organizing brain: from growth cones to functional networks.

Ramachandran, B., Ahmed, S., Zafar, N., & Dean, C. (2015). Ethanol inhibits long-term potentiation in hippocampal CA1 neurons, irrespective of lamina and stimulus strength, through neurosteroidogenesis. *Hippocampus*, *25*(1), 106-118. https://doi.org/10.1002/hipo.22356

Reeves, B. C., Karimy, J. K., Kundishora, A. J., Mestre, H., Cerci, H. M., Matouk, C., Alper, S. L., Lundgaard, I., Nedergaard, M., & Kahle, K. T. (2020). Glymphatic System Impairment in Alzheimer's Disease and Idiopathic Normal Pressure Hydrocephalus. *Trends Mol Med*, *26*(3), 285-295. https://doi.org/10.1016/j.molmed.2019.11.008

Reilly, J. F., Maher, P. A., & Kumari, V. G. (1998). Regulation of astrocyte GFAP expression by TGF-beta1 and FGF-2. *Glia*, *22*(2), 202-210. https://doi.org/10.1002/(sici)1098-1136(199802)22:2<202::aid-glia11>3.0.co;2-1

Risher, M. L., Fleming, R. L., Boutros, N., Semenova, S., Wilson, W. A., Levin, E. D., Markou, A., Swartzwelder, H. S., & Acheson, S. K. (2013). Long-term effects of chronic intermittent ethanol exposure in adolescent and adult rats: radial-arm maze performance and operant food reinforced responding. *PLoS One*, *8*(5), e62940. https://doi.org/10.1371/journal.pone.0062940

Risher, M. L., Fleming, R. L., Risher, W. C., Miller, K. M., Klein, R. C., Wills, T., Acheson, S. K., Moore, S. D., Wilson, W. A., Eroglu, C., & Swartzwelder, H. S. (2015). Adolescent intermittent alcohol exposure: persistence of structural and functional hippocampal abnormalities into adulthood. *Alcohol Clin Exp Res*, *39*(6), 989-997. https://doi.org/10.1111/acer.12725

Risher, M. L., Sexton, H. G., Risher, W. C., Wilson, W. A., Fleming, R. L., Madison, R. D., Moore, S. D., Eroglu, C., & Swartzwelder, H. S. (2015). Adolescent Intermittent Alcohol

Exposure: Dysregulation of Thrombospondins and Synapse Formation are Associated with Decreased Neuronal Density in the Adult Hippocampus. *Alcohol Clin Exp Res*, *39*(12), 2403-2413. https://doi.org/10.1111/acer.12913

Risher, W. C., Patel, S., Kim, I. H., Uezu, A., Bhagat, S., Wilton, D. K., Pilaz, L. J., Singh Alvarado, J., Calhan, O. Y., Silver, D. L., Stevens, B., Calakos, N., Soderling, S. H., & Eroglu, C. (2014). Astrocytes refine cortical connectivity at dendritic spines. *Elife*, *3*. https://doi.org/10.7554/eLife.04047

Risher, W. C., Ustunkaya, T., Singh Alvarado, J., & Eroglu, C. (2014). Rapid Golgi analysis method for efficient and unbiased classification of dendritic spines. *PLoS One*, *9*(9), e107591. https://doi.org/10.1371/journal.pone.0107591

Ristuccia, R. C., & Spear, L. P. (2008). Autonomic responses to ethanol in adolescent and adult rats: a dose-response analysis. *Alcohol*, *42*(8), 623-629. https://doi.org/10.1016/j.alcohol.2008.08.002

RJC, D. G. (1742). *Splanchnologie ou l'anatomie des visceres* (C. Osmond, Ed. Vol. 2nd).

Roberts, A. C., Diez-Garcia, J., Rodriguiz, R. M., Lopez, I. P., Lujan, R., Martinez-Turrillas, R., Pico, E., Henson, M. A., Bernardo, D. R., Jarrett, T. M., Clendeninn, D. J., Lopez-Mascaraque, L., Feng, G., Lo, D. C., Wesseling, J. F., Wetsel, W. C., Philpot, B. D., & Perez-Otano, I. (2009). Downregulation of NR3A-containing NMDARs is required for synapse maturation and memory consolidation. *Neuron*, *63*(3), 342-356. https://doi.org/10.1016/j.neuron.2009.06.016

Rolls, E. T. (2019). Orbitofrontal cortex: anatomy and connections. In E. T. Rolls (Ed.), *The Orbitofrontal Cortex* (p. 10-16) Oxford University Press. https://doi.org/10.1093/oso/9780198845997.003.0002

Rolls, E. T., Cheng, W., & Feng, J. (2020). The orbitofrontal cortex: reward, emotion and depression. *Brain Commun*, *2*(2), fcaa196. https://doi.org/10.1093/braincomms/fcaa196

Romer, D., Duckworth, A. L., Sznitman, S., & Park, S. (2010). Can adolescents learn self-control? Delay of gratification in the development of control over risk taking. *Prev Sci*, *11*(3), 319-330. https://doi.org/10.1007/s11121-010-0171-8

Rossetti, M. G., Patalay, P., Mackey, S., Allen, N. B., Batalla, A., Bellani, M., Chye, Y., Cousijn, J., Goudriaan, A. E., Hester, R., Hutchison, K., Li, C. R., Martin-Santos, R., Momenan, R., Sinha, R., Schmaal, L., Sjoerds, Z., Solowij, N., Suo, C., . . . Lorenzetti, V. (2021). Gender-related neuroanatomical differences in alcohol dependence: findings from the ENIGMA Addiction Working Group. *Neuroimage Clin*, *30*, 102636. https://doi.org/10.1016/j.nicl.2021.102636

Roth, B. L. (2016). DREADDs for Neuroscientists. *Neuron*, *89*(4), 683-694. https://doi.org/10.1016/j.neuron.2016.01.040

Rubia, K. (2013). Functional brain imaging across development. *Eur Child Adolesc Psychiatry*, *22*(12), 719-731. https://doi.org/10.1007/s00787-012-0291-8

Rushworth, M. F., Kolling, N., Sallet, J., & Mars, R. B. (2012). Valuation and decision-making in frontal cortex: one or many serial or parallel systems? *Curr Opin Neurobiol*, *22*(6), 946-955. https://doi.org/10.1016/j.conb.2012.04.011

Sabeti, J., & Gruol, D. L. (2008). Emergence of NMDAR-independent long-term potentiation at hippocampal CA1 synapses following early adolescent exposure to chronic intermittent ethanol: role for sigma-receptors. *Hippocampus*, *18*(2), 148-168. https://doi.org/10.1002/hipo.20379

Sacks, J. J., Gonzales, K. R., Bouchery, E. E., Tomedi, L. E., & Brewer, R. D. (2015). 2010 National and State Costs of Excessive Alcohol Consumption. *Am J Prev Med*, *49*(5), e73-e79. https://doi.org/10.1016/j.amepre.2015.05.031

Santos, F. J., Oliveira, R. F., Jin, X., & Costa, R. M. (2015). Corticostriatal dynamics encode the refinement of specific behavioral variability during skill learning. *Elife*, *4*, e09423. https://doi.org/10.7554/eLife.09423

Sawyer, K. S., Adra, N., Salz, D. M., Kemppainen, M. I., Ruiz, S. M., Harris, G. J., & Oscar-Berman, M. (2020). Hippocampal subfield volumes in abstinent men and women with a history of alcohol use disorder. *PLoS One*, *15*(8), e0236641. https://doi.org/10.1371/journal.pone.0236641

Sawyer, S. M., Afifi, R. A., Bearinger, L. H., Blakemore, S. J., Dick, B., Ezeh, A. C., & Patton, G. C. (2012). Adolescence: a foundation for future health. *Lancet*, *379*(9826), 1630-1640. https://doi.org/10.1016/S0140-6736(12)60072-5

Schubert, M. I., Porkess, M. V., Dashdorj, N., Fone, K. C., & Auer, D. P. (2009). Effects of social isolation rearing on the limbic brain: a combined behavioral and magnetic resonance imaging volumetry study in rats. *Neuroscience*, *159*(1), 21-30. https://doi.org/10.1016/j.neuroscience.2008.12.019

Scofield, M. D., Li, H., Siemsen, B. M., Healey, K. L., Tran, P. K., Woronoff, N., Boger, H. A., Kalivas, P. W., & Reissner, K. J. (2016). Cocaine Self-Administration and Extinction Leads to Reduced Glial Fibrillary Acidic Protein Expression and Morphometric Features of Astrocytes in the Nucleus Accumbens Core. *Biol Psychiatry*, *80*(3), 207-215. https://doi.org/10.1016/j.biopsych.2015.12.022

Shackman, A. J., Salomons, T. V., Slagter, H. A., Fox, A. S., Winter, J. J., & Davidson, R. J. (2011). The integration of negative affect, pain and cognitive control in the cingulate cortex. *Nat Rev Neurosci*, *12*(3), 154-167. https://doi.org/10.1038/nrn2994

Shenhav, A., Botvinick, M. M., & Cohen, J. D. (2013). The expected value of control: an integrative theory of anterior cingulate cortex function. *Neuron*, *79*(2), 217-240. https://doi.org/10.1016/j.neuron.2013.07.007

Sherwood, M. W., Arizono, M., Hisatsune, C., Bannai, H., Ebisui, E., Sherwood, J. L., Panatier, A., Oliet, S. H., & Mikoshiba, K. (2017). Astrocytic IP(3) Rs: Contribution to Ca(2+) signalling and hippocampal LTP. *Glia*, *65*(3), 502-513. https://doi.org/10.1002/glia.23107

Shigetomi, E., Bushong, E. A., Haustein, M. D., Tong, X., Jackson-Weaver, O., Kracun, S., Xu, J., Sofroniew, M. V., Ellisman, M. H., & Khakh, B. S. (2013). Imaging calcium microdomains within entire astrocyte territories and endfeet with GCaMPs expressed using adeno-associated viruses. *J Gen Physiol*, *141*(5), 633-647. https://doi.org/10.1085/jgp.201210949

Shimizu, K., Matsubara, K., Uezono, T., Kimura, K., & Shiono, H. (1998). Reduced dorsal hippocampal glutamate release significantly correlates with the spatial memory deficits produced by benzodiazepines and ethanol. *Neuroscience*, *83*(3), 701-706. https://doi.org/10.1016/s0306-4522(97)00339-4

Siddiqui, T. J., Pancaroglu, R., Kang, Y., Rooyakkers, A., & Craig, A. M. (2010). LRRTMs and neuroligins bind neurexins with a differential code to cooperate in glutamate synapse development. *J Neurosci*, *30*(22), 7495-7506. https://doi.org/10.1523/JNEUROSCI.0470-10.2010

Silveri, M. M., & Spear, L. P. (1998). Decreased sensitivity to the hypnotic effects of ethanol early in ontogeny. *Alcohol Clin Exp Res*, *22*(3), 670-676. https://doi.org/10.1111/j.1530-0277.1998.tb04310.x

Silvers, J. M., Tokunaga, S., Berry, R. B., White, A. M., & Matthews, D. B. (2003). Impairments in spatial learning and memory: ethanol, allopregnanolone, and the hippocampus. *Brain Res Brain Res Rev*, *43*(3), 275-284. https://doi.org/10.1016/j.brainresrev.2003.09.002

Silvestre de Ferron, B., Bennouar, K. E., Kervern, M., Alaux-Cantin, S., Robert, A., Rabiant, K., Antol, J., Naassila, M., & Pierrefiche, O. (2015). Two Binges of Ethanol a Day Keep the Memory Away in Adolescent Rats: Key Role for GLUN2B Subunit. *Int J Neuropsychopharmacol*, *19*(1). https://doi.org/10.1093/ijnp/pyv087

Simmonds, D. J., Hallquist, M. N., Asato, M., & Luna, B. (2014). Developmental stages and sex differences of white matter and behavioral development through adolescence: a longitudinal diffusion tensor imaging (DTI) study. *Neuroimage*, *92*, 356-368. https://doi.org/10.1016/j.neuroimage.2013.12.044

Singh, S. K., Stogsdill, J. A., Pulimood, N. S., Dingsdale, H., Kim, Y. H., Pilaz, L. J., Kim, I. H., Manhaes, A. C., Rodrigues, W. S., Jr., Pamukcu, A., Enustun, E., Ertuz, Z., Scheiffele, P., Soderling, S. H., Silver, D. L., Ji, R. R., Medina, A. E., & Eroglu, C. (2016). Astrocytes Assemble Thalamocortical Synapses by Bridging NRX1alpha and NL1 via Hevin. *Cell*, *164*(1-2), 183-196. https://doi.org/10.1016/j.cell.2015.11.034

Song, H., Stevens, C. F., & Gage, F. H. (2002). Astroglia induce neurogenesis from adult neural stem cells. *Nature*, *417*(6884), 39-44. https://doi.org/10.1038/417039a

Song, J. Y., Ichtchenko, K., Sudhof, T. C., & Brose, N. (1999). Neuroligin 1 is a postsynaptic cell-adhesion molecule of excitatory synapses. *Proc Natl Acad Sci U S A*, *96*(3), 1100-1105. https://doi.org/10.1073/pnas.96.3.1100

Sotres-Bayon, F., & Quirk, G. J. (2010). Prefrontal control of fear: more than just extinction. *Curr Opin Neurobiol*, *20*(2), 231-235. https://doi.org/10.1016/j.conb.2010.02.005

Spear, L. P. (2000). The adolescent brain and age-related behavioral manifestations. *Neurosci Biobehav Rev*, *24*(4), 417-463. https://doi.org/10.1016/s0149-7634(00)00014-2

Spear, L. P. (2013). Adolescent neurodevelopment. *J Adolesc Health*, *52*(2 Suppl 2), S7-13. https://doi.org/10.1016/j.jadohealth.2012.05.006

Spear, L. P., & Swartzwelder, H. S. (2014). Adolescent alcohol exposure and persistence of adolescent-typical phenotypes into adulthood: a mini-review. *Neurosci Biobehav Rev*, *45*, 1-8. https://doi.org/10.1016/j.neubiorev.2014.04.012

Spinka, M., Newberry, R. C., & Bekoff, M. (2001). Mammalian play: training for the unexpected. *Q Rev Biol*, *76*(2), 141-168. https://doi.org/10.1086/393866

Squeglia, L. M., Schweinsburg, A. D., Pulido, C., & Tapert, S. F. (2011). Adolescent binge drinking linked to abnormal spatial working memory brain activation: differential gender effects. *Alcohol Clin Exp Res*, *35*(10), 1831-1841. https://doi.org/10.1111/j.1530-0277.2011.01527.x

Steinberg, L. (2008). A Social Neuroscience Perspective on Adolescent Risk-Taking. *Dev Rev*, *28*(1), 78-106. https://doi.org/10.1016/j.dr.2007.08.002

Steinberg, L. (2010). A dual systems model of adolescent risk-taking. *Dev Psychobiol*, *52*(3), 216-224. https://doi.org/10.1002/dev.20445

Steinberg, L., Adams, G., Montemayor, R., & Gullota, T. (1989). Advances in adolescent behavior and development. In: Newbury Park, CA: Sage Publications.

Stevens, F. L., Hurley, R. A., & Taber, K. H. (2011). Anterior cingulate cortex: unique role in cognition and emotion. *J Neuropsychiatry Clin Neurosci*, *23*(2), 121-125. https://doi.org/10.1176/jnp.23.2.jnp121

Stevens, M. C., Pearlson, G. D., & Calhoun, V. D. (2009). Changes in the interaction of resting-state neural networks from adolescence to adulthood. *Hum Brain Mapp*, *30*(8), 2356-2366. https://doi.org/10.1002/hbm.20673

Stogsdill, J. A., Ramirez, J., Liu, D., Kim, Y. H., Baldwin, K. T., Enustun, E., Ejikeme, T., Ji, R. R., & Eroglu, C. (2017). Astrocytic neuroligins control astrocyte morphogenesis and synaptogenesis. *Nature*, *551*(7679), 192-197. https://doi.org/10.1038/nature24638

Sudhof, T. C. (2008). Neuroligins and neurexins link synaptic function to cognitive disease. *Nature*, *455*(7215), 903-911. https://doi.org/10.1038/nature07456

Sullivan, E. V., Adalsteinsson, E., Sood, R., Mayer, D., Bell, R., McBride, W., Li, T. K., & Pfefferbaum, A. (2006). Longitudinal brain magnetic resonance imaging study of the alcohol-preferring rat. Part I: adult brain growth. *Alcohol Clin Exp Res*, *30*(7), 1234-1247. https://doi.org/10.1111/j.1530-0277.2006.00145.x

Sullivan, E. V., Brumback, T., Tapert, S. F., Fama, R., Prouty, D., Brown, S. A., Cummins, K., Thompson, W. K., Colrain, I. M., Baker, F. C., De Bellis, M. D., Hooper, S. R., Clark, D. B., Chung, T., Nagel, B. J., Nichols, B. N., Rohlfing, T., Chu, W., Pohl, K. M., & Pfefferbaum, A. (2016). Cognitive, emotion control, and motor performance of adolescents in the NCANDA study: Contributions from alcohol consumption, age, sex, ethnicity, and family history of addiction. *Neuropsychology*, *30*(4), 449-473. https://doi.org/10.1037/neu0000259

Supekar, K., Musen, M., & Menon, V. (2009). Development of large-scale functional brain networks in children. *PLoS Biol*, *7*(7), e1000157. https://doi.org/10.1371/journal.pbio.1000157

Supekar, K., Uddin, L. Q., Prater, K., Amin, H., Greicius, M. D., & Menon, V. (2010). Development of functional and structural connectivity within the default mode network in young children. *Neuroimage*, *52*(1), 290-301. https://doi.org/10.1016/j.neuroimage.2010.04.009

Swartzwelder, H. S., Acheson, S. K., Miller, K. M., Sexton, H. G., Liu, W., Crews, F. T., & Risher, M. L. (2015). Adolescent Intermittent Alcohol Exposure: Deficits in Object Recognition Memory and Forebrain Cholinergic Markers. *PLoS One*, *10*(11), e0140042. https://doi.org/10.1371/journal.pone.0140042

Swartzwelder, H. S., Wilson, W. A., & Tayyeb, M. I. (1995). Age-dependent inhibition of long-term potentiation by ethanol in immature versus mature hippocampus. *Alcohol Clin Exp Res*, *19*(6), 1480-1485. https://doi.org/10.1111/j.1530-0277.1995.tb01011.x

Takesian, A. E., & Hensch, T. K. (2013). Balancing plasticity/stability across brain development. *Prog Brain Res*, *207*, 3-34. https://doi.org/10.1016/B978-0-444-63327-9.00001-1

Testen, A., Ali, M., Sexton, H. G., Hodges, S., Dubester, K., Reissner, K. J., Swartzwelder, H. S., & Risher, M. L. (2019). Region-Specific Differences in Morphometric Features and Synaptic Colocalization of Astrocytes During Development. *Neuroscience*, *400*, 98-109. https://doi.org/10.1016/j.neuroscience.2018.12.044

Testen, A., Sepulveda-Orengo, M. T., Gaines, C. H., & Reissner, K. J. (2018). Region-Specific Reductions in Morphometric Properties and Synaptic Colocalization of Astrocytes Following Cocaine Self-Administration and Extinction. *Front Cell Neurosci*, *12*, 246. https://doi.org/10.3389/fncel.2018.00246

Tomlinson, K. L., Brown, S. A., & Abrantes, A. (2004). Psychiatric comorbidity and substance use treatment outcomes of adolescents. *Psychol Addict Behav*, *18*(2), 160-169. https://doi.org/10.1037/0893-164X.18.2.160

Toyoizumi, T., Miyamoto, H., Yazaki-Sugiyama, Y., Atapour, N., Hensch, T. K., & Miller, K. D. (2013). A theory of the transition to critical period plasticity: inhibition selectively suppresses spontaneous activity. *Neuron*, *80*(1), 51-63. https://doi.org/10.1016/j.neuron.2013.07.022

Trimpop, R. M., Kerr, J. H., & Kirkcaldy, B. (1998). Comparing personality constructs of risk-taking behavior. *Personality and Individual differences*, *26*(2), 237-254.

Ullian, E. M., Sapperstein, S. K., Christopherson, K. S., & Barres, B. A. (2001). Control of synapse number by glia. *Science*, *291*(5504), 657-661. https://doi.org/10.1126/science.291.5504.657

Ullsperger, M., Fischer, A. G., Nigbur, R., & Endrass, T. (2014). Neural mechanisms and temporal dynamics of performance monitoring. *Trends Cogn Sci*, *18*(5), 259-267. https://doi.org/10.1016/j.tics.2014.02.009

Van den Oever, M. C., Spijker, S., Smit, A. B., & De Vries, T. J. (2010). Prefrontal cortex plasticity mechanisms in drug seeking and relapse. *Neurosci Biobehav Rev*, *35*(2), 276-284. https://doi.org/10.1016/j.neubiorev.2009.11.016

van Kerkhof, L. W., Damsteegt, R., Trezza, V., Voorn, P., & Vanderschuren, L. J. (2013). Social play behavior in adolescent rats is mediated by functional activity in medial prefrontal cortex and striatum. *Neuropsychopharmacology*, *38*(10), 1899-1909. https://doi.org/10.1038/npp.2013.83

Varlinskaya, E. I., & Spear, L. P. (2002). Acute effects of ethanol on social behavior of adolescent and adult rats: role of familiarity of the test situation. *Alcohol Clin Exp Res*, *26*(10), 1502-1511. https://doi.org/10.1097/01.ALC.0000034033.95701.E3

Varlinskaya, E. I., Truxell, E., & Spear, L. P. (2014). Chronic intermittent ethanol exposure during adolescence: effects on social behavior and ethanol sensitivity in adulthood. *Alcohol*, *48*(5), 433-444. https://doi.org/10.1016/j.alcohol.2014.01.012

Ventura, R., & Harris, K. M. (1999). Three-dimensional relationships between hippocampal synapses and astrocytes. *J Neurosci*, *19*(16), 6897-6906. https://doi.org/10.1523/JNEUROSCI.19-16-06897.1999

Verguts, T., Vassena, E., & Silvetti, M. (2015). Adaptive effort investment in cognitive and physical tasks: a neurocomputational model. *Front Behav Neurosci*, *9*, 57. https://doi.org/10.3389/fnbeh.2015.00057

Vetreno, R. P., & Crews, F. T. (2012). Adolescent binge drinking increases expression of the danger signal receptor agonist HMGB1 and Toll-like receptors in the adult prefrontal cortex. *Neuroscience*, *226*, 475-488. https://doi.org/10.1016/j.neuroscience.2012.08.046

Vetreno, R. P., & Crews, F. T. (2015). Binge ethanol exposure during adolescence leads to a persistent loss of neurogenesis in the dorsal and ventral hippocampus that is associated with impaired adult cognitive functioning. *Front Neurosci*, *9*, 35. https://doi.org/10.3389/fnins.2015.00035

Vetreno, R. P., Yaxley, R., Paniagua, B., & Crews, F. T. (2016). Diffusion tensor imaging reveals adolescent binge ethanol-induced brain structural integrity alterations in adult rats that correlate with behavioral dysfunction. *Addict Biol*, *21*(4), 939-953. https://doi.org/10.1111/adb.12232

Vollstadt-Klein, S., Hermann, D., Rabinstein, J., Wichert, S., Klein, O., Ende, G., & Mann, K. (2010). Increased activation of the ACC during a spatial working memory task in alcohol-dependence versus heavy social drinking. *Alcohol Clin Exp Res*, *34*(5), 771-776. https://doi.org/10.1111/j.1530-0277.2010.01149.x

Walker, C. D., Kuhn, C. M., & Risher, M. L. (2021). The effects of peri-adolescent alcohol use on the developing hippocampus. *Int Rev Neurobiol*, *160*, 251-280. https://doi.org/10.1016/bs.irn.2021.08.003

Walker, C. D., Risher, W. C., & Risher, M. L. (2020). Regulation of Synaptic Development by Astrocyte Signaling Factors and Their Emerging Roles in Substance Abuse. *Cells*, *9*(2). https://doi.org/10.3390/cells9020297

Walker, C. D., Sexton, H. G., Hyde, J., Greene, B., & Risher, M. L. (2022). Diverging Effects of Adolescent Ethanol Exposure on Tripartite Synaptic Development across Prefrontal Cortex Subregions. *Cells*, *11*(19). https://doi.org/10.3390/cells11193111

Warren, B. L., Mendoza, M. P., Cruz, F. C., Leao, R. M., Caprioli, D., Rubio, F. J., Whitaker, L. R., McPherson, K. B., Bossert, J. M., Shaham, Y., & Hope, B. T. (2016). Distinct Fos-Expressing Neuronal Ensembles in the Ventromedial Prefrontal Cortex Mediate Food Reward and Extinction Memories. *J Neurosci*, *36*(25), 6691-6703. https://doi.org/10.1523/JNEUROSCI.0140-16.2016

Weissenborn, R., & Duka, T. (2003). Acute alcohol effects on cognitive function in social drinkers: their relationship to drinking habits. *Psychopharmacology (Berl)*, *165*(3), 306-312. https://doi.org/10.1007/s00213-002-1281-1

White, A. M., Castle, I. P., Hingson, R. W., & Powell, P. A. (2020). Using Death Certificates to Explore Changes in Alcohol-Related Mortality in the United States, 1999 to 2017. *Alcohol Clin Exp Res*, *44*(1), 178-187. https://doi.org/10.1111/acer.14239

White, A. M., Castle, I. P., Powell, P. A., Hingson, R. W., & Koob, G. F. (2022). Alcohol-Related Deaths During the COVID-19 Pandemic. *JAMA*, *327*(17), 1704-1706. https://doi.org/10.1001/jama.2022.4308

White, A. M., Truesdale, M. C., Bae, J. G., Ahmad, S., Wilson, W. A., Best, P. J., & Swartzwelder, H. S. (2002). Differential effects of ethanol on motor coordination in adolescent and adult rats. *Pharmacol Biochem Behav*, *73*(3), 673-677. http://www.ncbi.nlm.nih.gov/entrez/query.fcgi?cmd=Retrieve&db=PubMed&dopt=Citation&list_uids=12151043

Wiese, S., Karus, M., & Faissner, A. (2012). Astrocytes as a source for extracellular matrix molecules and cytokines. *Front Pharmacol*, *3*, 120. https://doi.org/10.3389/fphar.2012.00120

Wiesel, T. N., & Hubel, D. H. (1963). Single-Cell Responses in Striate Cortex of Kittens Deprived of Vision in One Eye. *J Neurophysiol*, *26*, 1003-1017. https://doi.org/10.1152/jn.1963.26.6.1003

Witcher, M. R., Kirov, S. A., & Harris, K. M. (2007). Plasticity of perisynaptic astroglia during synaptogenesis in the mature rat hippocampus. *Glia*, *55*(1), 13-23. https://doi.org/10.1002/glia.20415

Wong, D., Dorovini-Zis, K., & Vincent, S. R. (2004). Cytokines, nitric oxide, and cGMP modulate the permeability of an in vitro model of the human blood-brain barrier. *Exp Neurol*, *190*(2), 446-455. https://doi.org/10.1016/j.expneurol.2004.08.008

Wood, J. N., & Grafman, J. (2003). Human prefrontal cortex: processing and representational perspectives. *Nat Rev Neurosci*, *4*(2), 139-147. https://doi.org/10.1038/nrn1033

Wood, R. L., & Worthington, A. (2017). Neurobehavioral Abnormalities Associated with Executive Dysfunction after Traumatic Brain Injury. *Front Behav Neurosci*, *11*, 195. https://doi.org/10.3389/fnbeh.2017.00195

World Health Organization. (2001). The Second Decade: Improving Adolescent Health and Development. Geneva.

World Health Organization. (2019). *Global Status Report on Alcohol and Health 2018*.

World, H. O. (2001). The Second Decade: Improving Adolescent Health and Development. Geneva.

Wyss-Coray, T. (2006). Inflammation in Alzheimer disease: driving force, bystander or beneficial response? *Nat Med*, *12*(9), 1005-1015. https://doi.org/10.1038/nm1484

Xi, B., Veeranki, S. P., Zhao, M., Ma, C., Yan, Y., & Mi, J. (2017). Relationship of Alcohol Consumption to All-Cause, Cardiovascular, and Cancer-Related Mortality in U.S. Adults. *J Am Coll Cardiol*, *70*(8), 913-922. https://doi.org/10.1016/j.jacc.2017.06.054

Xu, G., Liu, X., Yin, Q., Zhu, W., Zhang, R., & Fan, X. (2009). Alcohol consumption and transition of mild cognitive impairment to dementia. *Psychiatry Clin Neurosci*, *63*(1), 43-49. https://doi.org/10.1111/j.1440-1819.2008.01904.x

Yang, Y., Wang, Z. H., Jin, S., Gao, D., Liu, N., Chen, S. P., Zhang, S., Liu, Q., Liu, E., Wang, X., Liang, X., Wei, P., Li, X., Li, Y., Yue, C., Li, H. L., Wang, Y. L., Wang, Q., Ke, D., . . . Wang, J. Z. (2016). Opposite monosynaptic scaling of BLP-vCA1 inputs governs hopefulness- and helplessness-modulated spatial learning and memory. *Nat Commun*, *7*, 11935. https://doi.org/10.1038/ncomms11935

Yu, X., Moye, S. L., & Khakh, B. S. (2021). Local and CNS-Wide Astrocyte Intracellular Calcium Signaling Attenuation In Vivo with CalEx(flox) Mice. *J Neurosci*, *41*(21), 4556-4574. https://doi.org/10.1523/JNEUROSCI.0085-21.2021

Zahr, N. M., Pohl, K. M., Saranathan, M., Sullivan, E. V., & Pfefferbaum, A. (2019). Hippocampal subfield CA2+3 exhibits accelerated aging in Alcohol Use Disorder: A preliminary study. *Neuroimage Clin*, *22*, 101764. https://doi.org/10.1016/j.nicl.2019.101764

Zakharova, M., & Ziegler, H. K. (2005). Paradoxical anti-inflammatory actions of TNF-alpha: inhibition of IL-12 and IL-23 via TNF receptor 1 in macrophages and dendritic cells. *J Immunol*, *175*(8), 5024-5033. https://doi.org/10.4049/jimmunol.175.8.5024

Zamanian, J. L., Xu, L., Foo, L. C., Nouri, N., Zhou, L., Giffard, R. G., & Barres, B. A. (2012). Genomic analysis of reactive astrogliosis. *J Neurosci*, *32*(18), 6391-6410. https://doi.org/10.1523/JNEUROSCI.6221-11.2012

Zlatkine, P., Mehul, B., & Magee, A. I. (1997). Retargeting of cytosolic proteins to the plasma membrane by the Lck protein tyrosine kinase dual acylation motif. *J Cell Sci*, *110 (Pt 5)*, 673-679. https://doi.org/10.1242/jcs.110.5.673

Appendix A: Letter from the Office of Research Integrity

MARSHALL UNIVERSITY.
w w w . m a r s h a l l . e d u

Office of Research Integrity

April 27, 2023

Chris Walker
PO Box 4118
Pikeville, KY 41502

Dear Chris,

This letter is in response to the submitted dissertation abstract entitled *"Adolescence, Alcohol, and Astrocytes: The Impact of Adolescent Alcohol use on Astrocyte-Synaptic Interactions, Structure, Function, and Behavior."* After assessing the abstract, it has been deemed not to be human subject research and therefore exempt from oversight of the Marshall University Institutional Review Board (IRB). The Institutional Animal Care and Use Committee (IACUC) has reviewed and approved the study under protocol #750 and VA protocol #1608259. The applicable human and animal federal regulations have set forth the criteria utilized in making this determination. If there are any changes to the abstract, you provided then you would need to resubmit that information to the Office of Research Integrity for review and a determination.

I appreciate your willingness to submit the abstract for determination. Please feel free to contact the Office of Research Integrity if you have any questions regarding future protocols that may require IRB review.

Sincerely,

Bruce F. Day, ThD, CIP
Director
Office of Research Integrity

WE ARE... MARSHALL.
One John Marshall Drive • Huntington, West Virginia 25755 • Tel 304/696-4303
A State University of West Virginia • An Affirmative Action/Equal Opportunity Employer

Figure 25

Physiological Recordings and Protein Analysis Reveal Increased K^+ Clearance and Kir4.1 Expression at the Synapse in Adulthood Following AIE.
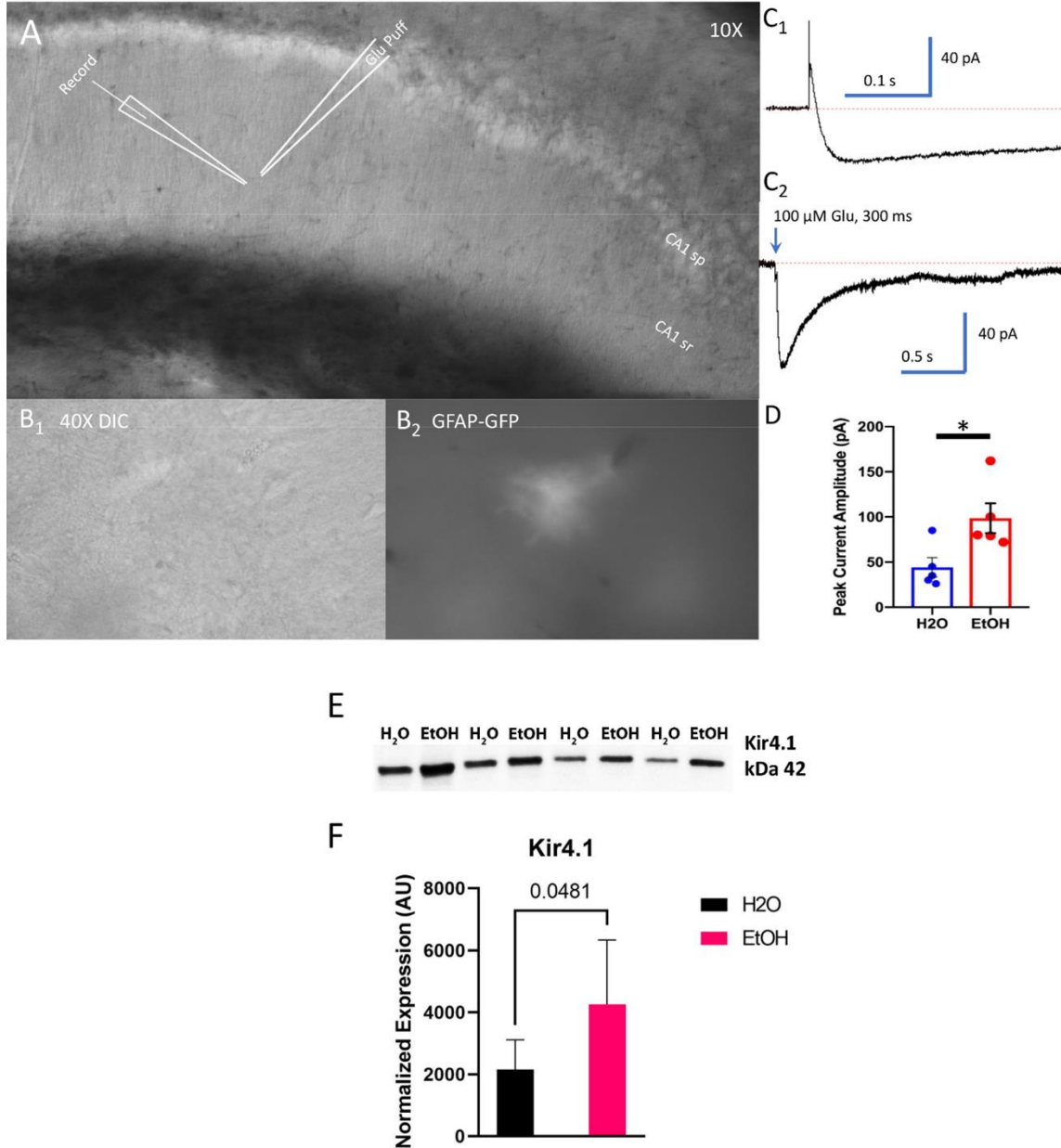
Physiological recordings of astrocytes in the male dHipp following AIE. A) shows the setup of our slice preparation on the recording stage and the orientation of the probe collecting recordings from the astrocyte of interest following glutamate puff in the stratum radiatum. B1 and B2 show the astrocyte of interest before and after the excitation of GFP, respectively. Figure C1 shows a representative trace of the holding potential of the astrocyte, while C2 is a representative trace

following 100 µM glutamate puff for 300 ms. D) AIE results in a protracted increase in astrocyte peak current amplitude in AIE animals following forced abstinence (p<0.05*; n=5 animals/treatment). E) Representative Western blot probing for Kir4.1 in subcellular fraction lysates prepared from dhipp tissue. F) Analysis of Western Blot protein assay revealed that AIE results in an increase in Kir4.1 expression following AIE in male rats. (t(10) = 2.251, p = 0.0481/ n=6 animals/treatment group). Statistical analysis: Student's t-test, n = 6 animals/treatment.

We observed a significant increase in peak current amplitude following glutamate puff in AIE animals compared to age matched controls. Astrocytes are electrically inert cells. However, recordings of changes in resting membrane potentials can still be collected using electrophysiology techniques. As glutamatergic signaling occurs, there is an increase in K^+ concentration. The astrocytes remove K^+ ions to maintain synaptic homeostasis to maintain neuronal function. K^+ is removed by inward rectifying K^+ channels (Kir4.1 channels) located on the membrane of the PAP. This data shows that AIE increases Kir4.1 expression at the PAP that correlates to an increase in astrocyte membrane potential. Further research is needed to determine if this is a compensatory mechanism in response to increased synaptic glutamate concentrations or if this is a response to the disruption of normal astrocyte function.

Appendix C: Glutamate Synthetase (GS) Activity

Figure 26

AIE Results in an Increase In Glutamate Synthetase (GS) Activity Following a 26-Day Forced Abstinence Period That is Not Seen During Peak Withdrawal.
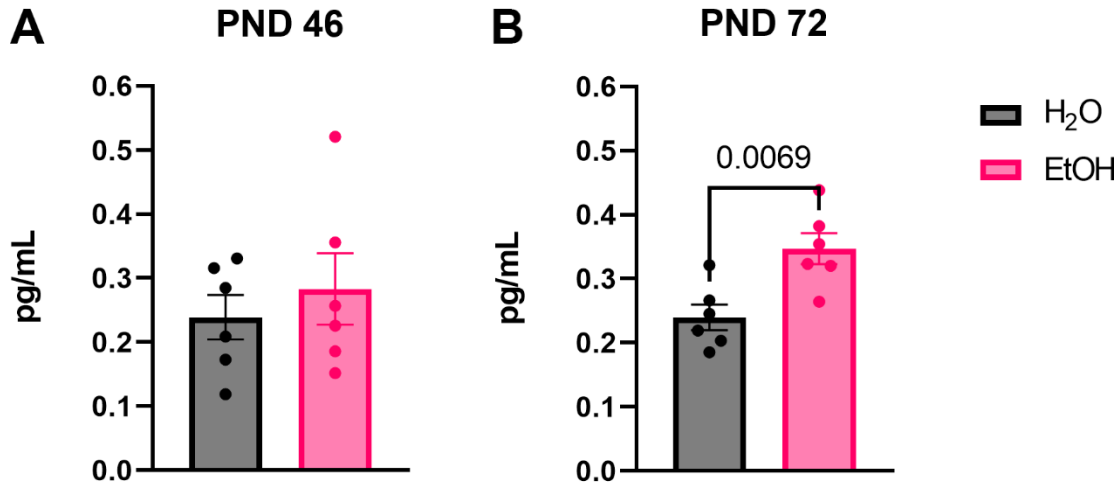

Analysis of enzyme assay to observe AIE-induced effects on GS activity during peak withdrawal (A) and adulthood following a 26-day forced abstinence period (B). We found no changes in GS activity at PND 46, during peak withdrawal ($t(10) = 0.6745$, $p = 0.5153$; n=5). However, there was a significant increase in GS activity in adulthood following forced abstinence (PND 72; $t(10) = 3.392$, $p = 0.0069$; n=6). Statistical analysis: Student's t-test, n = 6 animals/treatment.

GS plays a critical role in astrocyte mediated recycling of glutamate from the tripartite synapse. Glutamate is removed from the tripartite synapse via glutamate transporters found on the ensheathing astrocyte. Astrocyte GS converts glutamate to glutamine by adding a nitrogen atom to glutamate in the form of nitrogen. The glutamine molecule is then shuttled back to the presynaptic neuron where it can be used as the backbone for the formation of new glutamate molecules. These data show that AIE is not only having an impact on astrocyte morphology and PAP-synaptic interactions, but also altering intracellular pathways that are critical for normal neuronal function. Further research is needed to determine how this change in GS is affecting glutamatergic signaling and astrocyte cellular respiration.

Appendix D: IP3R2 Expression in the Adult Male Rat Hippocampus

Figure 27

AIE Results in an Increase in IP3R2 Expression in the Adult Male Hippocampus.
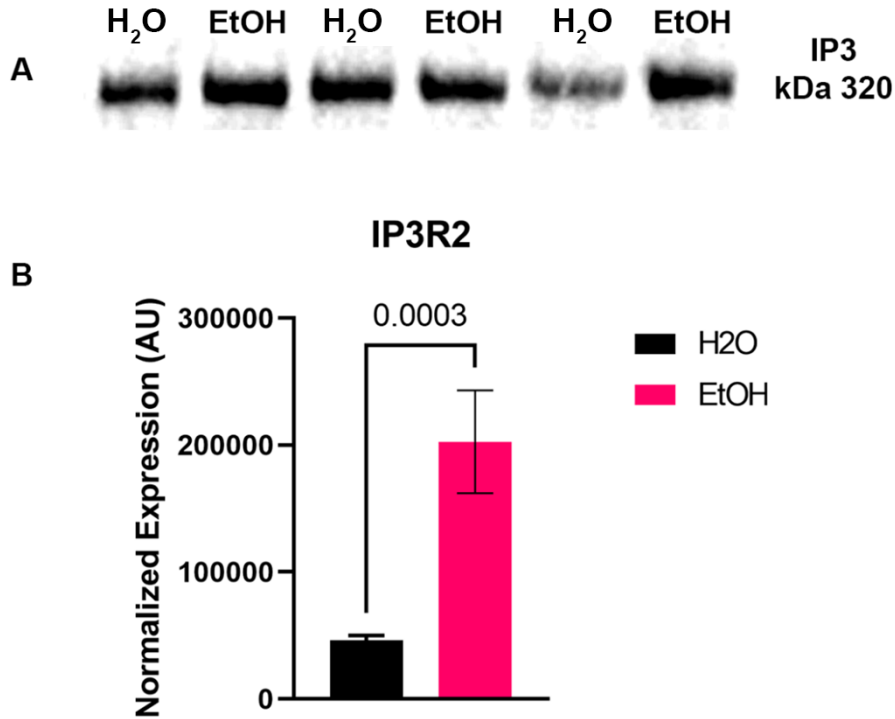

A) Representative image from Western Blot analysis of whole cell lysates prepared from hippocampal tissue. B) Analysis of Western Blot normalized to total protein. there was a significant increase in IP3R expression in the hippocampus of AIE treated animals following a 26-day period of forced abstinence when compared to age matched controls ($t(6) = 7.691$, $p = 0.0003$; n=5). IP3R2 plays a significant role in the induction of Ca^{2+} activity throughout astrocytes. Statistical analysis: Student's t-test, n = 4 animals/treatment.

These data tell us that IP3R2 expression is not contributing to the loss of astrocyte Ca^{2+} responsivity observed in our physiological assays. However, we have yet to explore the impact of AIE on overall expression of IP3 or other IP3 receptors.

Figure 28

Differing Effects of AIE on Adenosine Receptors in Adulthood.
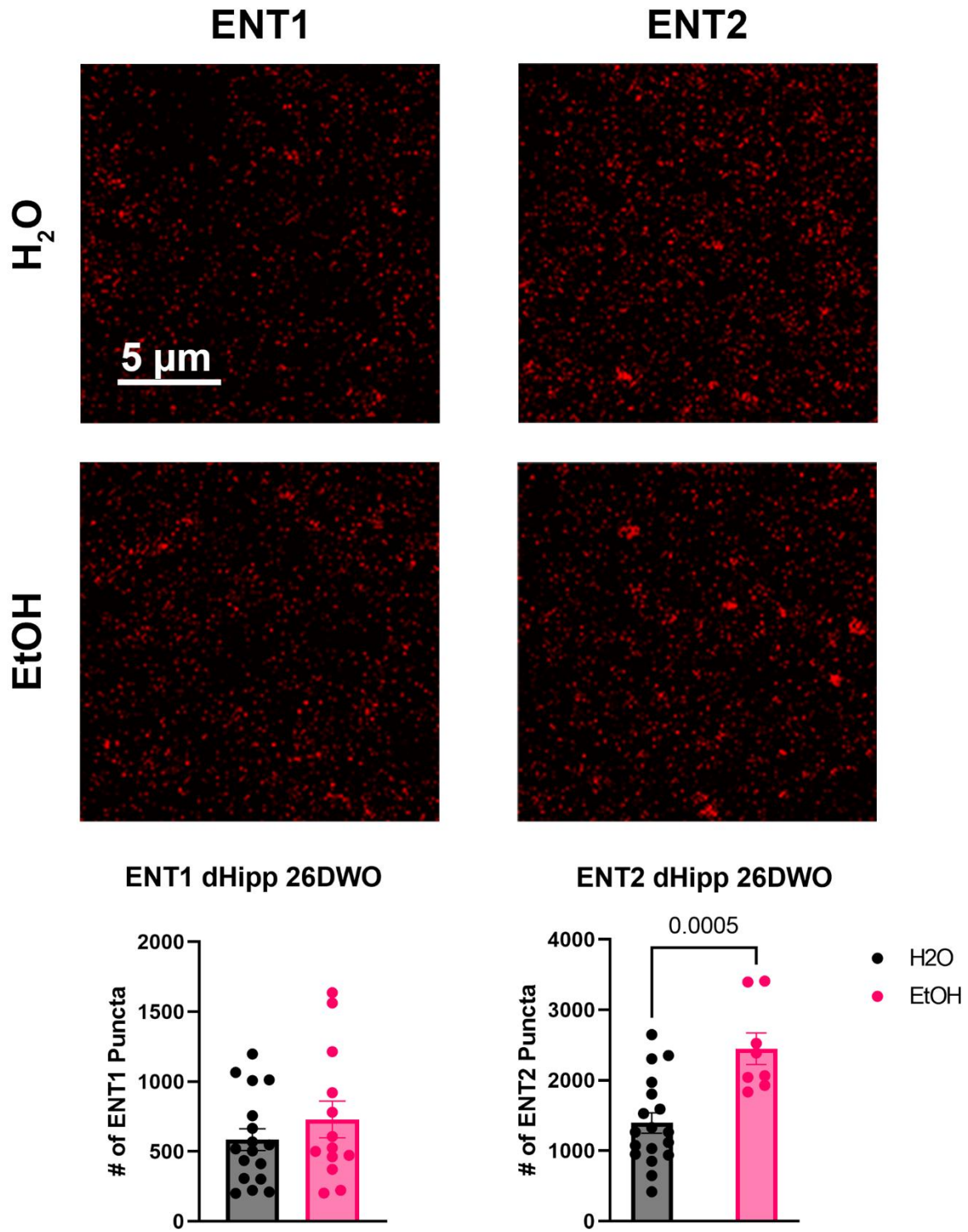
A) Representative images of IHC staining of the equilibrative nucleoside transports (ENT1 and ENT2). B) Puncta analysis to determine expression of ENT1 and ENT2 in the adult hippocampus following a 26-day forced abstinence period. We see no change in the ENT1 adenosine transporters in adulthood following AIE when compared to age matched controls (t(28) = 0.9973; p = 0.3272; n=4/treatment). However we found a significant increase in the expression of ENT2 in AIE animals when compared to age matched controls (t(24) = 4.001; p = 0.0005; n=4/treatment). Statistical analysis: Student's t-test, n = 2-3 images/animals (3-4 animals/treatment).

These transporters are responsible for transporting adenosine molecules in to and out of the cell. Changes in these transporters can affect extracellular concentrations of adenosine which is critical for modulation of glutamatergic neuronal transmission. Therefore, the changes observed here may indicate a mechanism by which astrocyte mediated modulation of glutamate transmission is increasing glutamate concentrations in the tripartite synapse. However, more research is necessary to determine if there are AIE induced changes in adenosine receptors on the corresponding neurons and, or changes in adenosine release from the astrocyte. These experiments will be key in better understanding astrocyte-neuronal bidirectional communication in our model of AIE.

Appendix F: Funding